

Strength in Flexibility;

Research into Innovative Flexible Bearing Designs for
Wave Convertor Permanent Magnet Generators

Adam Bedford

Lancaster University
Faculty of Science and Technology
Engineering Department

PhD Thesis

November 15, 2011

Supervisor(s): Dr. George A. Aggidis

Second Supervisors

Internal: Stephen Quayle

External: Dr. Markus Mueller

Declaration

The author declares that this thesis has not been previously submitted for a degree to this or any university and that the concepts, except where otherwise stated, are the authors own work.

Unless specifically referenced the figures and concepts within this document are all the work of the author.

Signed: _____

Date: _____

Table of Contents

Declaration	i
Abstract	ix
Nomenclature	xi
Abbreviations	xv
Acknowledgements	xxiii
Chapter 1 - Introduction	1
1.1 Renewable Energy	2
1.1.1 Limitations of renewable power	4
1.2 Wave Power	5
1.2.1 History	6
1.2.2 Resource Availability	6
1.2.3 Types of Resource	7
1.3 Linear Generators	8
1.3.1 What are linear generators?	8
1.3.2 What advantage do they offer?	10
1.3.3 What are the problems?	11

1.4	Why this work?	14
1.5	Thesis Structure	16
Chapter 2 - Literature		18
2.1	Foreword	19
2.2	Magnetic Theory	19
2.2.1	Magnetic Basics	20
2.2.2	Magnetic Circuit Theory	21
2.2.3	Attractive Forces	28
2.2.4	Opposing Magnets	29
2.3	Generator Theory	30
2.3.1	Magnetic Forces	30
2.3.2	Power Generation	32
2.4	Wave Theory	35
2.4.1	Wave Motion	35
2.4.2	Sea Spectra	36
2.4.3	Wave Device Tuning	38
2.5	Linear Generator Theory	39
2.5.1	Key Elements	40
2.5.2	Topologies	41
2.5.3	Motion	50
2.6	Hydrostatic Theory	51
2.6.1	Non-Dynamic Hydrostatic Analysis	53
2.6.2	Approximating Dynamic Hydrostatic Response	57
2.6.3	Industrial Bearings	61
2.6.4	Pumps	62

2.7	Analytical Stress Analysis	70
2.7.1	Bending Moments	70
2.7.2	Vibration	75
Chapter 3 - Methodology		77
3.1	Criteria	78
3.1.1	Bearing Power Usage	78
3.1.2	Power Generation	79
3.1.3	Economic Factors	80
3.1.4	Reliability Factors	83
3.1.5	Control Strategy	84
3.2	Summary	85
Chapter 4 - Evaluation of Rigidly Structured Generators		86
4.1	Introduction	87
4.1.1	Defining a Rigidly Structured Generator	87
4.1.2	Issues	87
4.1.3	Applying Hydrostatic Bearings	88
4.2	Bearing Spacing	90
4.3	Defects	98
4.3.1	Hydrostatic Bearings	99
4.3.2	Non-fluid Bearings	102
4.4	Performance & Losses	104
4.5	Scaling	107
4.5.1	Hydrostatic Bearing Scaling	108
4.5.2	Permanent Magnet Scaling	109
4.5.3	Effect on Efficiency	109

4.5.4	Summary	110
4.6	Test Case	112
4.6.1	Parameters	112
4.6.2	Assumptions	112
4.6.3	Performance & Losses	117
4.7	Additional Concerns	118
Chapter 5 - Moving to Non-Rigidly Structured Generators		120
5.1	Theory	121
5.2	2-Stage Bearings	121
5.2.1	Theory	123
5.2.2	Conclusion	126
5.3	Multi-Machine Architecture	128
5.3.1	Theory	129
5.3.2	Conclusion	130
5.4	Fast Replace MMA (FR-MMA)	131
5.4.1	Theory	131
5.4.2	Complexities of FR-MMA	135
5.4.3	Conclusion	136
5.5	Segmented FR-MMA - SFR-MMA	138
5.5.1	2-Stage Cell Operation	139
5.5.2	MMA Cell Operation	140
5.5.3	Theory	142
5.5.4	Conclusion	142
5.6	Ring Supported Segmented FR-MMA	144
5.6.1	Theory	144

5.6.2	Conclusion	145
5.7	Simplified FR-MMA	146
5.7.1	Theory	146
5.7.2	Conclusion	149
5.8	Multi-Purpose Modules	150
5.8.1	Theory	151
5.8.2	Conclusion	152
5.9	Lateral FR-MMA Module	154
5.9.1	Theory	154
5.9.2	Conclusion	156
5.10	Additional Work on FR-MMA Modules	158
5.10.1	Failure Response Mechanism	158
5.10.2	3-Point Pinning Strategy	166
5.11	Designing a Working Generator Module	168
5.11.1	Basic Requirements	169
5.11.2	Structural Implications	170
5.11.3	Pump Choice	176
5.11.4	Material Selection	177
5.11.5	Predicting Performance	181
5.12	Other Areas of Research	184
5.12.1	Re-circulating Bearings	184
5.12.2	Jet Bearing	186
5.12.3	Hybrid Ball-Fluid Bearing	190
5.12.4	Sacrificial Bearings	193
5.12.5	Protective Measures	194

Chapter 6 - Real World Impacts	197
6.1 Manufacturing Costs	198
6.2 Reliability	199
6.3 Operation & Maintenance Costs	200
6.4 Efficiency	201
Chapter 7 - Conclusions	203
7.1 Conclusions	204
7.1.1 Hydrostatic Evaluation	204
7.1.2 Additional Benefits	206
7.1.3 The Next Step	207
7.1.4 Overall Conclusions	209
7.2 Future Work	210
Appendices	212
Appendix A - Derivations	213
A.1 Pressure Distribution	213
A.2 Generalised Reynolds Equation	214
A.3 Hydrostatic Lubrication Equation	215
A.4 Polar Hydrostatic Derivation	216
A.5 Effective Area	218
A.6 Dynamic Hydrostatic Force	219
A.6.1 Pressure	219
A.6.2 Force	220
A.7 Air-gap Flux Relationship	221
A.8 Maximum Usable Air-Gap Relationship	222

Appendix B - Design Gallery	223
Appendix C - Laser Position Sensor	232
References	249

Abstract

Originally this research was to investigate the use of hydrostatic bearings in large linear machines, such as linear generators, and determine their viability in a power generation context. It quickly became clear that it was possible to make hydrostatic bearings viable, however the methods employed to do so gave rise to new possibilities which altered the scope of the research. The overall aim of the research has become to look at flexible construction, using modular generation units, as a means of creating more reliable and cost effective generators.

The methods employed to do this involved modularising the generator's structure. Each module then acts as a generator in its own right transferring its power to the parent machine. The potential for each module design was assessed based on its losses, due to the bearings, and its economic potential, such as how it impacted the operation and maintenance costs or transport costs and consideration of how each design affected the power density of the parent machine.

The basic structural analysis showed that, of the arrangements tried, there was a distinct advantage to restricting the number of bearings because it reduces energy losses. This is particularly true of designs that take advantage of the MMA concepts. The magnitude of the forces within the generators, during operation, lead to the creation 2-stage bearing and MMA concepts. The key reasons for them being to reducing dynamic forces within the generator and increase tolerance to design flaws and damage. Reducing the dynamic forces reduces losses in all types of bearings improving overall efficiency. Not all the concepts present in this document show commercial promise, however from the basic principles used to understand their working, there are some whose potential is clear. In general the modules have reduced the weight necessary to operate a successful generator and reduced the bearing losses no matter the type of bearing being used. Predicted force reductions mean that less strength critical and more cost effective materials can be used in the machines construction.

Given that the original scope of the research was to assess a single type of bearing it has come a long way to incorporate construction methods that will reduce operation and transport costs, as well as being more efficient on some of the construction materials. The final module designs show great promise to increase the power density of generators whilst making them easy to maintain. Although hydrostatic bearings provide excellent lubrication the basic analysis performed herein shows that their energy consumption exceeds the energy loss of normal roller bearings reducing overall generator efficiency. The modular constructions presented may not provide a great jump in efficiency over previous designs however they do show a way to simplify operation and maintenance costs improving overall commercial viability.

All 3D/CAD models contained herein were created by the author for this work unless otherwise stated/referenced.

Nomenclature

α	Laser Alignment Angle (<i>rad</i>)
Γ	Efficiency Product (%)
ϵ	Strain (<i>dimensionless</i>)
ε	Electro-motive Force (<i>Volts</i>)
ζ	Damping Ratio (<i>dimensionless</i>)
η	Efficiency (%)
η_{pump}	Overall Efficiency of a Pump (%)
η_k	Efficiency of Component k (%)
θ	Angular Position in a Rotating Device (<i>rad</i>)
κ	Ratio of Magnet Thickness to Air-gap (<i>dimensionless</i>)
μ_0	Permeability of free space (Hm^{-1})
μ_h	Dynamic Viscosity ($Pa\ s$)
μ_r	Relative Permeability (<i>dimensionless</i>)
ρ_f	Fluid Density ($kg\ m^{-1}$)
ρ_r	Resistivity of Conductor (Ωm)
σ	Stress (Pa)
σ_{max}	Maximum Stress (Pa)
σ_S	Magnetic Shear Stress (Pa)
σ_T	Transverse Magnetic Stress (Pa)
ϕ	Phase Shift (<i>radians</i>)
φ	Magnetic Flux (Wb)
$\varphi'(t)$	First Derivative of $\varphi(t)$
φ_m	Flux Constant for Permanent Magnets (Wb)
φ_c	Flux Constant for Circuit Current (H)
ψ	Vibrational Coefficient (<i>dimensionless</i>)
ω	Driving Frequency ($rad\ s^{-1}$)
ω_0	Natural Frequency ($rad\ s^{-1}$)
ω_1	Angular Frequency of Reciprocating Motion ($rad\ s^{-1}$)
ω_2	Translator Slot frequency (m^{-1})
ω_p	Angular Velocity of Pump ($rad\ s^{-1}$)
a	Distance from Start Point (Beam Bending) (m)

A	Area (m^2)
A_C	Cross-Sectional Area of Coil (m^2)
A_e	Effective Area (m^2)
A_i	Initial Amplitude of Oscillation in Bearing (m)
A_m	Magnet Area (Perpendicular to Field Direction) (m^2)
A_t	Reciprocating Linear Motion Amplitude (m)
A_x	Cross-Sectional Area of Conductor (m^2)
B	Flux Density (B-Field) (T)
B_{rem}	Remnant Flux Density (B-Field) (T)
B_{xy}	Buffer value at x, y (<i>dimensionless</i>)
C_f	Coefficient of Friction (<i>dimensionless</i>)
C_H	Dynamic Hydrostatic Bearing Constant
d	Coil Conductor Diameter (m)
E	Young's Modulus (Pa)
EMF	Electromotive Force ($Volts$)
f	Perspective Factor (<i>dimensionless</i>)
$f(t)$	Variation with Respect to Time (<i>dimensionless</i>)
$f'(t)$	First Derivative of $f(t)$ (s^{-1})
f_A	Packing Coefficient (<i>dimensionless</i>)
f_{rc}	Ratio of radius to circumference (<i>dimensionless</i>)
F_f	Friction Force(N)
F_T	Transverse Force(N)
h	Bearing Land Clearance (m)
H	Magnetic Field Strength (Am^{-1})
H_i	Magnetic Field Strength for Segment i (Am^{-1})
H_P	Equivalent Pumping Power (w)
I	Current (A)
I	Second moment of area (m^4)
$I'(t)$	First Derivative of $I(t)$ (As^{-1})
k	Spring Coefficient (Nm^{-1})
K	Current Loading (Am^{-1})
l	Length (m)
$l_{air-gap}$	Thickness of Air-gap (m)

l_{magnet}	Thickness of Magnet for the Purposes of Magnetic Circuits (m)
l_i	Length of Segment i (m)
l_t	Thickness (m)
l_x	Width of Coil Cross-Section (m)
l_y	Height of Coil Cross-Section (m)
L	Inductance (H)
L_H	Hydrostatic Bearing Constant ($N s$)
$\overline{L_P}$	Average Path Length (m)
m, m_n	Mass (kg)
m_a, m_b	Pole Strength Values ($m s^{-1} \sqrt{kg H}$)
m_g	Laser Beam Gradient (<i>dimensionless</i>)
MMF	Magnetomotive Force (<i>Ampere-turns</i>)
n	Number of Magnets & Air-Gaps (<i>dimensionless</i>)
N	Number of Turns (<i>dimensionless</i>)
N_x	Number of Conductors per Width (<i>dimensionless</i>)
N_y	Number of Conductors per Height (<i>dimensionless</i>)
p	Pressure (Pa)
p_i	Inlet Pressure (Pa)
P	Power (w)
P_{in}	Power In (w)
P_{input}	Power Input to a Pump (w)
P_{out}	Power Out (w)
P_{pipe}	Power Loss in the Pipes (w)
Q	Volumetric Flowrate ($m^3 s^{-1}$)
Q_{in}	Volumetric Flowrate In ($m^3 s^{-1}$)
Q_{out}	Volumetric Flowrate Out ($m^3 s^{-1}$)
q_0	Volume Displaced per Rotation (Volumetric Pumps) (m^3)
r	Radius (m)
r_i	Inner Radius (m)
r_o	Outer Radius (m)
R	Resistance (Ω)
R_{coil}	Coil Resistance (Ω)
R_{grid}	Grid Resistance (Ω)

s	Displacement (m)
S	Reluctance ($Ampere - Turns Wb^{-1}$)
S_i	Reluctance of Segment i ($Ampere - Turns Wb^{-1}$)
t	Time (s)
T	Torque (Nm)
u_i, v_i, w_i	x, y and z Components of Velocity at a point i (ms^{-1})
v	Volume (m^3)
v_t	Translator Velocity (ms^{-1})
V	Voltage ($Volts$)
V_{xy}	Pixel value at x,y ($dimensionless$)
V_s	Fluid velocity in the Axial direction in polar form (ms^{-1})
W	Load (N)
W_D	Force Applied to Achieve a given rate of change of h (N)
W_k	Load at a point k (N)
x_c, y_c	Interpolated centre coordinates ($Pixels$)
x_w, y_w	Weighted pixel coordinates ($Pixels$)
$z(s), Z(s)$	Force per m in Hybrid Bearings (N)

Abbreviations

CCD	Charged Couple Device
CFD	Computational Fluid Dynamics
EMF	Electromotive Force
FEA	Finite Element Analysis
FPA	Focal Plane Array
FR-MMA	Fast-Replace Multi-Machine Architecture
MMA	Multi-Machine Architecture
MMF	Magnetomotive Force
O&M	Operation & Maintenance
RMS	Root Mean Square
SFR-MMA	Segmented Fast-Replace Multi-Machine Architecture
SiFR-MMA	Simplified Fast-Replace Multi-Machine Architecture

List of Figures

1.1	Global Wave Resource ^[44]	7
1.2	”Useful” Wave Resource ^[44]	7
1.3	Sea-bed Mounted Linear Generator	9
1.4	Hydraulic Linear Power Take-off Arrangement	10
1.5	Original Concept AWS Linear Generator Design ^[27]	13
1.6	The Air-Cored linear generator (2.5.2)	15
1.7	The Variable-Reluctance linear generator (2.5.2)	15
1.8	The Transverse-Flux linear generator (2.5.2)	15
2.1	Electromagnetic Induction	20
2.2	Motor Force	20
2.3	Eddy Currents in a Conductor	21
2.4	Example of a Flux Path within a C-shaped Flux Carrier	21
2.5	Appropriately Dimensioned Breakdown of Flux Path	23
2.6	Saturation Curves for Magnetic Materials. (See Table 2.1)	27
2.7	Opposing Permanent-Magnet Arrangement	30
2.8	Displacement-Force Curve for Opposing Magnets	31
2.9	Distribution of conductors in a square packed coil	33
2.10	Wire Packing Arrangements	34
2.11	Elliptical Motion and Depth Effects of Waves ^[40]	35

List of Figures

2.12 Primary Modes of Wave Energy Capture	36
2.13 Pierson-Moskowitz Spectra for differing wind speeds	37
2.14 Example of Air-Cored Topology	42
2.15 Possible Arrangements of Magnets & Translator	43
2.16 Variable Reluctance Generator Configurations	43
2.17 Example of Magnetic Short Circuit (shorted field shown in red) . . .	44
2.18 Power Generation Equivalent Circuit	46
2.19 Constant Inductance Simulation of Variable Reluctance Output . . .	47
2.20 Potential Linear Transverse Flux Generator	49
2.21 Schematic Rotary Transverse Flux Machine with Flux Paths	49
2.22 Hybrid Transverse Flux and Variable Reluctance Machine	50
2.23 Basic Hydrostatic Bearing Circular Step Bearing	52
2.24 Load/Clearance Curves	56
2.25 Fluid Compression Plates	58
2.26 Compressed Annulus	58
2.27 Vibration in a single hydrostatic bearing supporting a direct load . .	60
2.28 Self-Compensating Bearing + Fluid Direction Markers	62
2.29 Core of a Vane Pump	64
2.30 Illustration of basic piston pump mechanism	65
2.31 Basic Components of a Swash Plate Pump	65
2.32 Log-Log Chart of Flow-Rate against Pressure for a Perfect Pump . .	67
2.33 Loaded Beam Supported at 2 Points	72
2.34 Moment about x involving W_1	73
2.35 Moments about x involving W_1 & W	73
4.1 Example Arrangement of Bearings for a Linear Generator ($n = 5$) . .	90
4.2 Test Beam Layout	94

List of Figures

4.3	Deflection of an Arbitrary Beam Supported at 2, 3 and 5 Points . . .	95
4.4	Variable Reluctance Generator Cross-Section	96
4.5	Flawed Bearing Arrangement (B displaced from ideal position) . . .	98
4.6	Load/Displacement Plot	99
4.7	Layout of Test Case Generator	112
4.8	Loaded Beam	114
4.9	Deflection of a 5-point supported beam due to an external load. . .	115
4.10	Net Force/Displacement Plot	115
4.11	Net Force/Power Plot	116
4.12	Partially Clogged Filter Plate with Fluid-Flow	118
5.1	2-Stage Bearing	122
5.2	1 st Stage System	124
5.3	Second Stage System	125
5.4	MMA System	128
5.5	Principle of FR-MMA	132
5.6	An Example of Self-Supporting FR-MMA	132
5.7	Example FR-MMA Module	134
5.8	Classic Tubular Air-Cored Arrangement	135
5.9	Collection of Alternative Coil Arrangements	136
5.10	AWS Translator with Bed of Magnets During Construction ^[27] . . .	136
5.11	AWS Stator Section with Coils Visible ^[27]	137
5.12	SFR-MMA Machine Schematic	139
5.13	SFR-MMA MMA Cell	140
5.14	Bayonet Ring Support	145
5.15	Basic Concept SiFR-MMA 2-Stage Module	147
5.16	Basic Concept SiFR-MMA Generator Module	147

List of Figures

5.17 Exploded View of Complete Generator	147
5.18 Modules inserted into welded support frame	148
5.19 Simple Multi-Purpose Module	151
5.20 Simple Multi-Purpose Modules Used for Rotational Generator . . .	152
5.21 Constructed Multi-Purpose Module	153
5.22 Lateral FR-MMA Concept Module	154
5.23 Lateral Module Translator	155
5.24 Example of Lateral Modules in a Rotational Device	156
5.25 Overall Operation of Positional Modules & Complete Generator . .	159
5.26 Generator Schematic	160
5.27 Close-up of bearing group	163
5.28 Close-up of bearing group	166
5.29 Concept Generator Module	168
5.30 Module and Translator Showing Motions	168
5.31 Close-up of magnet air-gap	170
5.32 Basic C-Core Arrangement & Onion Skin Image of Deformed Shape	171
5.33 Translator Section with Bearing Paths	175
5.34 Support Frame	175
5.35 Back Iron/Flux Carrier	177
5.36 Hydrostatic Bearing Insert	178
5.37 Translator Section	179
5.38 Cross-section of a Variable Reluctance Generator Head	181
5.39 Triangle wave Approximated with a 4-term Fourier Series	182
5.40 Characteristic EMF Output Profile	183
5.41 Translator Position and Instantaneous Flux	184
5.42 Generated EMF	184

List of Figures

5.43	Output Frequency	185
5.44	Concept Re-Circulating Bearing	185
5.45	Jet Bearing Concept	187
5.46	Jet Bearing inc. CFD modelled flows	188
5.47	2-Jet Recirculating Flow	188
5.48	2-Jet Additional Flow	188
5.49	4-Jet Recirculating Flow	189
5.50	4-Jet Additional Flow	189
5.51	2-Jet Pressure Distribution	189
5.52	4-Jet Pressure Distribution	189
5.53	2-Jet Velocity Vectors	190
5.54	4-Jet Velocity Vectors	190
5.55	Hybrid Bearing Frame	190
5.56	Example of Conductors Embedded in Bearing material	194
B.1	Complete Concept 2-Stage Generator	223
B.2	Complete Concept MMA Module	224
B.3	Exploded View of Concept MMA Module	225
B.4	3-Section FR-MMA Module in a Partially Expanded State	226
B.5	SFR-MMA Tower with Faulty Module Ejected	227
B.6	Concept SFR-MMA & SFR-2Stage Arrangement	228
B.7	SFR-MMA Module & Concept Empty Mounting	228
B.8	Lateral Module Superstructure & Shown in Cut-away	229
B.9	Final Design for Proof of Concept Generator	230
B.10	Linear-Rotary Generator with Sections	231
C.11	Schematic Device Arrangement	233
C.12	Perspective Projection	235

List of Figures

C.13 Interpolation Method	238
C.14 Flood Selection Method	240
C.15 Multi-Area Flood Selection Method	241
C.16 Range Point Discrimination	243
C.17 Motion Vector Point Discrimination	243
C.18 Original Concept Design of Device	245
C.19 Comparison of Experimental & Practical Data	247

List of Tables

2.1	Materials for Figure 2.6	28
2.2	Wire Packing Arrangement Factors	35
4.1	Support Reaction Forces	94
4.2	Extension to Table 4.1 including power and offset	101
4.3	Additional parameters required for Table 4.2	101
4.4	Mechanical Bearing Data Table	103
4.5	Test Case Parameters	113
4.6	Loads, Deflections and Total Power Consumption	114
4.7	Loads and Hydrostatic Offsets	116
5.1	Cases 1-3	160
5.2	Cases 4-6	161
5.3	Weighting values for stability function	163
5.4	Example Stability Values	163
5.5	Magnet Classifications	171
5.6	Example Variables	173
5.7	Output Profile Parameters	183

Acknowledgements

I would like to give thanks for the support I have received from my family, my friends and my supervisors, without whom completion of this work would not have been possible. This work is dedicated to my family and to hopes of a cleaner, brighter tomorrow.

Chapter 1:

Introduction

Chapter 1: Introduction

The primary aim of this research was initially to investigate the possibility of using hydrostatic bearings as an alternative to existing mechanical bearing technologies in direct drive linear generators. The main application being the design of flooded linear generators for wave energy applications, potentially using hydrostatic bearings fed with sea water.

This initial work led onto new approaches to the design of linear generators, including the introduction of flexible component design. This had implications for all aspects of design and construction of the generators, therefore the focus shifted from purely the viability of linear generators to the overall economic viability of the generators.

The final aim of the research is to improve the economic viability of linear generator technology to aid in the development and deployment of wave energy devices and any other devices that currently employ mechanisms to convert linear to rotational motion.

1.1 Renewable Energy

Renewable energy is going to play a big part in the future of power generation. Renewable energy exists in a number of forms, and most are derived from the solar energy in some way.

- Solar Power
 - Photo-voltaic cells
 - Solar-Thermal conversion

Chapter 1: Introduction

- Wind Power
 - Vertical Axis
 - Horizontal Axis
- Wave Power
- Tidal Power
 - Vertical Axis
 - Horizontal Axis
 - Venturi
 - Oscillating Hydrofoil
- Geothermal Power
- Hydroelectricity

With the exception of Photo-voltaic cells all of the other power generation techniques make use of electromagnetic power take-off devices (PTO). The majority of these devices require rotational electromagnetic devices, except for wave power which, depending on the type of wave power, uses both rotational and linear direct drive generators.

Renewable energy has been making significant growth in recent years, exceeding both nuclear and oil in the area of electrical power generation^[43]. However at present this growth has only really been seen in hydropower such as hydroelectric dams^[43]. The exploitation of other renewable resources have improved over the same period but by a far smaller degree. It is predicted that by 2050, renewable

energy will constitute 60% of european energy generation with 20% nuclear and the remainder being fossil fuels^[40].

1.1.1 Limitations of renewable power

Ideally, with sufficient resource exploitation, renewable energy would be able to supply all the power to the planet. This would be the final goal of renewable energy research, however as it is likely a long way off. With currently available technologies and the current economic climate it is likely that renewable energy sources will need to be supplimented with fossil fuel and nuclear technologies to be viable for some time to come.

Although the eventual goal of renewable energy is to replace other sources of energy, the current level of power usage is too high for a complete transfer to renewable sources however if a big enough reduction in the use of fossil fuels can be achieved then carbon emissions could be reduced to a sustainable level.

In either case to make renewable energy sources viable they must operate at very high efficiencies and become relatively inexpensive. At present, renewable energy, through lack of exploited resource and efficiency, is only supplying a tiny fraction of the power demand around the world, and that demand is growing rapidly.

To give renewable energy the chance to make a difference a focus must not only be made on the generating technology itself but also the devices that it is powering. If efficiency is increased at both ends then supply would increase and demand would drop. Additionally most renewable energy sources are dependent on very localized resources, wind turbines generally need to be on hills, tidal devices need to be high current areas, solar arrays need lots of sunshine

Due the limitations in how much energy they can capture, wind turbines and solar panels need to be large in order to generate reasonable quantities of power. In a lot of cases there is resistance from people around sites for the these devices, amid concerns about spoiling the natural landscape or concerns about noise and safety. These must also be addressed if renewable energy is to be accepted en-mass.

1.2 Wave Power

Oceanic waves carry a huge amount of energy, the waves around the world contains an estimated $2\text{TW}^{[44]}$ of accessible energy in deep water waves. Technologically wave power is among the renewable energy technologies that are in its infancy. Most wave energy devices are designed to operate in shallow water because of the way waves work in shallow water and the complexities of deploying wave energy devices in deep water.

It may seem easy to put a buoy in the water and take power from it as it bobs up and down but there are numerous additional effects that need to be considered. From an ecological standpoint, by taking energy from the water using the device there is a change in the energy reaching nearby coastlines, this in turn has an effect on the eco system in those areas. There are also concerns about tourism in some areas, for example those that rely on surfing or watersports in general. The change in the wave behaviour may drive tourists to move to other sites causing a drop in revenue or damage to other sites.

1.2.1 History

The first known patent for a device to capture energy from ocean waves dates from 1799^[9]. The first practical wave power application was constructed in around 1910 to light and power a house, potentially the first oscillating water column device^[22]. Since then numerous designs have been created and tried, perhaps the most famous being Salters Duck^[32], invented by Stephen Salter at University of Edinburgh in 1973. A plethora of devices have been designed and tried in recent years, probably the most well known recent device is Pelamis^[45,18] which operates as a wave attenuator.

1.2.2 Resource Availability

Wave power resources are scattered all over the world, the greatest sources of wave energy can be seen in Figure 1.1. The orange/yellow areas show the highest levels of energy. As can be seen the greatest resources are in deep open water. Deploying devices in these areas present numerous challenges both in deploying the devices and connecting them to shore.

Although there is ample wave resource worldwide, due to restrictions with placement and feasibility of routing power lines, the areas that have a useful wave resource are pretty small and the total available power is substantially less. Figure 1.2 shows the how useful a particular wave resource is around the world, that being a wave resource that can be readily exploited coupled with the population density. As an example Japan has lots of waves and a very high population density

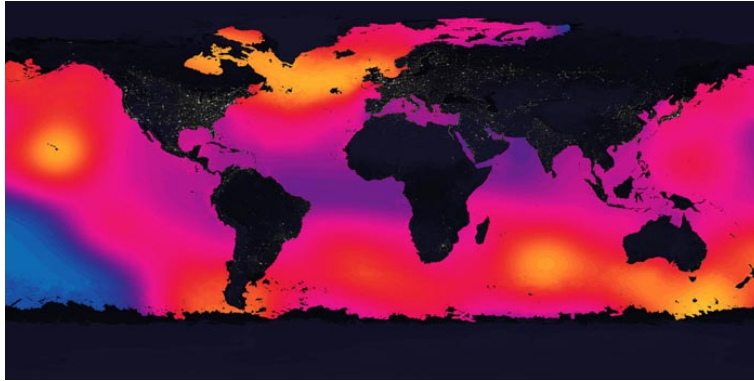


Figure 1.1: Global Wave Resource^[44]

therefore that wave resource would be very useful, and the same could be said of Americas eastern seaboard.

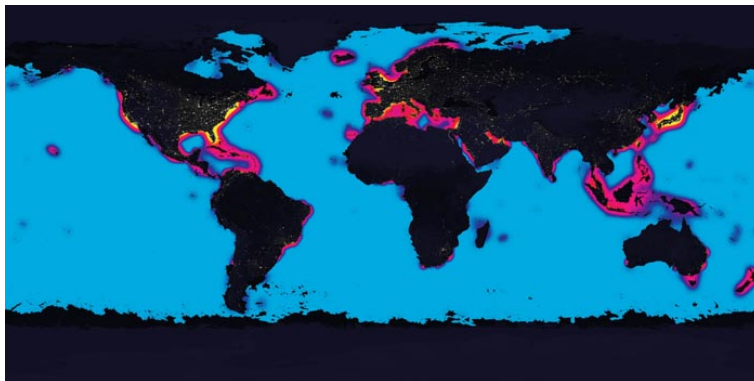


Figure 1.2: "Useful" Wave Resource^[44]

1.2.3 Types of Resource

Wave energy devices are often classified by the area they will be placed in and the type of wave motion they are designed to respond to. Some types of devices are more suited to certain areas than others. Numerous designs have been proposed that sit close to shore, working in relatively shallow water. Comparatively few are

proposed for deep water, hence the problems with extracting energy from those waves found in the middle of the oceans. The twin problems of mounting devices on the seabed and carrying the extracted energy back to shore make deep water devices less desirable from an economic standpoint, however in the future these sites might need to be considered since they have a large proportion of the available wave energy.

1.3 Linear Generators

1.3.1 What are linear generators?

A linear generator is device that is designed to extract energy from a any linear motion or series of linear motions. Most current research is directed towards their use in wave generators such as shown in Figure 1.5.

There are many ways to create a linear generator, ranging from hydraulic systems to direct drive electromagnetic devices. In general the term linear generator applies to a direct drive device rather than a composite hydraulic arrangement such as the one shown in Figure 1.4.

A direct drive linear generator uses electromagnetic affects to generate electricity directly from a linear motion. There are numerous devices that can be used for these applications some using field windings and others using permanent magnets. Either way a linear generator consists primarily of a translator and stator and as the translator moves past the stator it induces and EMF.

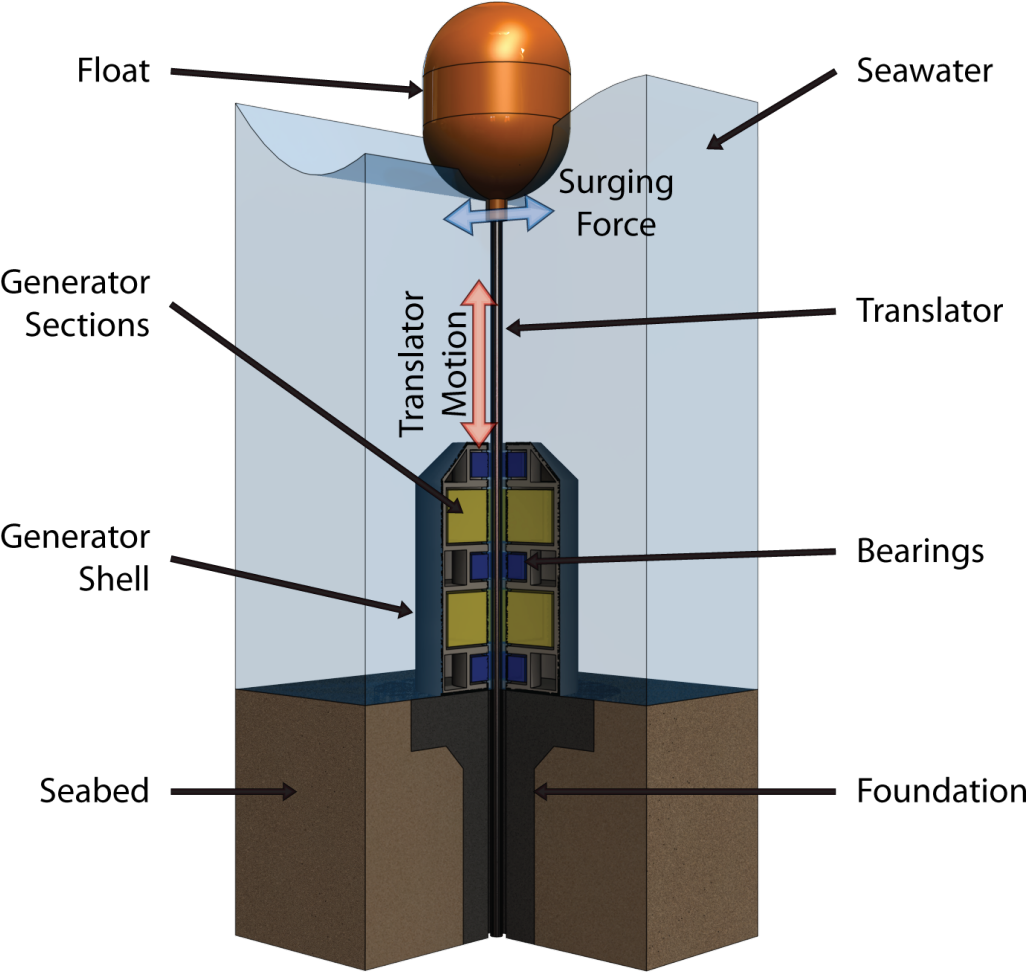


Figure 1.3: Sea-bed Mounted Linear Generator

1.3.2 What advantage do they offer?

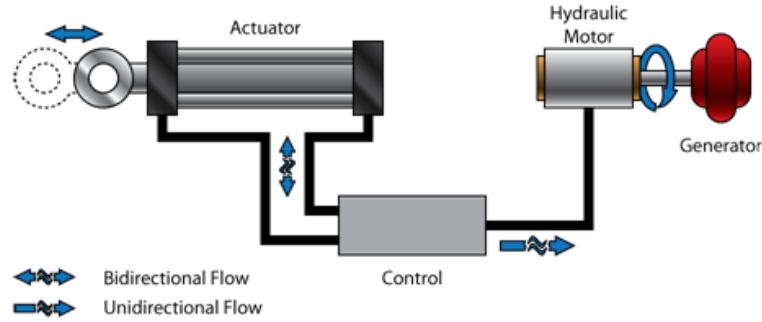


Figure 1.4: Hydraulic Linear Power Take-off Arrangement

In any standard linear power take-off system a linear actuator, such as a piston is connected to a fluid control mechanism which provides a flow to a device such as a hydraulic motor which is in turn is connected to a generator. In any system the efficiency is defined as^[14];

$$\eta = \frac{P_{out}}{P_{in}} \quad (1.1)$$

Where P_{out} is the power reaching the generator, P_{in} is the incident power of the system, in the case of Figure 1.4 the power being absorbed at the actuator, and η is the efficiency. Therefore the power transferred to the generator is of the form of;

$$P_{out} = \prod_k^n \eta_k P_{in} \quad (1.2)$$

Where η_k is the efficiency of specific system component. In the case of a hydraulic system such as the one in Figure 1.4 is composed of 3 components all of which cause an efficiency drop. A direct drive linear generator is only one device and

Chapter 1: Introduction

therefore, if designed correctly, then the overall efficiency is much greater than a hydraulic equivalent;

$$P_{out} = \eta P_{in} \quad (1.3)$$

$$\eta > \prod_k^n \eta_k$$

Linear generators, in theory, would also help to improve the reliability of the system since there is only one mechanism to fail.

In systems such as internal combustion engines the linear motion of the pistons is used to drive a rotating shaft by means of hinged rods. The effect of this method of power transfer is that some of the power is lost as a result of the changing angle of the rods. Although controlling such an engine with purely linear devices would be far harder, in theory linear generators could be attached directly to the pistons without the rods reducing the power losses. In this way linear generators could be applied to many applications outside their current remit.

1.3.3 What are the problems?

Direct drive generators may be the future of wave energy, however the hefty price tag associated with them and maintaining their potentially high efficiencies are major problems yet to be overcome. Much of the expense involved comes from the number of magnets in the design, in the case of permanent magnet based machines the cost of the magnets themselves and in purely electromagnetic machines the cost of the copper in the field windings.

Chapter 1: Introduction

From an economic point of view, the technology must enter the market at a cost that makes it economically viable when compared with other sources of energy in order for it to be taken seriously and be mass produced. Having a generator that costs five times more whilst delivering five times less would never be viable and as such the drive must be to reduce the cost of mass producing these devices whilst maintaining their high efficiencies. The precise nature of linear generators adds to the costs since they require precisely controlled clearances along their length to function correctly. Maintaining separations of a few millimetres on devices a few metres long is far from easy, especially when the magnets within the machine encourage the components to move away from their proper positions.

Additionally there is the problem of maintenance, wave devices need to operate in an extremely harsh environment, suffering from corrosion and being battered by heavy weather. They are hard to reach and access because of the same conditions they must be designed to withstand. Therefore, designing devices that can be easily repaired, or replaced, and ones that reduce the need for heavy equipment and extended periods at sea should also be a major focus. Exposed metal components, including any permanent magnets, must be protected from the sea, incurring more expenses and increasing construction lead times.

Even without the savage conditions at the sites where these devices will operate, current designs are subject to large internal stresses, putting great demands on the components within. To maintain the efficiency of the device the bearings that support the moving parts become increasingly important, and to further complicate things, bearings that work well in air often become less efficient when submerged in water.

Chapter 1: Introduction

All in all, there are a lot of problems to be faced if linear generators are to rise to the challenge of becoming the dominant technology extracting power from the sea.

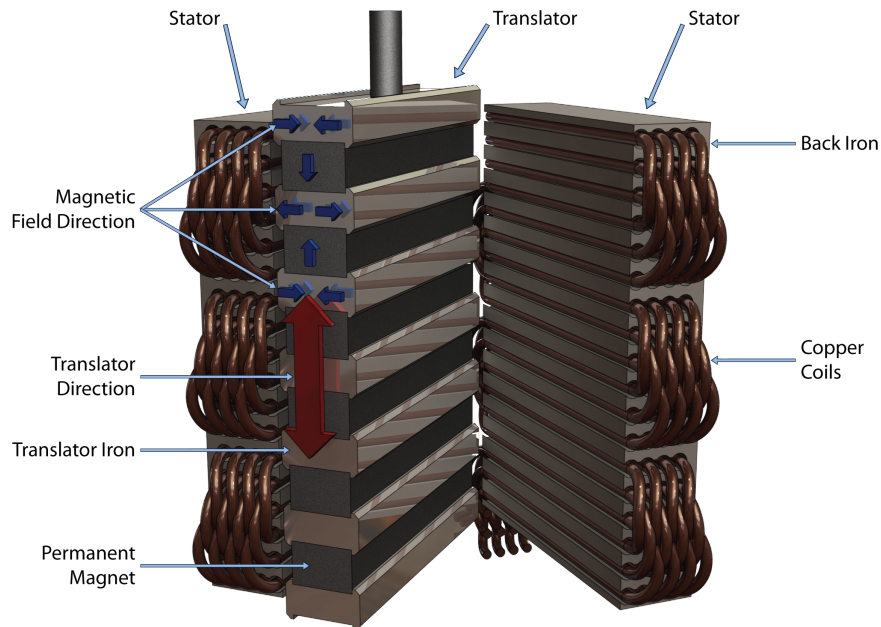


Figure 1.5: Original Concept AWS Linear Generator Design^[27]

To date, only a few linear generators have been deployed at sea and they have generally been sealed units. Oregon State University is currently exploring an off-shore wave farm utilising linear generator technology^[29], and the first AWS used a permanent magnet linear generator devices by Dr. Henk Pollinder.^[27] The design shown in Figure 1.5 is one of the designs considered for the AWS. Another version of this design discarded the back iron and worked as an Air-cored design. See Section 2.5.2.

1.4 Why this work?

In 2008 the total worldwide energy consumption was estimated at $474 \times 10^{18} \text{J}$ ^[42]. This is equivalent to a continuous global power consumption of 15TW ^[42]. This includes all forms of power consumption, including domestic, industrial, transport, etc., not just electrical demand. Even if it were possible to extract all available wave energy available it would make up only a fraction of the total. As such it is necessary to make the generators as efficient, reliable and cheap as possible to aid in their deployment and the capture of wave energy.

Originally the focus of this research was simply the bearings and looking at possibly replacing traditional bearings with hydrostatic bearings, however the focus has widened to include all aspects of generator design and a possible shift in thinking about linear generator design.

The primary areas of study have looked at the viability of hydrostatic bearings for this application and methods of making linear generators more economically viable for use in the mass market. The primary focus for their use is still wave energy but as the work progressed some aspects appeared to be applicable to other areas of power generation as well.

Key linear generator topologies that have been considered during this work are shown in Figures 1.6 to 1.8.

It should be noted that much of the advantage of the transverse flux machine is lost when applied to modular systems, such as those detailed herein.

For this work the assumed generator structure is similar to that shown in Figure 1.5. A translator, either round or flat, passes through the centre of the machine

Chapter 1: Introduction

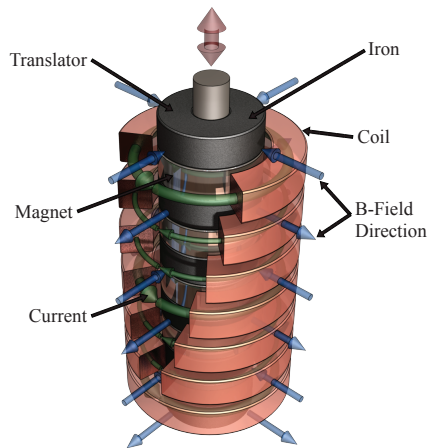


Figure 1.6: The Air-Cored linear generator (2.5.2)

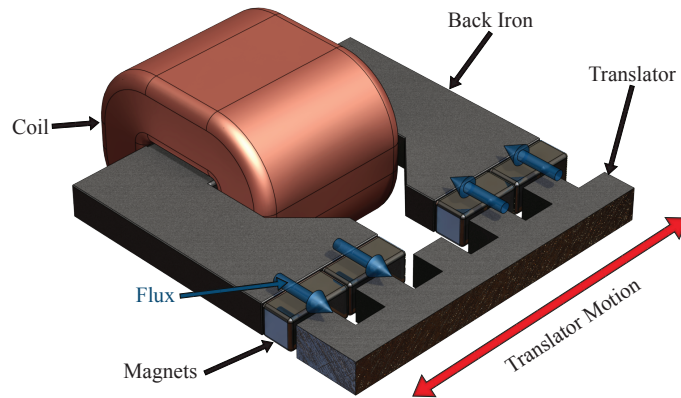


Figure 1.7: The Variable-Reluctance linear generator (2.5.2)

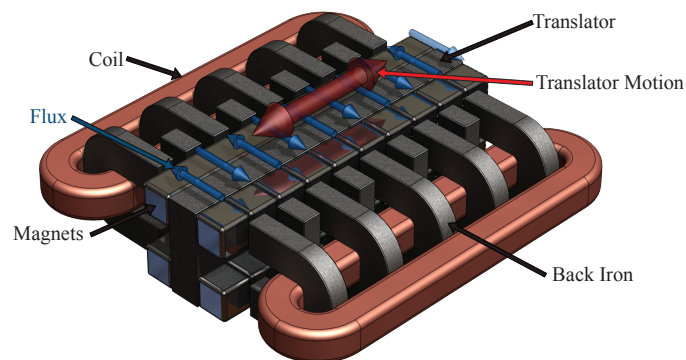


Figure 1.8: The Transverse-Flux linear generator (2.5.2)

and is supported on a series of bearings. Although Figure 1.5 shows a generator with 3 sets of bearings this is just for illustration and the merits of different bearing numbers is discussed in the investigation in Chapter 4. Between the bearings are generator sections and the structure of these sections is the major focus of this research.

1.5 Thesis Structure

The following sections will outline the theory and concepts that make up this research.

Section 2 will cover the basic theory for electromagnetism, magnetic circuit theory, hydrostatic theory and the basics of wave motion and theory. Section 2 will also explain the various topologies of linear generators and introduce some new work for hydrostatics. This should provide adequate grounding and reference for the rest of the document.

Section 3 covers the methods of assessment and what is being looked for in each of the concepts that has been explored.

Section 4 contains the theoretical assessment of the behaviour of a basic, rigidly structured/non-flexible, linear generator for a given generating topology. This includes estimations of internal forces, and deflections in the translating components.

Section 5 introduces all the concepts that have been explored during this research, along with their origins and reasons for pursuing each concept. As well as concepts relating directly to generator design a couple also deal with bearing design and power generation.

Chapter 1: Introduction

Section 6 discusses the potential real world impacts of this work and the concepts there in, exploring the economic and material advantages offered by generators based on the final concepts explored.

Section 7 contains the conclusions and opportunities for future work based on these concepts.

Chapter 2:

Literature

2.1 Foreword

During the initial review of material on hydrostatic bearings it became apparent that although they are mentioned in a lot of documents, there is very little material making real world comparisons between analytical and practical data, and even less dealing with the dynamic loading of such bearings. Similarly there are few references towards magnetic circuit theory even within Hopkinson's collected papers. As such, although the theory should be adequately explained here for the work that has been done, in places references may not be available.

2.2 Magnetic Theory

Magnets are key to numerous modern applications. The majority of generators operate using magnetic principles. Most people will be aware of the properties of magnets as well as where they can be found but few know how they are produced and the finer points of their use.

The effect a material has on a magnet varies with the material, however its ability to carry a magnetic field is known as the permeability. This is most often represented as the relative permeability, μ_r , which is the permeability compared to the permeability of free space, μ_0 .

The key to magnetic generators is to create a changing magnetic field from which energy can be extracted. This can be done by moving magnets past metal, metal past magnets or even metal past metal in the right circumstances.

2.2.1 Magnetic Basics

The key to the operation of most generators is electromagnetic induction. As a conductor moves through a magnetic field a voltage is induced in the conductor. Also if a conductor is subject to a changing magnetic field then a voltage is induced. If a current-carrying conductor is subject to a magnetic field it will experience a force.

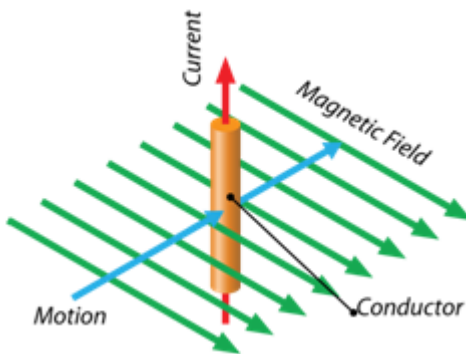


Figure 2.1: Electromagnetic Induction

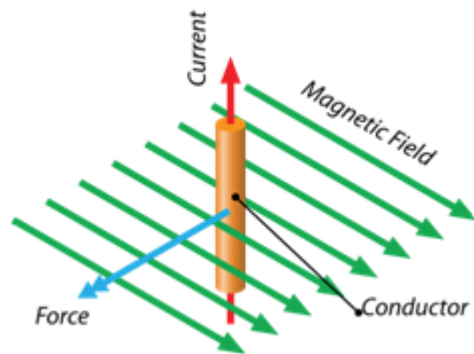


Figure 2.2: Motor Force

Therefore, if a magnet is moved past a coil of wire, in the correct manner, a voltage will be induced due to the changing magnetic field. At the same time, the induced voltage will drive a current in the conductor (assuming a load is present) and the conductor will experience a force related to that current.

The most common form of an electromagnet is a coil. The rotating current in the coil produces almost parallel magnetic field lines through its centre. This process is not one way, a straight field line passing through a conductive medium (except diamagnetic materials) will produce a rotating current. These currents, called eddy currents, are self contained, existing freely within the conductor. Although generally not very large, the eddy currents dissipate energy and therefore cause additional losses.

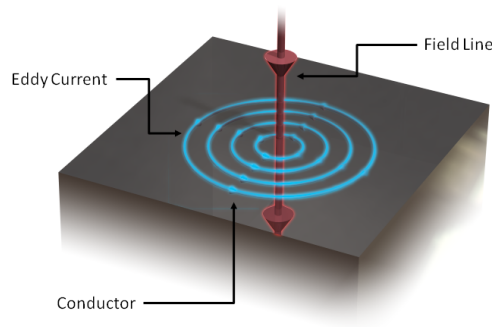


Figure 2.3: Eddy Currents in a Conductor

2.2.2 Magnetic Circuit Theory

Magnetic circuit theory^[12] equates magnetic field paths to electrical circuits. The laws governing these circuits are analogous to Kirchoff's Laws in electrical circuits. The driving potential in these circuits is the Magneto-Motive-Force (MMF) in place of Electro-Motive-Force (EMF), and the resistance of circuit paths is replaced with reluctance. The current in a magnetic circuit is known as flux and is represented as φ .

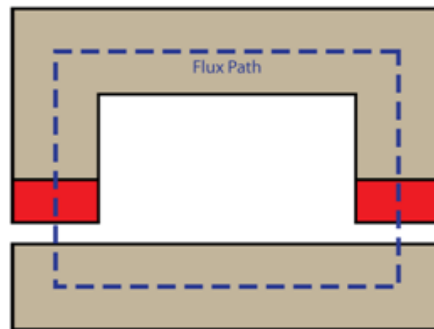


Figure 2.4: Example of a Flux Path within a C-shaped Flux Carrier

The MMF is defined as;

$$\text{MMF} = \oint H dl \quad (2.1)$$

Chapter 2: Literature

In practical terms this would be;

$$\text{MMF} = \sum_{i=0}^n H_i l_i \quad (2.2)$$

Where l is the length of a path section and H is the magnetic field strength. The field strength, H , can be related to the B-field through;

$$B = \mu_0 \mu_r H \quad (2.3)$$

and magnetic flux expressed as;

$$\varphi = BA \quad (2.4)$$

where A is the cross-sectional area of the flux path. The flux can therefore be derived as;

$$\varphi = \mu_0 \mu_r H A \quad (2.5)$$

and H as;

$$H = \frac{\varphi}{\mu_0 \mu_r A} \quad (2.6)$$

Reluctance is the equivalent to resistance in this analogy. As a result the expression for the total resistance of a circuit is very similar;

$$\text{MMF} = \varphi S \quad (2.7)$$

where S is the total reluctance of the circuit. By replacing S with the summation

Chapter 2: Literature

of S values for each point in the circuit , we get;

$$\text{MMF} = \varphi \sum S \quad (2.8)$$

$$\therefore \varphi \sum_{i=1}^n S_i = \sum_{i=1}^n H_i l_i$$

$$\therefore S_i = \frac{H_i l_i}{\varphi} = \frac{l_i}{\mu_0 \mu_{r_i} A} \quad (2.9)$$

Therefore, for each path section, reluctance can be calculated and by using the total reluctance, the flux can be calculated.

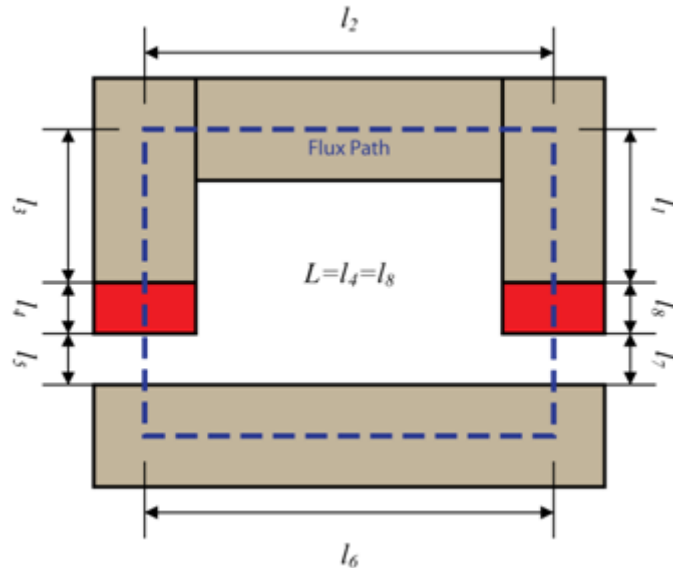


Figure 2.5: Appropriately Dimensioned Breakdown of Flux Path

At this point, one very important fact becomes apparent. The reluctance of the path section is inversely proportional to relative permeability of the medium that path is made of, much like conductivity in electrical circuits. The higher the permeability, the more easily it can conduct a magnetic field. As such, the best materials

Chapter 2: Literature

for constructing magnetic circuits are materials with high relative permeabilities such as Iron.

Permanent magnets are assumed to have a relative permeability of 1, as does air. This is also key as it indicates that, since air and permanent magnets are far less conductive to magnetic fields than Iron, if the rest of the circuit is composed of Iron, the size of magnets and air-gap is extremely important.

A complete circuit would be expressed as something like this;

$$\text{MMF} = \varphi \sum_{x=1}^n S_x = \varphi[S_1 + \dots + S_n] \quad (2.10)$$

Since the relative permeability of Iron is so great compared to air, the reluctance values for these paths are often forgotten because they make a negligible contribution to the overall reluctance.

As a result a typical circuit equation might be;

$$\text{MMF} = 2\varphi[S_{\text{magnet}} + S_{\text{air-gap}}] \quad (2.11)$$

This can be easily rearranged to give the flux within the circuit.

It is important to note that there is a maximum flux that can be carried by any particular circuit. In Iron, for example, the maximum b-field is about 1.2T because Iron begins to become saturated at this point and it becomes increasingly difficult to increase the flux within the circuit beyond this point.

The flux is important because a changing flux is required to generate an EMF. In

Chapter 2: Literature

its simplest form;

$$\varepsilon = N \frac{d\varphi}{dt} \quad (2.12)$$

Where N is the number of turns on the coil in which the EMF is being induced.

The MMF can be generated in a couple of ways, the first is electromagnetically.

This can be used with generators however much work is currently being done on the second method, which utilizes permanent magnets.

For an electromagnetic coil the MMF is;

$$\text{MMF} = NI \quad (2.13)$$

where N is the number of turns and I is the current passing through the coil, and for a permanent magnet the MMF is expressed as;

$$\text{MMF} = B_{rem} \frac{l_{magnet}}{\mu_0} \quad (2.14)$$

Where l_{magnet} is the length of the magnet in the magnetic path direction, and B_{rem} is the remnant magnetic field of the magnet.

In permanent magnet generator arrangements the MMF would be;

$$\text{MMF} = B_{rem} \frac{l_{magnet}}{\mu_0} - NI \quad (2.15)$$

since the rules of induction state that the induced current will apply a magnetic field in opposition to the driving field.

Chapter 2: Literature

Therefore a complete permanent magnet circuit, with no coil present, would look like;

$$2B_{rem} \frac{l_{magnet}}{\mu_0} = 2\varphi[S_{magnet} + S_{air-gap}] \quad (2.16)$$

Through rearrangement of the above an equation can be derived that can predict the air-gap required in order to achieve a certain circuit flux.

$$\varphi_{rem} = \varphi \left[\frac{l_{magnet} + l_{air-gap}}{l_{magnet}} \right] \quad (2.17)$$

(See derivation A.7)

By substituting a target flux, φ_{target} , into the equation, the air-gap for a given material and type of magnet can be found.

$$\left[\frac{B_{rem} - B_{target}}{B_{target}} \right] l_{magnet} = l_{air-gap} \quad (2.18)$$

(See derivation A.8)

If the air-gap exceeds the $l_{air-gap}$ value then the B-field in the circuit will drop below the target level. The choice of air-gap affects the design of the generator, having profound implications for construction tolerances.

According to the circuit theory, by varying the cross-sectional area of the circuit path it should be possible to vary the B-field within it for a given flux. The effect on the flux should be limited if the B-field is kept below the saturation point. If it is desirable to saturate a given part of a circuit, then reducing its area will force it to saturate at a lower flux.

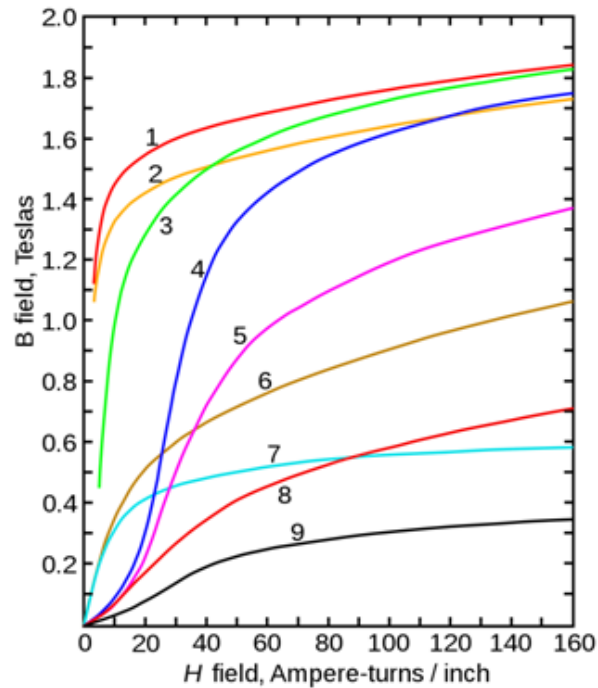


Figure 2.6: Saturation Curves for Magnetic Materials. (See Table 2.1)

Using the example of material 3, from Figure 2.6 and Table 2.1, the B-Field is predictable during the linear slope. In this region the B-Field varies linearly with the magnetizing H-Field. Once the B-Field rises much above 1.0T it no longer varies linearly. As a result the necessary air-gap cannot be predicted by the previous relationship and a function for the saturation must also be included.

If a greater amount of flux is required then cross section area of the flux carrier can be increased in accordance with;

$$\varphi = BA \quad (2.19)$$

However any increase in area has a corresponding increase in mass and will also affect the generating potential by increasing the length of wire used in any coils.

No.	Material Type
1	Standard Sheet Steel Annealed
2	Silicon Sheet Steel Annealed Si 2.5%
3	Soft Steel Casting
4	Tungsten Steel
5	Magnet Steel
6	Cast Iron
7	Cast Cobalt
8	Magnetite (Fe_2O_3)

Table 2.1: Materials for Figure 2.6

Also, because of the way magnetic fields distribute themselves through a material it there may be a limit to the effect of increasing the area.

2.2.3 Attractive Forces

Forces attracting the iron components to the magnets are a key issue in generator design. The force of attraction between them is determined by the B-field permeating the gap between them, which is linked to the flux. From equation (2.4) we can calculate the B-field as;

$$B = \frac{\varphi}{A} \quad (2.20)$$

This can then be applied to find the attractive forces using the following equation^[43];

$$\sigma_T = \frac{B^2}{2\mu_0} \quad (2.21)$$

The result of this is;

Chapter 2: Literature

$$\sigma_T = \frac{\left(\frac{\varphi}{A}\right)^2}{2\mu_0} = \frac{\varphi^2}{2A^2\mu_0}$$

$$F_T = A\sigma_T = \frac{\varphi^2}{2A\mu_0} \quad (2.22)$$

Alternatively if the magnets are looked at in terms of magnetic poles then it is generally accepted that two attractive poles will experience a force in line with;

$$F = \frac{m_a m_b}{4\mu_0 h^2} = M_m \frac{1}{h^2} \quad (2.23)$$

where for this case m_a and m_b are the pole strengths and h is the magnetic separation.^[28]

2.2.4 Opposing Magnets

As the translator moves from the central position the magnetic forces increase and act to pull the translator further out of position. However since there are forces from 2 opposing magnets they force from an individual magnet is reduced. As a result the force on any supporting bearing is reduced.

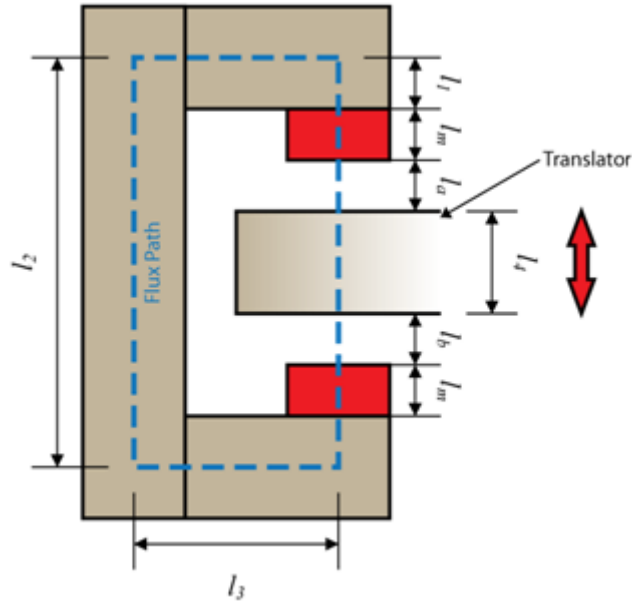


Figure 2.7: Opposing Permanent-Magnet Arrangement

2.3 Generator Theory

2.3.1 Magnetic Forces

While a generator is running there will be changing forces applied to it by the interactions of the magnets and internal components. In the case of the magnetic shear stress, $\sigma_S^{[43]}$, this is related to the power capture of the device.

$$\sigma_S = BK \quad (2.24)$$

The transverse magnetic stresses, $\sigma_T^{[43]}$, are less desirable as they can drag the internal components of a generator off centre leading to damage or failure.

$$\sigma_T = \frac{B^2}{2\mu_0} \quad (2.25)$$

Chapter 2: Literature

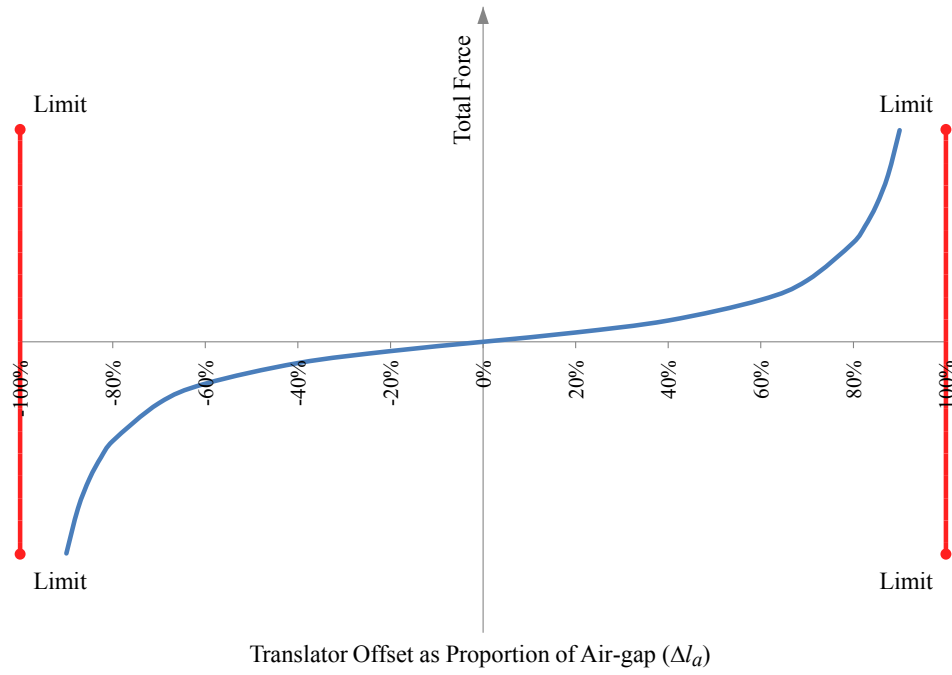


Figure 2.8: Displacement-Force Curve for Opposing Magnets

The magnetic shear stress is the most important from a power generation point of view, since there is a direct connection between the magnetic shear stress and the amount of power extracted by the device.

$$F_S = \sigma_S A \quad (2.26)$$

$$P = F_S v \quad (2.27)$$

2.3.2 Power Generation

The power output of the generator depends on the number of turns in the power take-off coils, the cross-sectional area of the conductor, the material used (generally copper) and the average path length of the conductor.

$$R_{coil} = \frac{\overline{L_P} N \rho_r}{A_x} \quad (2.28)$$

$$P = \frac{V^2}{\sum R} \quad (2.29)$$

As a first approximation of the power output it could be assumed that the grid it is attached to is a near infinite collection of parallel devices being fed from a common source. As such;

$$\begin{aligned} \frac{1}{R_{grid}} &= \sum_{n=0}^k \frac{1}{R_n} \\ \frac{1}{R_{grid}} &\approx \frac{k}{\overline{R}} \\ k \rightarrow \infty : R_{grid} &\rightarrow 0 \end{aligned} \quad (2.30)$$

This does not account for the resistance of the transmission lines but does present a reasonable argument for doing initial calculations based on internal or short circuit resistance, especially if;

$$R_{coil} \gg R_{grid}$$

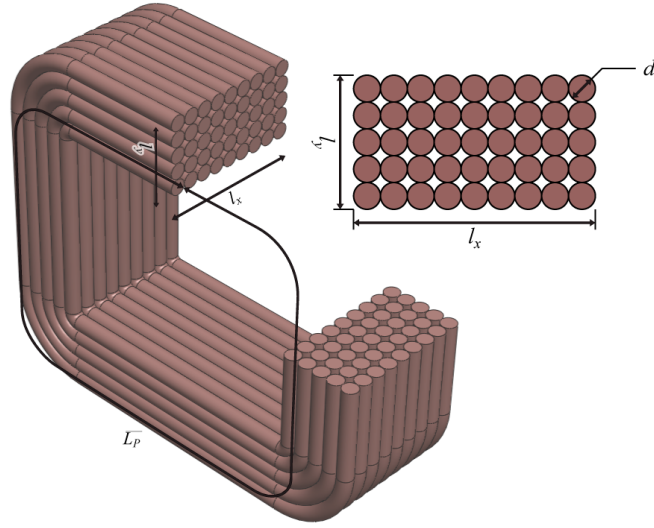


Figure 2.9: Distribution of conductors in a square packed coil

The number of conductors within a coil will determine, in part, the power output of the device in operation, therefore;

$$\begin{aligned}
 N_x &= \left\lfloor \frac{l_x}{d} \right\rfloor & N_y &= \left\lfloor \frac{l_y}{d} \right\rfloor \\
 N &= N_x N_y \\
 N &= \left\lfloor \frac{l_x}{d} \right\rfloor \left\lfloor \frac{l_y}{d} \right\rfloor
 \end{aligned} \tag{2.31}$$

The N_x and N_y values must be integers in order to be correct;

$$\begin{aligned}
 P &= \frac{A_x N}{\rho_r \overline{L_P}} \left(\frac{d\varphi}{dt} \right)^2 \\
 A_x &= \frac{\pi d^2}{4} \\
 P &= \left\lfloor \frac{l_x}{d} \right\rfloor \left\lfloor \frac{l_y}{d} \right\rfloor \frac{\pi d^2}{4 \rho_r \overline{L_P}} \left(\frac{d\varphi}{dt} \right)^2
 \end{aligned} \tag{2.32}$$

Chapter 2: Literature

$$\begin{aligned} \left[\frac{l_x}{d} \right] \left[\frac{l_y}{d} \right] \frac{\pi d^2}{4\rho_r \overline{L_P}} &\approx \frac{\pi l_x l_y}{4\rho_r \overline{L_P}} = \frac{\pi A_C}{4\rho_r \overline{L_P}} \\ &= f_A \frac{A_C}{\rho_r \overline{L_P}} \end{aligned} \quad (2.33)$$

The power calculated is directly related to the sectional area of the coil, and the average path length of the coil. The value for the wire diameter essentially cancels out from the N terms and the wire cross-sectional area. The N value still dictates the output voltage however the output power should be fixed.

Since the $\overline{L_P}$ term is on the bottom of the equation the coil should be kept as close to circular as possible in order to minimize $\overline{L_P}$ for any given area of flux carrier. It is important to retain the area, if not the shape, because of the relationship between flux and the B-field.

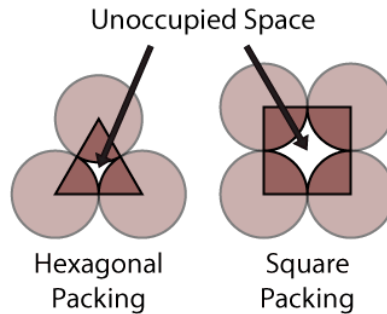


Figure 2.10: Wire Packing Arrangements

The f_A term refers to different packing arrangements, two are listed below.

Hexagonal packing is usually the way wires will lie within a coil when wound, square packing is more difficult to achieve. Since hexagonal packing is the more efficient on area anyway it makes sense to use it in the calculations.

Arrangement	f_A	
Square	$\frac{\pi}{4}$	0.785
Hexagonal	$\frac{\pi}{2\sqrt{3}}$	0.907

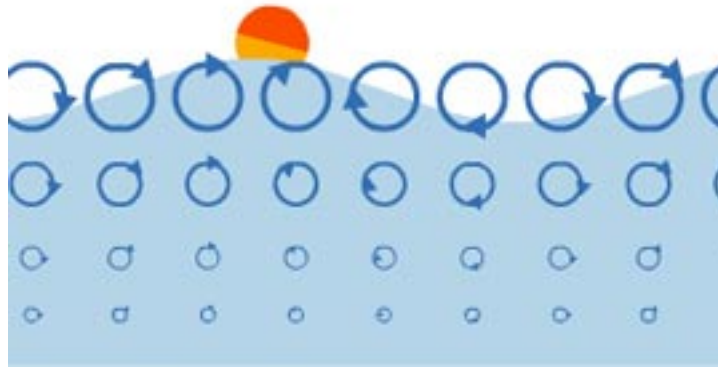
Table 2.2: Wire Packing Arrangement Factors

2.4 Wave Theory

Since the primary focus of this research is linear generators for wave power applications, it is important to understand the forces that are applied by waves.

2.4.1 Wave Motion

Although the classic image of a wave is that they only move up and down, the particles in ocean waves actually move in elliptical paths. An object placed atop the water will move in an elliptical motion, with both a vertical and 2 horizontal components.

Figure 2.11: Elliptical Motion and Depth Effects of Waves^[40]

Each of these components applies force to the object. However the force applied varies with depth, as can be seen in Figure 2.11, and as such, if an object is large

enough it can experience a moment instead, therefore there are 6 possible ways that an object can move in ocean waves.

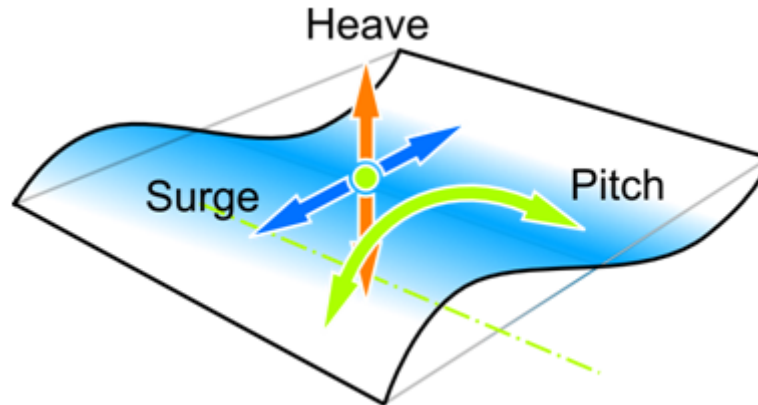


Figure 2.12: Primary Modes of Wave Energy Capture

The primary modes of motion are heave, surge and pitch which are illustrated in 2.12. There are 3 other modes which are used more infrequently; these are sway, roll and yaw. If a suitable object is placed on the surface of a wave they it will experience all 6 modes of motion. This can commonly be seen with buoys with masts. They can be seen to pitch and roll in the waves whilst heaving up and down.

2.4.2 Sea Spectra

As is readily observable, ocean waves do not exist at a specific frequency but across a range. There are a number of sea spectra which have been developed and used over the years. A sea spectrum tells us the number of waves of a given frequency that occur per square metre of ocean surface. This is affected by many factors and each region will have a dominant wave frequency. An example of a wave spectrum is the Pierson-Moskowitz (PM)^[26] spectrum.

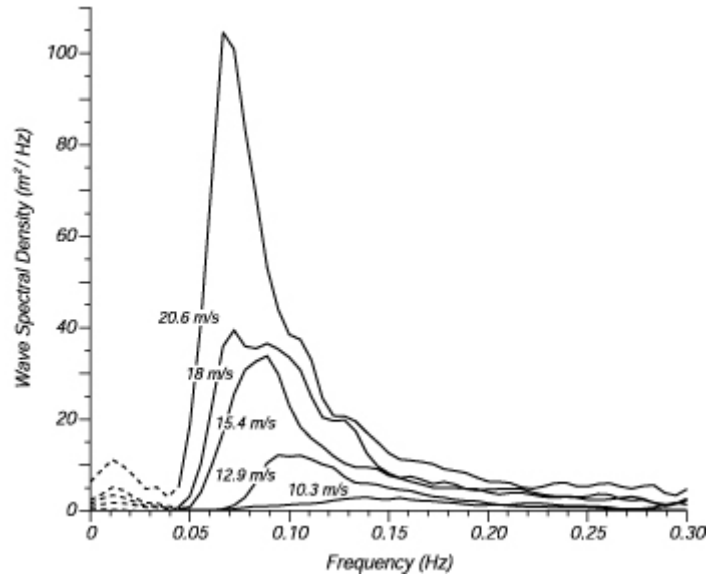


Figure 2.13: Pierson-Moskowitz Spectra for differing wind speeds

The chart in Figure 2.13 shows the wave spectral density which is the effect number of square metres of that frequency wave that exist in that particular region. In essence it provides information about which frequencies a device should be tuned to in order to extract the maximum amount of power. Unfortunately it is not that simple since tuning a wave energy device is generally very difficult. However the sea spectra provide information vital to correctly operating a wave energy device in a given climate.

It is important to remember that all devices are subject to all forces. Just because a device is designed to utilise a particular force, does not mean it does not have to deal with the others. In some cases these forces can be rather substantial. For example a heaving buoy will be subject to cycling shearing forces from surge and sway. If these forces are not anticipated they could cause serious damage to the generator.

2.4.3 Wave Device Tuning

There are many difficulties to do with the tuning of a wave device, the variable damping caused when a device changes position in the water, the added mass of the water that is being moved with/by the device and the variety of frequencies it will be subjected to being some of the major ones. As the components of wave energy device move, they experience variable damping forces from the internal components and the interactions with the water. In a simple, sinusoidally driving, harmonic system the damping affects the timing/phase of the device, ϕ , as follows^[39];

$$\phi = \arctan \left(\frac{2\omega\omega_0\zeta}{\omega^2 - \omega_0^2} \right) \quad (2.34)$$

where ω_0 is the natural frequency, defined as^[33];

$$\omega_0 = \sqrt{\frac{k}{m}} \quad (2.35)$$

As the device moves there is also a volume of water that for all intents and purposes moves with it. This is referred to as the added mass. This volume is not always constant and since it changes the effective mass of the device it alters the natural frequency.

Many devices, especially those which use a pitching motion, experience a variable spring force as well due to the buoyancy of the individual components, this also upsets the natural frequency. The natural frequency is important because the intention is to design wave energy devices to operate at resonance so as to extract the maximum amount of power. If the natural frequency of the device keeps

changing then making it resonate is difficult.

Although there is much research into how to make devices tune the parallel line of research into linear generators is intended to create generators which can operate in all circumstances and with good part load characteristics. As a result, linear generators should be able to extract energy from the device whether it is resonant or not.

This has been a very brief explanation of the difficulties of wave device tuning because it has little impact on the design of linear generators. Further information on some attempts to tune wave energy devices can be found in [1,17,34,36,37,38]

2.5 Linear Generator Theory

The design of linear generators is in many ways similar to that of rotational generators. They are based on the same principles but the number of variations in design can be staggering. There are two basic classes of linear generators, direct-drive and non-direct drive. Direct-drive generators generate power without using any kind of mechanical power conversion.

One of the key issues with linear generators is that in order to generate an equivalent output of a rotational generator they must have small stages to create the necessary frequency of flux changes. Since a linear generator is used in circumstances where there is an oscillating motion it will not be able to generate a continuous output as it moves, resulting in a cyclic power output.

2.5.1 Key Elements

Energy Density

Energy Density refers to the amount of energy that can be generated by a generator for a given volume occupied by or weight of the device. Therefore a large device with a small output will have a low density where as a small device that generates a large output will have a high energy density. Different generator topologies will have different energy density ranges.

The energy density has other implications too. If a device has a high energy density then it will make a difference to the transport and installation costs. Also a device will repay itself more quickly, offsetting the incurred costs if it has a high energy density since there should be lower transport and installation costs.

Translator

The translator is key to the generator. In variable reluctance generators it is constructed of iron or other highly permeable materials. Other topologies use translators with integrated magnets or integrated coils. The air-cored tubular design uses a translator of permanent magnets interspersed with steel rings. The AWS^[27] uses a bed of magnets moving against a set of coils and so in the end either part could be used as the translator or the stator.

Back Iron

Back Iron is iron within the design that is intended to help improve the Energy Density of the generator. As stated in the Magnetic Theory section, the amount of

Chapter 2: Literature

iron used in a generator is key to how well that generator will perform, depending on its topology. However, it is also responsible for the degree of transverse force generated by the magnets present in the generator.

The amount of Iron in a design also has a marked impact on its weight, affecting design and construction of the rest of the generator. The iron is usually made as a laminate to improve its magnetic characteristics. The magnetic saturation point of the material chosen for the back iron is important also because it will affect the area of material required to carry a given flux.

Air-cored generators do not use back iron in an attempted to reduce weight and the attractive forces inside the generators. In general they use a magnetic translator which contains some iron.

2.5.2 Topologies

Air Cored

As the name suggests, and Air Cored generator is one where there is little or no Back Iron in the design. This has two important effects, firstly the removal of the Back Iron results in a marked reduction in the forces present in the design and secondly its removal results in a substantially reduced magnetic flux. So an Air Cored generator will be easier to construct and operate than other topologies, but will have a lower energy density.

Primarily an Air Cored design will consist of a magnet passing through or past an open wound coil. As the magnet passes the field it creates fluctuates. These fluctuations induce an EMF in the coil, which in turn will drive a current. There

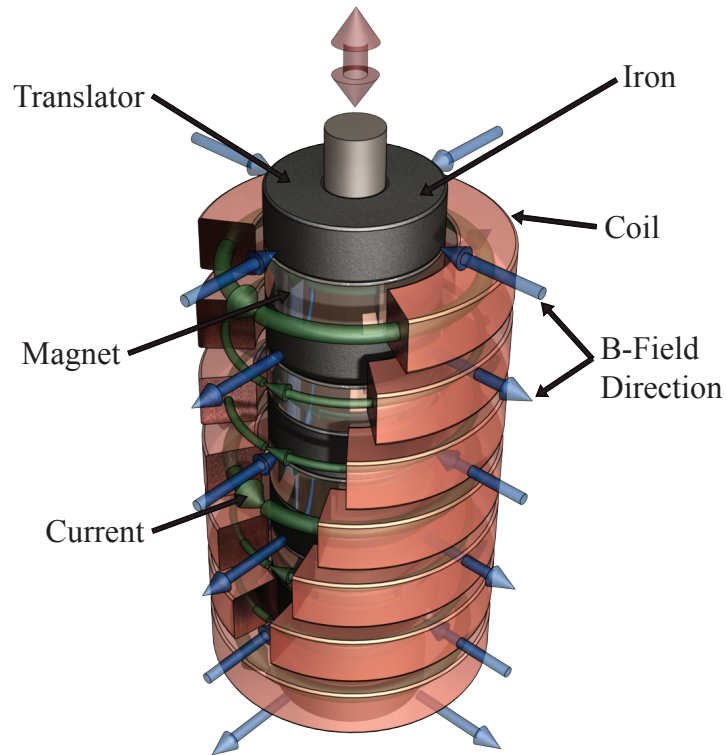


Figure 2.14: Example of Air-Cored Topology

have been numerous different designs of air-cored generators, only some of which resemble Figure 2.14. (The magnets are the silver discs, the flux is shown in blue and the coils are in orange.) An air-cored design was implemented in the Archimedes Wave Swing^[27], consisting of a flat array of magnets and coils rather than the tubular arrangement shown in Figure 2.14.

Air-cored machines have been tested at a number of institutions, including Edinburgh and Durham Universities^[2,23,3], and have been deployed in offshore wave energy devices, AWS^[27] and Oregon State University's Prototype Wave Buoy^[30].

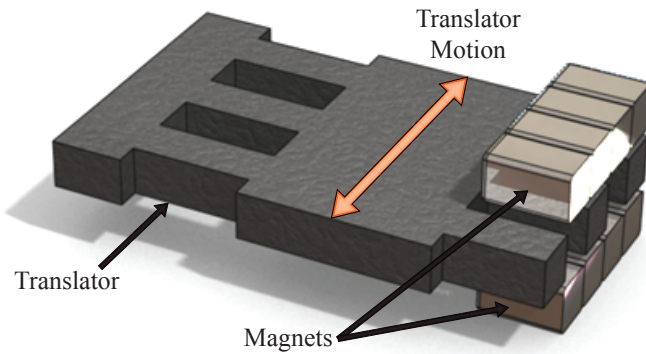


Figure 2.15: Possible Arrangements of Magnets & Translator

Variable Reluctance

A Variable reluctance generator operates by creating alternating low reluctance paths for a bed of alternate magnets. As the translator moves it essentially closes one magnetic circuit after another, in doing so the flux direction changes rapidly generating an EMF.

The translator for this work is essentially a slotted iron bar. (See Figure 2.15) The magnets in the generator are aligned with the slots in the translator.

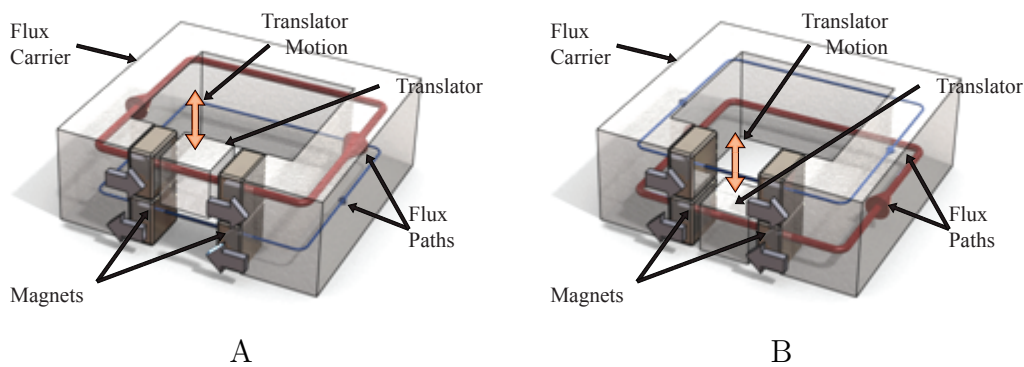


Figure 2.16: Variable Reluctance Generator Configurations

When the translator is in position 1 (See Figure 2.16A) then a strong magnetic

Chapter 2: Literature

circuit is formed along the top path. When in position 2 (See Figure 2.16B) a strong magnetic circuit forms on the bottom path. The field direction for the top path is the opposite of the bottom path therefore the flux of the magnetic circuit completely reverses once for each tooth on the translator. Ideally the translator is kept within a few millimetres of the magnets resulting in high magnetic fields and forces, putting high loads on whatever bearings/support mechanisms are in use. The advantage of the stronger magnetic fields is that potentially a greater flux can be generated.

From (2.12)

$$\text{EMF} = N \frac{d\phi}{dt}$$

Since the direction of the flux reverses for every tooth on the translator the translation rate and distribution of the teeth determines the rate of change of flux. Since the flux varies with the distance between the magnets and the translator's surface, the shape of the teeth would alter the waveform of the flux.

The coils would be wrapped around arms of the C-core in Figure 2.16 in order to get the most out of the available flux.

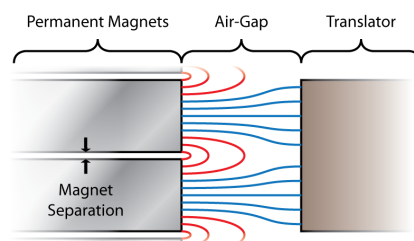


Figure 2.17: Example of Magnetic Short Circuit (shorted field shown in red)

Unfortunately the proximity of the magnets in such a design causes a degree of flux loss due to a magnetic short-circuit. Since the magnets have opposing poles

Chapter 2: Literature

there is a connection formed between them through the back iron and through the air. As a result the basic approximation from circuit theory will always over predict the flux that is generated by the arrangement. In theory, by seperating the magnets, using plastic spacers or similar, the amount of flux in the short-circuits can be reduced. By creating the cores out of suitable laminates the field can be channelled reducing the effect of the short circuit.

The following is a first approximation as to how a variable reluctance generator will behave. From magnetic circuit theory the following can be derived;

$$\frac{nB_{rem}l_{magnet}}{\mu_0} - NI = \frac{n}{\mu_0 A}(l_{air-gap} + l_{magnet})\varphi \quad (2.36)$$

To look current and flux with respect to time $f(t)$ will be used to vary the MMF, due to the permanent magnets, within the circuit. $f(t)$ is a non-dimensional function with a range of -1 to 1.

$$\begin{aligned} \frac{nB_{rem}l_{magnet}}{\mu_0}f(t) - NI(t) &= \frac{n}{\mu_0 A}(l_{air-gap} + l_{magnet})\varphi(t) \\ \frac{AB_{rem}l_{magnet}}{(l_{air-gap} + l_m)}f(t) - \frac{\mu_0 AN}{n(l_{air-gap} + l_{magnet})}I(t) &= \varphi(t) \end{aligned} \quad (2.37)$$

By substituting the values φ_m and φ_C for the constants a simpler relationship develops. The φ_m is the value of the maximum flux generated by the magnets in static circumstances and φ_C is the flux per Amp generated from the current in the coil. φ_C is negative because, due to the rules of induction, it will oppose the direction of the existing field.

Chapter 2: Literature

$$\varphi_m = \frac{AB_{rem}l_{magnet}}{l_{air-gap} + l_{magnet}}$$

$$\varphi_c = -\frac{\mu_0 AN}{n(l_{air-gap} + l_{magnet})} \quad (2.38)$$

$$\varphi(t) = \varphi_m f(t) + \varphi_c I(t) \quad (2.39)$$

$$\varphi'(t) = \varphi_m f'(t) + \varphi_c I'(t) \quad (2.40)$$

If the EMF can be taken to be the supply voltage then the device can be modelled with an electrical circuit by equating voltages. Figure 2.27 shows the equivalent circuit for the model.

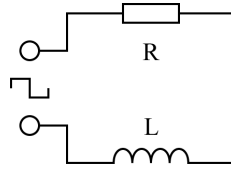


Figure 2.18: Power Generation Equivalent Circuit

The input is a square wave because it has been assumed that the flux is represented by a triangle wave, as such the slopes of the triangle wave give constant $\varphi'(t)$ values and therefore constant EMF values have a square waveform.

$$V = \varepsilon = N\varphi'(t) = RI(t) - LI'(t)$$

$$N\varphi_m f'(t) + N\varphi_c I'(t) = RI(t) - LI'(t)$$

$$I(t)R - N\varphi_m f'(t) - (L + N\varphi_c)I'(t) = 0 \quad (2.41)$$

This function, when modelled, gives rise to characteristic curves shown in Figure

2.19;

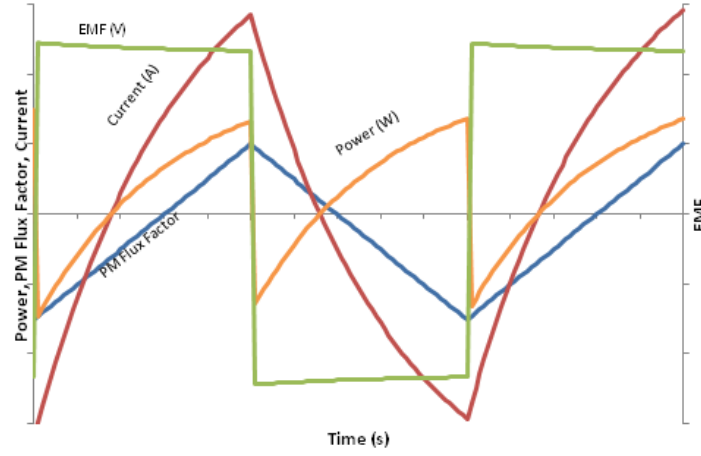


Figure 2.19: Constant Inductance Simulation of Variable Reluctance Output

In this simulation it is clear to see that both the current and the power are out of phase with the EMF and because of the interdependency of the flux and the current the current and EMF do not vary linearly. The current in the windings works in opposition to the permanent magnets to reduce the total flux and therefore the EMF, in turn the reduced EMF reduces the rate of current growth.

If L is not longer assumed to be a constant then the derived functions are as follows;

$$I(t)^2 R + N\varphi(t)I'(t) - N\varphi'(t)I(t) = 0 \quad (2.42)$$

By substituting from (2.40);

$$I(t)^2 R + N\varphi_m f(t)I'(t) - N\varphi_m f'(t)I(t) = 0 \quad (2.43)$$

Chapter 2: Literature

Testing of the principles has been performed and documented at Edinburgh University, by Dr. M. Mueller^[24,5] and by the wave energy team of Oregon State University.^[13] The tests performed at Edinburgh used a toothed iron bar held a distance away from a c-core to induce the changing air-gap. This machine, referred to as the Vernier Hybrid generator, has been well documented.^[24]

Since at its core this research is about developing support mechanisms for linear generator modules it makes sense to design said mechanisms for high force designs so that they are feasible for all designs, high and low force. For this reason the majority of this work, with a few exceptions, has focused on the variable reluctance type generator although a little work has been done surrounding air-cored tubular machines as well.

Transverse Flux

Transverse flux machines^[20,25] generally use a bed of magnets moving past sections of back iron. Unlike other designs however, the coils are not wrapped around the back iron. Instead of the back iron being wrapped in the coil the coil is wrapped in the back iron. The iron is used to channel the flux around the copper conductors of the coil producing a similar effect to having the coil wrapped around it.

The design in Figure 2.20 would operate by sliding a translator composed of two beds of magnets past an array of iron sections. The field generated by the magnets as they pass induces a current in the copper. This effect is easier to see in Figure 2.21;

As the bed of magnets move past the back iron it drives a flux change within the iron. This flux then creates the EMF within the copper. The magnets reverse di-

Chapter 2: Literature

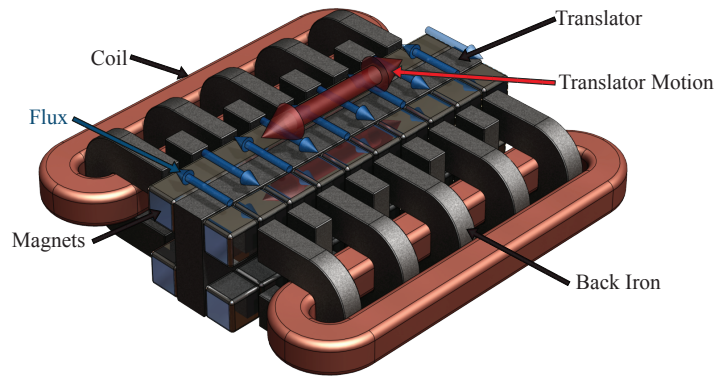


Figure 2.20: Potential Linear Transverse Flux Generator

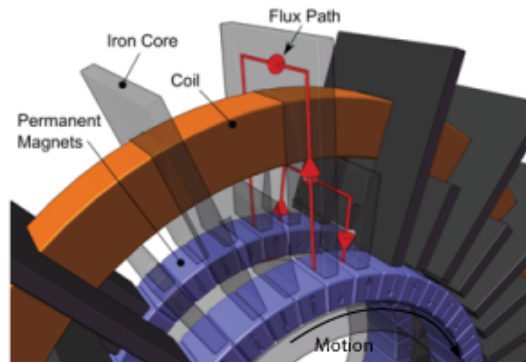


Figure 2.21: Schematic Rotary Transverse Flux Machine with Flux Paths

rection with each row or 2 rows causing the alternating flux when the machine is in motion. If the magnets are staggered correctly in the design then it is theoretically possible to produce a smoother output from the combined flux variations.

By using this arrangement the amount of copper and therefore the cost of the machine can be reduced. Transverse flux machines are readily available for rotational applications and can be fairly compact, as in Figure 2.21, however, as can be seen in Figure 2.20, the arrangement of coil and iron becomes more complicated when it is applied to linear applications.

Like the Variable Reluctance generators a transverse flux machine is a high force

machine due to the inclusion of the back iron loops, however, compared to the variable reluctance machine it uses substantially more back iron and, in the linear case, marginally less copper. Since the forces on the internal components, for a given air-gap, will be similar and due to its structural complexity the Variable Reluctance topology was chosen for study rather than the Transverse Flux.

A linear transverse flux machine, such as the one shown in Figure 2.20, a large number of magnets would be required in order to construct the translator making the design rather expensive. Other designs may be possible by hybridising the transverse flux and variable reluctance designs which could reduce the number of magnets required.

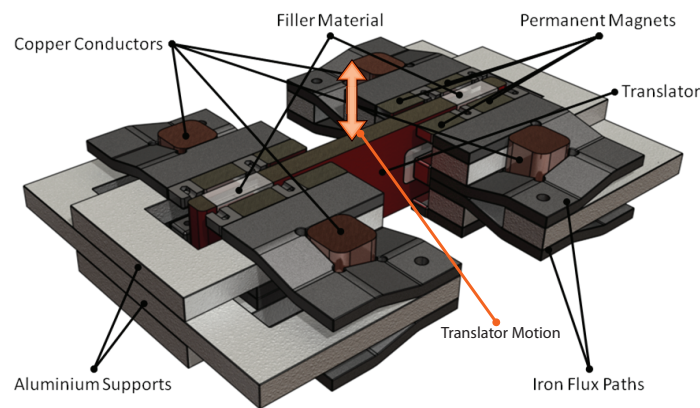


Figure 2.22: Hybrid Transverse Flux and Variable Reluctance Machine

2.5.3 Motion

Reciprocating Linear Motion

All linear generators are designed to extract power from cyclic linear motions. As such there is a governing wave function that describes the relative motion of

Chapter 2: Literature

translator and stator. No matter what topology of linear generator is being used the motion of the translator is described in the same way. The simplest waveform to use in evaluating designs would be a sine wave displacement;

$$\begin{aligned} s &= A_t \cos \omega_1 t \\ \frac{ds}{dt} &= -A_t \omega_1 \sin \omega_1 t \end{aligned} \tag{2.44}$$

These values are key to all the output calculations for linear generators and will be used in later sections to describe their motion.

Constant Velocity Rotational Motion

In the case of a rotational device using similar technology it will instead be assumed that;

$$\begin{aligned} \theta &= \omega t \\ \frac{d\theta}{dt} &= \omega \end{aligned} \tag{2.45}$$

Where $\frac{d\theta}{dt}$ is analogous to $\frac{ds}{dt}$, ($ds = r d\theta$).

Since later work will rely on the $\frac{ds}{dt}$ value this is important for both the linear and rotational motions.

2.6 Hydrostatic Theory

Hydrostatic bearings were first introduced in 1878 at the Paris Industrial Exposition^[19] under the name of “La Chemin de For de Glace,” “The Ice Railway.” They con-

Chapter 2: Literature

sist of a surface with a recess, into which fluid is pumped, and a smooth opposing surface upon which the bearing acts. It is important that the opposing surfaces be smooth since all the theory presented here relies on the ideas of ideal laminar flow. A rough or uneven surface will not produce evenly distributed surface flows. A rough or uneven surface will not produce evenly distributed surface flows.

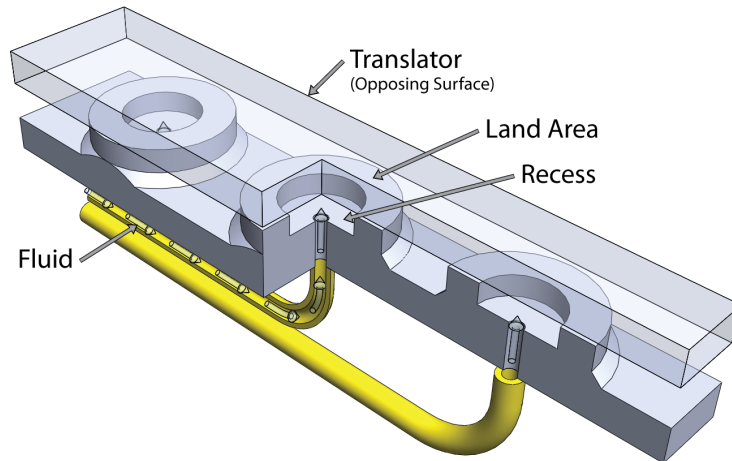


Figure 2.23: Basic Hydrostatic Bearing Circular Step Bearing

The recess fluid is at a higher pressure than the surroundings, as a result of the exit flow being restricted, and flows across the land area of the bearing to escape. As it does so the internal pressure drops until it matches the ambient pressure at the outside. Since the internal pressure is high across the land and in the recess this generates a net force to separate the bearing and the surface.

The equations used in hydrostatic theory are derived from Reynolds Equation for Hydrostatic Lubrication^[4] of two parallel plates.

$$\frac{\partial}{\partial r} \left(h^3 \frac{\partial p}{\partial r} \right) + \frac{\partial}{\partial y} \left(h^3 \frac{\partial p}{\partial y} \right) = 12\mu_h u \frac{\partial h}{\partial r} \quad (2.46)$$

When properly derived this equation is key to understanding how fluid moves

between two flat parallel surfaces, it also tells us the pressure required in order to support a given load.

2.6.1 Non-Dynamic Hydrostatic Analysis

Crucial to the operation of hydrostatic bearings is the way in which the internal pressure of the lubricating fluid is distributed across the land area, the shared area of the surface and the bearing. The approximate pressure distribution is described by the following differential.

$$p = \int_0^{p_i} dp = \int_{r_o}^{r_i} \frac{1}{r} dr \quad (2.47)$$

From this an expression can be derived for any hydrostatic bearing, the following is for a simple circular step bearing, such as that shown in Figure 2.23.

$$p = p_i \frac{\ln \frac{r}{r_o}}{\ln \frac{r_i}{r_o}} \quad (2.48)$$

Where r_i is the inner radius or the radius of the recess and r_o is the outer radius of the bearing. The optimum value for r_i/r_o is approximately 53%^[21].

(See derivation A.1)

Using this it is possible to calculate the load to be supported by the bearing by integrating it across the surface of the bearing.

$$W = \int_A p dA \quad (2.49)$$

Chapter 2: Literature

The final form of this equation is as follows;

$$W = p_i A_e \quad (2.50)$$

where W is the load and A_e is the effective area of the bearing. Since the pressure varies across the land area the true area will not give an accurate value for the force. The inlet pressure is found from Reynolds equation for hydrostatic lubrication, which is in turn derived from the Generalised Reynolds Equation^[4]. The Generalised Reynolds Equation is as follows;

$$\begin{aligned} \frac{\partial}{\partial x} \left(\frac{\rho h^3}{12\mu_h} \frac{\partial p}{\partial x} \right) + \frac{\partial}{\partial y} \left(\frac{\rho h^3}{12\mu_h} \frac{\partial p}{\partial y} \right) &= \frac{\partial}{\partial x} \left[\frac{\rho h (u_a + u_b)}{2} \right] \\ &+ \frac{\partial}{\partial y} \left[\frac{\rho h (v_a + v_b)}{2} \right] \\ &+ \rho \left[(w_a - w_b) - u_a \frac{\partial h}{\partial x} - v_a \frac{\partial h}{\partial y} \right] + h \frac{\partial \rho}{\partial t} \end{aligned} \quad (2.51)$$

(See derivation A.2)

$$\frac{\partial}{\partial r} \left(h^3 \frac{\partial p}{\partial r} \right) + \frac{\partial}{\partial y} \left(h^3 \frac{\partial p}{\partial y} \right) = 12\mu_h u \frac{\partial h}{\partial r} \quad (2.52)$$

From this the equation for the inlet pressure^[21] is;

$$p_i = \frac{6\mu_h Q}{\pi h^3} \ln \frac{r_o}{r_i} \quad (2.53)$$

(See derivation A.3)

This equation can also be derived using the Reynolds Equation in polar form^[21];

Chapter 2: Literature

$$\frac{\partial}{\partial r} \left(\frac{\rho r h^3}{12\mu_h} \frac{\partial p}{\partial r} \right) + \frac{1}{r} \frac{\partial}{\partial \theta} \left(\frac{\rho h^3}{12\mu_h} \frac{\partial p}{\partial \theta} \right) = \frac{1}{2} U \frac{\partial(\rho h)}{\partial \theta} - r \rho V_s \quad (2.54)$$

(See derivation A.4)

An example $A_e^{[21]}$ (Effective Area) for a circular step bearing would be;

$$A_e = \frac{\pi (r_o^2 - r_i^2)}{2 \ln r_o/r_i} \quad (2.55)$$

(See derivation A.5)

$$W = \frac{3\mu_h Q}{h^3} (r_o^2 - r_i^2) \quad (2.56)$$

$$W = L_H \frac{Q}{h^3} \quad (2.57)$$

where L_H is a bearing characteristic constant.

$$L_H = 3\eta (r_o^2 - r_i^2) \quad (2.58)$$

From equation 2.57 the flow-rate required to support a given load at a given clearance, on a given bearing can be calculated. The L_H value is individual to a bearing design. The results can be seen in Figure 2.24.

If a clearance and load is specified the required flow-rate can be calculated.

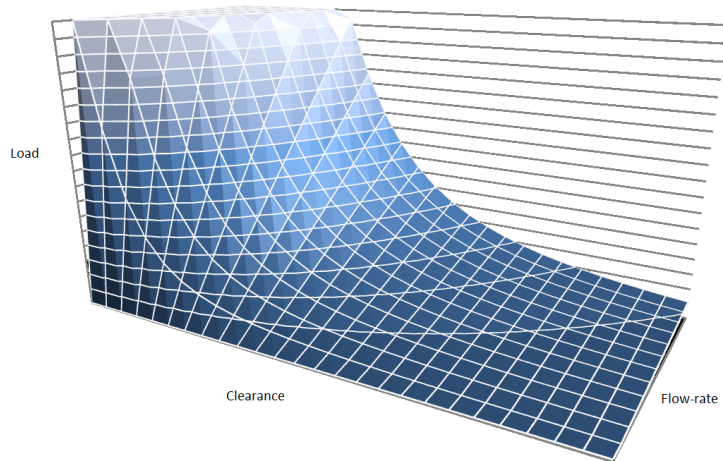


Figure 2.24: Load/Clearance Curves

Equivalent Pumping Power

$$H_P = pQ \quad (2.59)$$

Where H_P is the equivalent pumping power. This approximation for the equivalent pumping power is derived from thermodynamics^[7] where;

$$\delta W = p dv$$

This assumes that there is no change in entropy as the fluid is pressurised. In this case;

$$\frac{\delta W}{\delta t} = H_P = p \frac{dv}{dt} = pQ$$

From (2.50) and (2.57)

$$H_P = \frac{W^2 h^3}{A_e L_H} \quad (2.60)$$

This indicates that if applied to a real situation, the power required to operate the bearing is related to the land clearance (h), the load (W) and the effective area (A_e) for a given bearing design (L_H).

The equivalent pumping power gives an indication of the power required in order to use the hydrostatic bearings. This value combined with the losses from the fluid transport system supplying the bearings gives a true indication of the power usage.

$$P_{input} = \frac{1}{\eta_{pump}} (H_P + P_{pipe}) \quad (2.61)$$

This value is required in order to calculate the efficiency of any hydrostatically supported system.

2.6.2 Approximating Dynamic Hydrostatic Response

Traditional hydrostatic analysis is determined assuming that the land area does not change. Using these results in dynamic circumstances is an inherently bad idea since they contain no terms that can account for dynamic applications.

To provide an approximation to hydrostatic damping it was assumed that the dynamic effects were similar to the effect of squeezing two plates together.

By looking at an annulus between the two discs the change in flow with respect to radius can be derived as;

Chapter 2: Literature

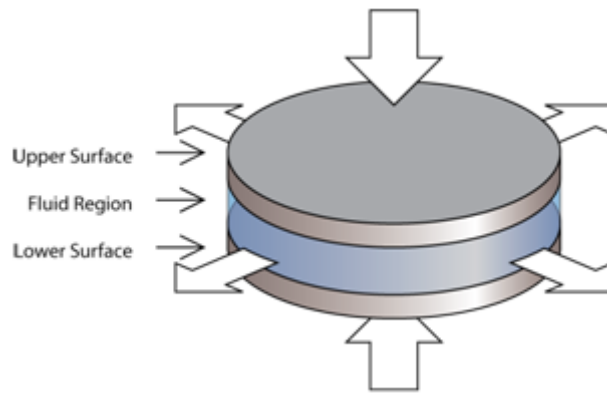


Figure 2.25: Fluid Compression Plates

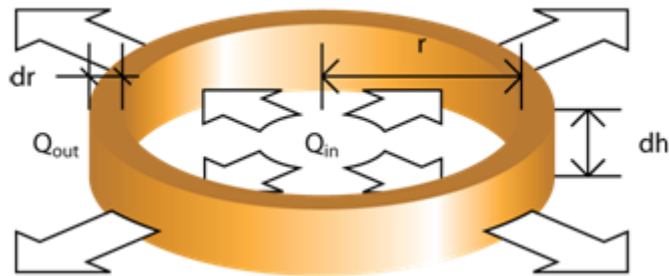


Figure 2.26: Compressed Annulus

$$Q_{out} = Q_{in} + dQ$$

$$dQ = 2\pi r \frac{dh}{dt} dr \quad (2.62)$$

from this;

$$Q = \pi r^2 \frac{dh}{dt} \quad (2.63)$$

By substituting Q into Reynold's Equation (as in previous sections) a function for pressure can be derived;

Chapter 2: Literature

$$p = \frac{3\mu_h r^2}{h^3} \frac{dh}{dt} \quad (2.64)$$

(See derivation A.6.1)

From this force is;

$$W_D = \frac{3\pi\mu_h r_o^4}{2h^3} \frac{dh}{dt} \quad (2.65)$$

(See derivation A.6.2)

The total force is the sum of the two forces;

$$\begin{aligned} W &= \frac{3\mu_h}{h^3} \left(Q (r_o^2 - r_i^2) + \frac{\pi}{2} r_o^4 \frac{dh}{dt} \right) \\ W &= \frac{1}{h^3} \left(L_H Q + C_H \frac{dh}{dt} \right) \end{aligned} \quad (2.66)$$

Where;

$$\begin{aligned} L_H &= 3\mu_h (r_o^2 - r_i^2) \\ C_H &= \frac{3\mu_h \pi}{2} r_o^4 \end{aligned} \quad (2.67)$$

This can now be used in the dynamic modelling of the hydrostatic bearing. When used in numerical simulations the addition of the dynamic term adds a substantial damping force, damping even fairly substantial oscillations away in fractions of a second. Figure 2.27 shows a decaying oscillation tending towards the equilibrium position for the bearing (the horizontal axis) as would result from (2.57).

Although not an exact match for a simple harmonic oscillation it is approximately

Chapter 2: Literature

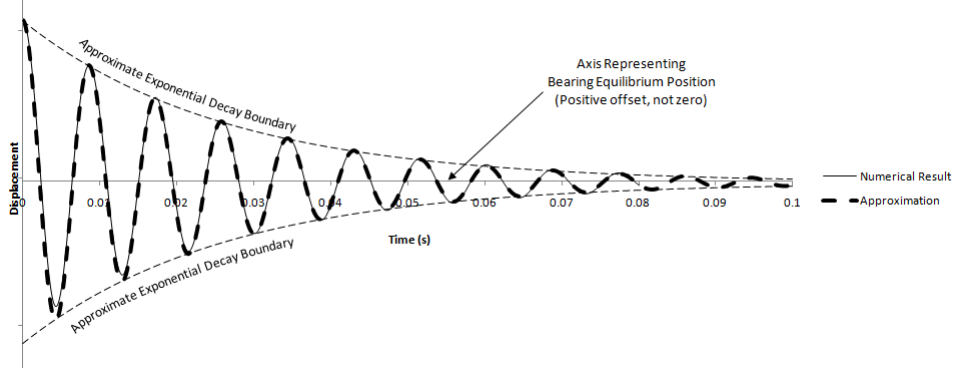


Figure 2.27: Vibration in a single hydrostatic bearing supporting a direct load the same as a damped oscillation of the form of;

$$x(t) = A_i e^{-\zeta \omega_0 t} \cos\left(\sqrt{1 - \zeta^2} \omega_0 t\right) \quad (2.68)$$

It is possible to match an exponential decay curve to the peaks of the data with an R^2 value of $R^2 = 1.000$ and from this determine both the decay rate and the amplitude.

A test case for this would have the following second order differential equation.

$$W = \frac{1}{h^3} \left(L_H Q + C_H \frac{dh}{dt} \right) - mg \quad \Rightarrow \quad mx'' = \frac{1}{x^3} (L_H Q + C_H x') - mg \quad (2.69)$$

L is the bearing constant and C is the dynamic bearing constant. Figure 2.27 shows a generic set of results from the numerical analysis of this equation. From the numerical analysis of these results, the vibration frequency for this case seems to follow;

$$\sqrt{1 - \zeta} \omega_0 \approx \psi \frac{m^{0.169}}{Q^{0.158}} \quad (2.70)$$

where ψ is a constant. The damping follows;

$$\zeta\omega_0 \approx \frac{\beta}{Q^{1.088}} \quad (2.71)$$

Therefore the highest damping is achieved at low flowrate, which from (2.57) requires a small clearance. It should be noted that there is a slight shift in frequency over time as the vibration diminishes. These equations are fitted to the numerical data but are consistent over a range of values when run.

2.6.3 Industrial Bearings

Hydrostatic bearings have a number of applications in industry. They are generally used in situations where high stability and low noise is required. An example would be a large telescope which needs to be very precisely controlled yet mobile. These bearings maintain sub-millimetre positions with very little noise. Hydrostatic bearings occur in tool beds for the same reasons, and have been used in hydroelectric turbines. Hydrostatic bearings, when fed with a clean lubricating fluid, water or oil, have impressive longevity. A measurement done on some hydrostatic bearings used for hydroelectric turbines suggested that the bearings might last up to 1,000 years if properly operated.^[46]

Many bearings used in industrial applications are self-compensating. These use in-built channels to act as pressure regulators, keeping the bearings aligned and giving very high positional accuracy. Such bearings occur in devices such as machine tools where they are used to support the work beds.

Self-compensating bearings use paired recesses as distance sensors, Figure 2.28

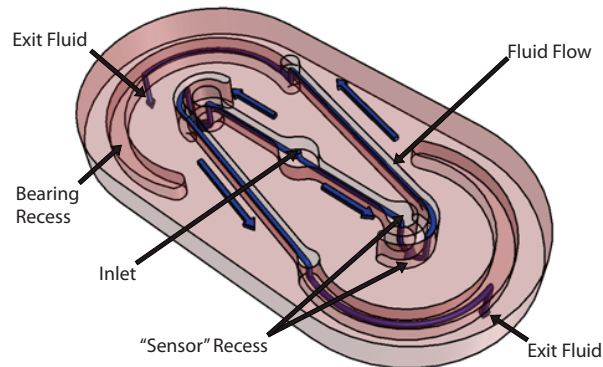


Figure 2.28: Self-Compensating Bearing + Fluid Direction Markers

shows an example of the self compensating bearing arrangement. If the gap is too small then the flow through these recesses is reduced feeding to the opposite bearing causing it to generate less pressure. Likewise if the gap is too large then the increased flow is fed to the opposite bearing to increase the gap there.

2.6.4 Pumps

Any pump can be used to supply fluid to a hydrostatic bearing; however some are better suited than others. The main types of pumps, along with advantages and disadvantages are listed below;

- Centrifugal Pump
 - A centrifugal pump uses a rotor to expel fluid radially. It is a simple design of pump and relatively easy to control. To determine the flow-rate from the pump however additional hardware is required. Because of its design a given rate of rotation of the main shaft of the pump will not necessarily result in a specific flow-rate.

Chapter 2: Literature

- A centrifugal pump can deliver a large volume at low pressure or a low volume at high pressure depending on the situation. The same rate of rotation of the rotor will do both depending on the pressure.
- Axial Flow Pump
 - Axial flow pumps essentially use a propeller/turbine to drive the fluid through the pump. It performs in a similar way to a centrifugal pump, in as much as its rate of rotation is not necessarily an indication of the flow-rate.
- Gear Pump
 - A gear pump, as the name suggests, uses paired gears to drive fluid. As the gears turn the meshing of the teeth exclude fluid from the centre of the pump, while fluid is carried around the unmeshed teeth on the outside. Ideal fluid cannot escape from between the teeth and for each rotation of the shaft the pump delivers the same amount of fluid, generating a constant flow-rate. As the pressure increases a greater torque is required in order to turn the shaft of the pump, but the volume displaced per rotation remains a constant.
 - A gear pump can deliver very high pressures but in general does not deliver a great volume. The output from a gear pump is very smooth.
- Vane Pump
 - A vane pump, like the gear pump, delivers a specific volume for each rotation of the shaft. It works by trapping a volume between sliding

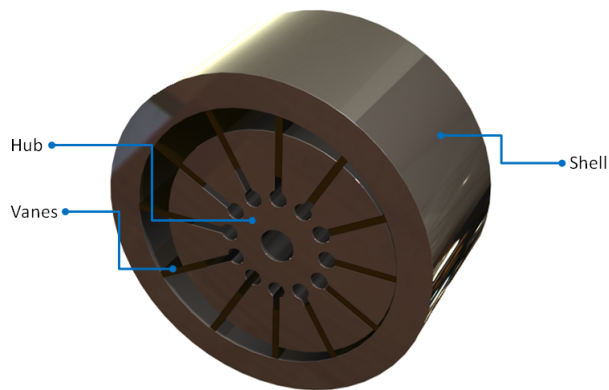


Figure 2.29: Core of a Vane Pump

vanes set in the hub/rotor. As the hub turns the volume trapped between the vanes is carried round. The rotor is circular and offset from the centre of the case it is mounted in, which is also circular. The fluid is expelled on the opposite side to where it entered.

- A vane pump can deliver greater volumes than a gear pump but at the expense of pressure. The profile of the vanes, specifically the angle at the tip, has an effect on the maximum pressure they can maintain. The output from a vane pump is also often not as smooth as a gear pump.

- Piston Pump

- A piston pump is made up of one or more radial pistons attached to a cam, as the cam rotates the piston(s) are extended and compressed. The torque varies as the cam rotates depending on the number of pistons attached to it. Unless a mechanism is in place to vary the length of the pistons stroke a piston pump is a constant flow-rate pump.
- As with previous types, this one delivers a constant volume of fluid per

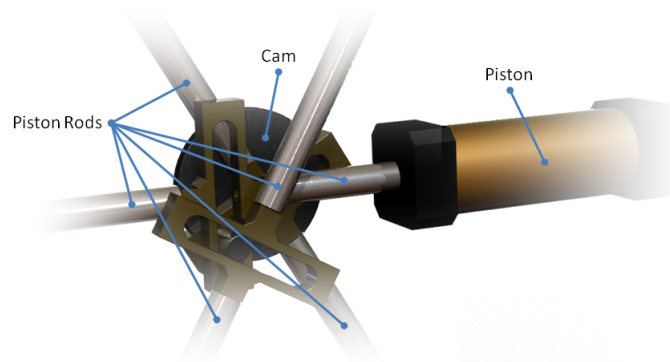


Figure 2.30: Illustration of basic piston pump mechanism

rotation of the shaft, depending on the number of pistons the output may not be as smooth as other designs, however the output is smoother as more pistons are added.

- Swash-Plate Pump

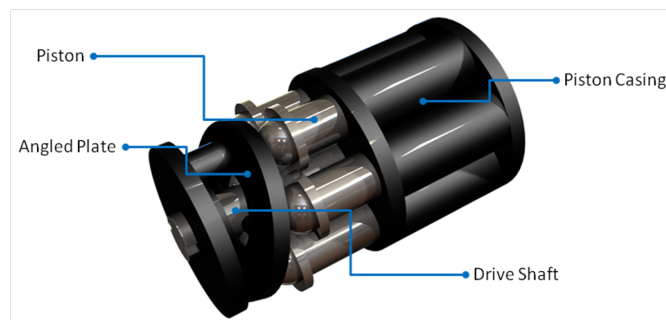


Figure 2.31: Basic Components of a Swash Plate Pump

- A swash-plate pump is a variation on a radial piston pump, however, rather than having the pistons attached to a cam, they are axial and attached to an angled rotating plate. As this plate turns it pushes the pistons which then extend with the aid of a spring. This produces a bi-

Chapter 2: Literature

direction flow from each piston which is then rectified to uni-directional flow using one way valves.

- Since the swash-plate pump is essentially a piston pump it has the same characteristics, the output gets smoother with increasing numbers of pistons. They do deliver a constant volume for each rotation; however it is possible to vary the angle of the plate in a swash-plate pump changing the flow-rate delivered.

The suitable pump for a hydrostatic bearing depends on the control strategy to be employed. If a constant load was to be supported and the clearance needed to be varied then any of the above pumps would do the job. However if a given force is required being able to control the flow-rate accurately would be an advantage which may in itself rule out the centrifugal pump. Certain types of pump cannot realistically be used in this application because they require a secondary driving pump such as an eductor-jet pump.

Figure 2.32 is derived from (2.59). Each line is essentially an isocline of pumping power. By taking a point described by a desired pressure and flow-rate the line for the power is simply the line that intersects that point.

From (2.59);

$$\begin{aligned} H_P &= Qp \\ &= T\omega_p \end{aligned} \tag{2.72}$$

For a constant flow-rate pump the value of ω is also constant. Therefore;

Chapter 2: Literature

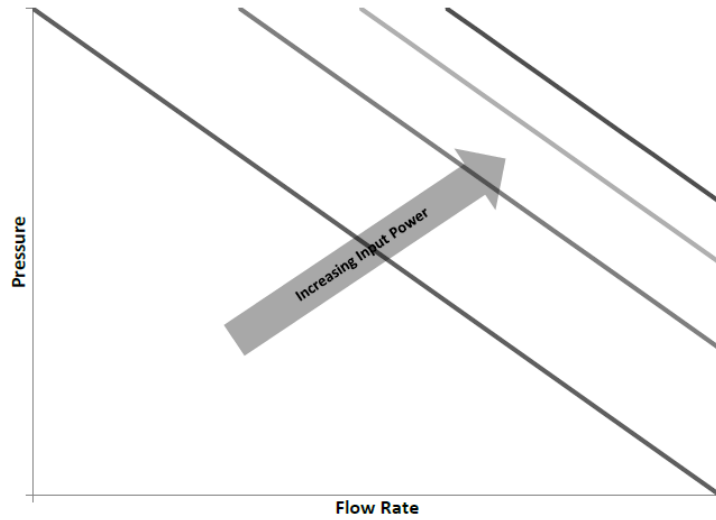


Figure 2.32: Log-Log Chart of Flow-Rate against Pressure for a Perfect Pump

$$\begin{aligned}Q &= q_0 \omega_p \\ q_0 \omega_p p &= T \omega_p \\ q_0 p &= T\end{aligned}\tag{2.73}$$

For a constant flow pump there is a direct relationship between the required pressure and the torque applied to the pump. Since there will be some mechanism for predicting the torque of a motor at a given speed, this information can be used to keep the motor running at a constant velocity until the required torque exceeds that motor's capability. All of this of course ignores the efficiency of the pump and the motor. If constant pressure is desired then a constant torque is required, if constant flow-rate is desired instead then the torque must be varied so that ω is constant.

Chapter 2: Literature

$$q_0 \frac{W}{A_e} = T \quad (2.74)$$

With more complex control it should be possible to match a variable load by varying the torque. So much so that;

$$\frac{q_0}{A_e} F(t) = T(t) \quad (2.75)$$

The torque at any given point should simply be a multiple of the load it is supporting. If a measure of the power being used by the motor is taken by the control system then if ω is known the pressure can be calculated.

$$\begin{aligned} Qp &= T\omega \\ q_0\omega p &= T\omega \\ q_0\omega p &= VI \\ \therefore T\omega &= VI \\ p &= \frac{VI}{q_0\omega} \end{aligned} \quad (2.76)$$

This is of use if a variable control strategy is employed because it forgoes the need for an additional pressure sensor. Once the efficiencies are taken into account;

Chapter 2: Literature

$$\begin{aligned} p &= \frac{VI}{q_0\omega} \prod_{k=1}^n \eta_k \\ \Gamma &= \prod_{k=1}^n \eta_k \\ \therefore p &= \frac{VI}{q_0\omega} \Gamma \end{aligned} \tag{2.77}$$

Where η_k is an efficiency for any part of the pump mechanism. Once the efficiencies, Γ , and q_0 are known, the pressure is simply a function of the power. By monitoring instantaneous values for ω and power a control mechanism should be able to regulate the pressure relatively easily.

Since there is a relationship between the pressure/load on a hydrostatic bearing and the flow-rate that the fluid is supplied, the simplest way to regulate it is to take advantage of this relationship and supply a constant flow to the bearing.

There are many different pumps that could be used for this application, however to eliminate the need for a real-time control system to balance the pressure of the pump a volumetric/positive displacement pump should be chosen. For each rotation of such a pump the same amount of fluid is expelled, therefore if the constant speed is maintained then a constant flow-rate is also maintained.

2.7 Analytical Stress Analysis

2.7.1 Bending Moments

To analyze the deformations caused by internal forces of the generator analytical stress analysis will be used^[14]. Analytical stress analysis reduces the components to beams and joints. A beam is considered to have no dimensions other than its length except to calculate the second moment of area, I .

If a horizontal beam is subject to a downward force and is mounted on a number of pins then the load on each in will obey the following;

$$W = \sum_{k=0}^n W_k \quad (2.78)$$

where W_k is the load on each pin and n is the number of pins.

The individual loads on each pin will depend on their location and the location of the other pins. The load on each pin is also its upward force therefore there numerous point forces located along the beam. By working from one end of the beam to the other the bending moment for the beam, $M(x)$, at any given point can be derived.

Since the loads are spread along the length of the beam the equation to model them will be discontinuous, this warrants the inclusion of singularity functions for each of the loads.

$$\langle x - a \rangle^n = \begin{cases} (x - a)^n & x \geq a \\ 0 & x < a \end{cases} \quad (2.79)$$

Chapter 2: Literature

where x is a position along the length of the beam and a is the location of a specific load on the beam. x and a share the same axis.

The integration of the singularity function is the same as integrating a normal set of brackets such as;

$$\begin{aligned}\int (x - a)^n dx &= \frac{(x - a)^{n+1}}{n + 1} + b \\ \int \langle x - a \rangle^n dx &= \frac{\langle x - a \rangle^{n+1}}{n + 1} + b\end{aligned}\quad (2.80)$$

The integration or differentiation of singularity functions does not affect the scope of the function. Therefore;

$$\begin{aligned}\int_0^l \langle x - a \rangle^n dx &= \int_0^a \langle x - a \rangle^n dx + \int_a^l \langle x - a \rangle^n dx \\ &= 0 + \int_a^l \langle x - a \rangle^n dx\end{aligned}\quad (2.81)$$

where $l > a$.

Once $M(x)$ has been defined the slope and displacement can be found by integrating;

$$\frac{d^2y}{dx^2} = \frac{M(x)}{EI}\quad (2.82)$$

where E is the Youngs/Elastic Modulus and I is the second moment of area. The second moment of area relates to the stiffness of the beam and is defined as;

Chapter 2: Literature

$$I = \int_a^b wy^2 dy \quad (2.83)$$

Once $M(x)$ is defined an approximation for the stress in a beam can be taken from;

$$\frac{\sigma}{y} = \frac{M(x)}{I} \quad (2.84)$$

where y is the distance from the neutral axis. The geometrical neutral axis is often used for these calculations, however because of the way materials deform in tension and compression the real neutral axis is usually biased closer to the side in compression than the geometrical neutral axis.

Example:

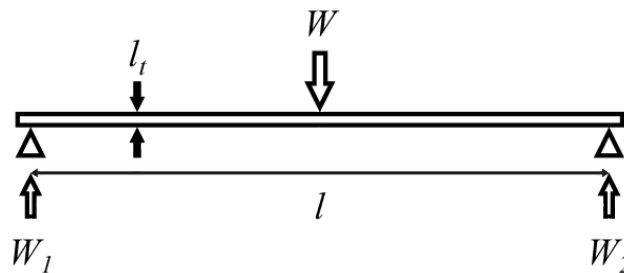


Figure 2.33: Loaded Beam Supported at 2 Points

In the case of 2.33, the load, W , is half-way between W_1 and W_2 , therefore the reaction force at both is equal to $\frac{W}{2}$ and W_1 & W_2 are separated by a distance l .

$$M(x) = W_1x$$

By taking a moment around the point x , an expression for $M(x)$ can be defined.

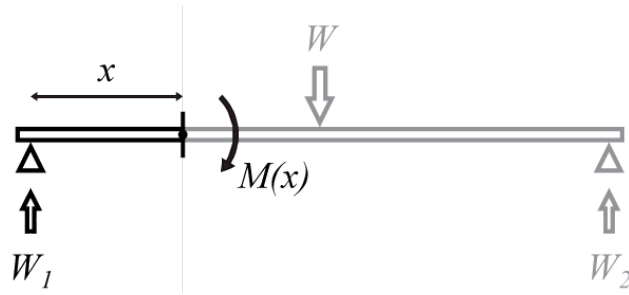


Figure 2.34: Moment about x involving W_1

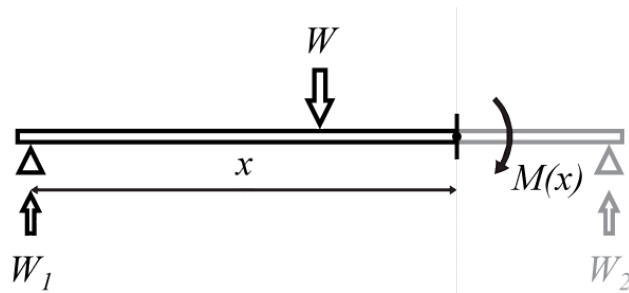


Figure 2.35: Moments about x involving W_1 & W

$$M(x) = W_1x - W \left\langle x - \frac{l}{2} \right\rangle^1$$

As x progresses this definition must be updated to include W . Since this function is now discontinuous it is necessary to include a singularity function for the effect of the load. This is true for every load applied to the beam however the form will vary depending on the type of load, i.e. distributed or point.

Since;

$$\int \frac{M(x)}{EI} dx = \frac{1}{EI} \int M(x) dx$$

Unless I is a function of x , $M(x)$ can be integrated separately.

Chapter 2: Literature

$$\frac{dy}{dx} = \frac{1}{EI} \left[\frac{W_1 x^2}{2} - \frac{W}{2} \left\langle x - \frac{l}{2} \right\rangle^2 + a \right]$$

$$y = \frac{1}{EI} \left[\frac{W_1 x^3}{6} - \frac{W}{6} \left\langle x - \frac{l}{2} \right\rangle^3 + ax + b \right]$$

Initials conditions apply;

$$\begin{aligned} @x = 0, \quad y &= 0 \\ @x = l, \quad y &= 0 \\ @x = \frac{l}{2}, \quad \frac{dy}{dx} &= 0 \end{aligned}$$

Since $dy/dx = 0$ at $x = l/2$ this is the point of maximum displacement between the two pins. To satisfy the initial conditions;

$$a = -\frac{W_1 l^2}{8} \quad b = 0$$

Therefore;

$$y = \frac{1}{EI} \left[\frac{W x^3}{12} - \frac{W}{6} \left\langle x - \frac{l}{2} \right\rangle^3 - \frac{W l^2}{16} x \right]$$

and the maximum value of y is;

$$y_{max} = -\frac{W l^3}{48EI}$$

and the maximum stress is;

$$\sigma_{max} = \frac{l_t W l}{8I}$$

where l_t is the thickness of the beam.

2.7.2 Vibration

The beam can be viewed as a linear spring where;

$$F = kx \tag{2.85}$$

or in this case;

$$W = ky \tag{2.86}$$

where, at $x = l/2$;

$$k = \frac{96EI}{5l^3}$$

As such the natural frequency^[35] of the beam between the two support points can be estimated;

$$\omega_0 = \sqrt{\frac{k}{m}} \tag{2.87}$$

This will not be the true frequency in most cases however due to the extra material beyond the supports and potential additional points of support. For these circum-

Chapter 2: Literature

stances a more complex analysis is required. However (2.87) should give at least indicate the order of magnitude of the frequency, and how it should behave. As expected, the frequency increases as the support spacing decreases. It also varies with the second moment of area and elastic modulus.

Since the majority of applications for linear generators will have very low driving frequencies, less than 1Hz, it is highly unlikely that any sympathetic vibrations would occur within the device.

Chapter 3:

Methodology

This thesis is not an attempt to completely model any given generator design but to present, discuss and evaluate different concept designs based on the criteria given in this chapter. Much of the technical portions have been included to give an understanding of why certain changes were beneficial and what the specific problems were. In some cases approximations have been made that aid in the comparison of these concepts.

3.1 Criteria

Since the research has expanded beyond the original brief its goal has become looking for ways to produce concepts & designs that make linear generators more economically viable. The assessment of each will primarily be based on power usage and generation, economics impacts and reliability changes inherent to the new concepts.

3.1.1 Bearing Power Usage

The bearing power usage will be looked at in two ways;

1. Determine the power necessary to support the generator on hydrostatic bearings and use that to calculate the efficiency of the system as a whole under different topologies and operating environments.
2. Determine the losses of standard bearings under the same conditions and compare the power loss in the bearings with the power usage in the hydrostatic bearings.

By investigating these two factors it should be possible to state a case for the viability of hydrostatics as an option and the viability of the other designs conceived in this research.

From equations 2.50 and 2.59 the power usage of hydrostatics bearings is assumed to be;

$$H_P = \frac{WQ}{A_e} \quad (3.1)$$

and throughout this work this equation or variations there of will be used to indicate power consumption.

3.1.2 Power Generation

The power generation will be assessed by looking at the potential power output of each varied design. In many cases this will be related to the magnet density in the machine, i.e., the volume of magnets that can be equipped per a given flux carrier cross section. Since the concepts will eventually be evaluated using magnetic circuit theory the total air-gap in the circuit will also have an impact on the potential power output of the generator. However, from section 2 it can be shown that the flux within a flux carrier can be predicted and that if a specific flux is desirable then it can be achieved by looking at the size of magnets and the air-gaps involved.

There is also a limiting factor introduced by the power generation criterion thanks to the need to efficiently use the permanent magnets installed. From equation 2.4 it is clear that there is a relationship between the flux within the flux carrier

Chapter 3: Methodology

and cross-sectional area of the flux carrier. Put simply if there is insufficient area the carrier will saturate and some of the strength of the magnets will be wasted. Likewise if the area is too large then the flux in the carrier will be too low and the output will be reduced, therefore it is important that there is enough flux carrier cross section to carry the required flux. Additionally, the placement will affect the flux too because of the magnetic short circuit effect, as shown in Figure 2.17.

Chapter 4 introduces an approximation for the maximum power output of a set of generating components and demonstrates how it is applied. The basic principles of this approximation are included in each of the concept designs. It should be noted that this approximation is intended solely for comparative purposes, and illustrates a mechanism by which designs can be compared regardless of the actual power output that such a generator would achieve in the real world.

3.1.3 Economic Factors

Economic factors will include;

- Manufacturing Costs
- Transport Costs
- Operation & Maintenance Costs
- Life-span, Reliability & Output

They will be affected by the simplicity of the designs, the power usage, material choices, and the weight of the devices. The weight of the device factors heavily into the transport costs and the operation and maintenance costs, dictating in part

Chapter 3: Methodology

the types of vehicles and equipment necessary to transport and install a generator. Material choices affect weight, manufacturing cost and lead times. Since a large proportion of the weight will be due to the weight of the flux carrier in each design it is important to remember what was stated about the necessities of flux carrier cross-sections in 3.1.2.

Manufacturing costs will be influenced by the material and the complexity of the components being made. As a rough guide the costing would look as follows;

$$Cost_{constructiontotal} = \frac{1}{1 - f_{failure-rate}} (Cost_{material} + Cost_{equipment} + Cost_{labour}) \quad (3.2)$$

Depending on materials and complexity different equipment will be required and differing levels of skill required by the labour force. A certain proportion of the components created will not be fit for purpose and this percentage will be the failure rate. Simple components will have a lower failure rate and cost in equipment and labour.

The major contributors to the mass of a generator will be the iron & copper in the generation components and the structural materials. Support hardware will introduce additional masses to the structure which will be particularly relevant to hydrostatic bearings since they require pumps.

$$m_{total} = m_{iron} + m_{copper} + m_{structural} + m_{support} \quad (3.3)$$

Since there is a relationship between the cost of transport and the mass of the devices reductions in each element will have a positive impact on the transport costs. Since there is a direct link between generating capacity and the volume of

Chapter 3: Methodology

copper in the machine reducing the copper in many cases may not be possible so reductions in iron and structural masses will be key.

Operation and maintenance costs are one of the greatest limiting factors in deployment of wave devices in general. The cost of performing maintenance on offshore structures such as wave generators, especially if they are fully submerged like the AWS^[27], is very high. If in-situ maintenance is not possible for one reason or another then the only option is to drydock the device requiring a crane barge and many man-hours of labour.

For the purposes of this work the operations and maintenance costs would be based on the amount of downtime or reduced capacity the generator suffers and the cost of equipment and personnel hired to perform the maintenance and repairs.

$$\begin{aligned} Cost_{O\&Mtotal} = & (Cost_{equipment-hire} + Cost_{personnel}) t_{repair} + \\ & (Income_{max} - Income_{reduced}) t_{downtime} \end{aligned} \quad (3.4)$$

In (3.4) the cost of equipment hire and personnel will be related to the length of the repairs, t_{repair} , and the lost revenue will be related to the length of the downtime, $t_{downtime}$, here taken to mean periods complete inactivity or operation at reduced capacity. A period of complete inactivity results in a $Income_{reduced}$ value of zero.

All of this means that operation & maintenance costs for these devices are high. Since this is a primary focus for the application of linear generators a drop in the operation and maintenance costs would increase the commercial viability of the devices in general. This can be achieved either by improving the amount of in-situ maintenance that is possible or by increasing the reliability of the device. Ideally

in-situ maintenance should not involve the larger vessels, such as crane barges, greatly reducing the costs.

3.1.4 Reliability Factors

Reliability factors will relate to;

- Component Redundancy
- Component/Superstructure Longevity
- Overall System Adaptability
- Failure and Disaster Control/Prevention

Overall system adaptability relates to the ability for the control system to compensate for failed components. Any generator structure must be able to account for a failed component and compensate for it and/or detect and imminent failure and shut down the generator before severe damage occurs. From an economic standpoint the reliability of a machine is key to whether it is commercially viable or not, the more downtime a machine incurs because of failures the less profitable it becomes. As such it is essential that, rather than being an after thought, the reliability and controllability of a design be considered during its inception.

By adding redundancy the devices reliability should increase, provided it is implemented properly. The longevity of the components based on normal use and material choices is also a key factor to reliability, for example using unprotected iron in sea-water would have very poor longevity. Choices of material and protection play a key role in all areas of generator design. In some areas it may not

be possible to exchange materials, such as in the flux carriers due to the need for magnetically permeable materials to be present.

The overall impacts of the reliability factors is the change of the t_{repair} and $t_{downtime}$ values in (3.4), due to the changed frequency of repairs for a given timescale.

3.1.5 Control Strategy

Hydrostatic Control

All designs within this work using hydrostatic bearings have a constant-flow control strategy. To achieve this, the pumps supplying fluid to the bearings are constant volume pumps driven by a motor attached to a constant velocity controller. As stated previously, a constant volume pump driven at a constant velocity will deliver a constant flow. The reason for choosing this control strategy is that if the flow-rate into a bearing is kept constant then the bearing acts like a non-linear spring. From equation 2.57;

$$\begin{aligned} W &= L_H \frac{Q}{h^3} \\ W &= L_H \frac{Q}{(h_0 + \Delta h)^3} \end{aligned} \tag{3.5}$$

Where h_0 is the land clearance at equilibrium and Δh is the variation in clearance under load. A variable flow-rate approach is possible but the control algorithms and hardware are more complex. Constant flow can be achieved with very basic and reliable hardware. Additionally, the power loss across a pipe is related to the

flow-rate through the pipe rather than the pressure within it. As such maintaining a constant or near-constant flow-rate should help to keep a constant power loss in the fluid supply pipes.

3.2 Summary

In summary, the concepts presented here will be compared on the basis of some, if not all, of the following;

- Power Losses/Usage in the bearings (Mechanical or Hydrostatic) and pumps
- Power Generation Potential based of the key elements of flux, coil dimensions and operational frequencies
- Economic factors such as reduction in material costs, O&M costs and transport costs
- Reliability of Generator as a whole, redundancy, adaptability and ease of maintenance

Chapter 4:

Evaluation of Rigidly Structured Generators

4.1 Introduction

This section of the work refers to the original evaluation of how hydrostatic bearings would perform in a linear generator. Most of the work has been done on a translator with a rectangular section. Also included in this section is information on other issues identified whilst doing this evaluation.

4.1.1 Defining a Rigidly Structured Generator

For the purposes of this research a rigidly structured generator is a device where the bearings used, to support a translator or rotor, are directly attached to the superstructure of the generator. In this circumstance whatever direct load is experienced by the bearing is transferred into the superstructure of the generator and is responsible for the stress there in.

For much of the work, a perfect rigid device will be assumed, meaning that the superstructure and translator is stable and dimensionally perfect. A perfect generator in real terms is an impossibility and later sections will cover the affect of defects in construction or caused by damage.

The superstructure will be assumed to be rigid; however the translator will be able to bend if necessary.

4.1.2 Issues

The primary issue with a rigidly framed generator is that any small deviations in the structure of translator, caused by improper manufacturing or damage suffered

during operation, cause increased bearing loadings which at best increases the power consumption of the machine and at worst can cause a catastrophic failure. In addition the increased bearing loadings increase the stresses applied to the superstructure of the generator, having implications to the design of the generator superstructure and choice of materials.

4.1.3 Applying Hydrostatic Bearings

The application of hydrostatic bearings to linear generators depends on the type of translator to be used and the degrees of freedom required. A device that uses a square or rectangular translator would require a minimum of 6 bearings to fix both position and rotation. The use of only 4 is possible, however the bearings would need to be paired up and supporting opposite corners. A device that uses a translator with a circular cross-section can use as few as 3 bearings to lock its position, but does not require that its rotation be fixed. Since hydrostatic bearings in essence function like non-linear springs, for a given flow-rate, any position and rotation is a matter of degrees. Any external force or torque will cause a change in the loading on bearings and a corresponding change in the land clearances. As a result the clearances may deviate from the design specification when sufficient external load is applied. With all designs there will be limitations in the range to which the clearances can change before a catastrophic failure would occur within the generator.

As the pressure is increased in the bearings they will offer greater support at the cost of increased power consumption. From the basics of hydrostatic bearing operation it became apparent that;

Chapter 4: Evaluation of Rigidly Structured Generators

- operating them at a constant pressure could be risky and prove generally costly
- adding a pressure control system to adapt to changing forces would add extra hardware and complexity to the system
- operating at a constant flow-rate, using the right pump and a constant velocity controller for the driving motor, would essentially create a hydrostatic spring which would serve the purpose and be simple to implement.

From (2.50) & (2.59);

$$H_P = pQ = \frac{WQ}{A_e}$$

Therefore, the flow-rate and bearing design will dictate the pump power consumption of a given load, or;

$$H_P = pQ = \frac{W^2 h^3}{A_e L_H}$$

where a fixed clearance and design would dictate the power consumption for a given load. It would seem, ideally, that it would pay to have the flow-rate as low as possible, however this links with the clearances. The practical upshot of this is that if the clearance is small for the hydrostatic bearings then a small flow-rate can be used and the power consumption will remain low. The clearances of the magnets and bearings do not need to be the same; therefore it is quite possible to use a much smaller clearance for the bearings.

4.2 Bearing Spacing

The spacing of the bearings will affect the maximum deflection caused by any applied force. As the spacing between the bearings is decreased the maximum deflection between them is also reduced, however it increases the number of bearings that are required in order to support the translator and the power consumed by them increases.

The maximum deflection has implications as far as power generation and tolerances is concerned, since too great a deflection would bring the translator too close to the magnets in the generating mechanism. Also since there is also a force from the magnets within the generating mechanism, too much of a deviation from the equilibrium position would result in increased stresses.

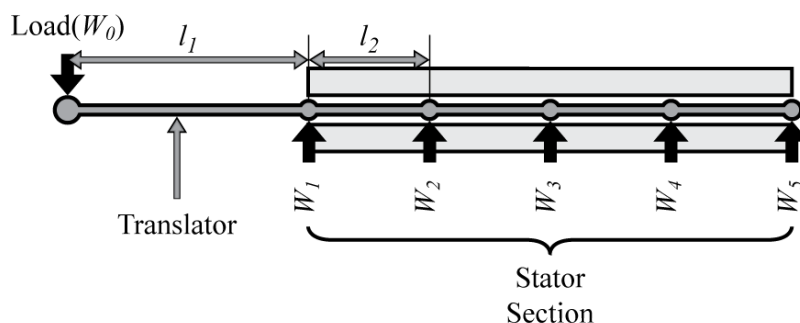


Figure 4.1: Example Arrangement of Bearings for a Linear Generator ($n = 5$)

An arrangement of n bearings is described by the following moments matrix;

$$\left[\begin{array}{ccc|c} 0 & \cdots & (k-1)l_2 & W_0 l_1 \\ \vdots & \ddots & \vdots & \vdots \\ (1-k)l_2 & \cdots & 0 & W_0(l_1 + (k-1)l_2) \end{array} \right] = \begin{bmatrix} W_1 \\ \vdots \\ W_k \end{bmatrix} \quad (4.1)$$

Chapter 4: Evaluation of Rigidly Structured Generators

When a load W_0 is applied a distance l_1 from the lead bearing and l_2 is the spacing between the bearings. To account for any number of bearings within the generator the moment at any given axial location x would be;

$$M(x) = W_0x + \sum_{k=1}^n W_k \langle f(x, k) \rangle^1$$

$$f(x, k) = x - l_1 - (k - 1)l_2 \quad (4.2)$$

From (2.63) the slope and displacement would be;

$$\frac{dy}{dx} = \frac{1}{6EI} \left\{ 3W_0x^2 + 3 \sum_{k=1}^n W_k \langle f(x, k) \rangle^2 + A \right\}$$

$$y = \frac{1}{6EI} \left\{ W_0x^3 + \sum_{k=1}^n W_k \langle f(x, k) \rangle^3 + Ax + B \right\} \quad (4.3)$$

If the value of y at any point exceeds the maximum tolerance for the generator then the bearing has failed. All the values for W_k , A and B are dependant on the number of bearings used in the design. The matrix in equation 4.1 will outline the relationships between the supports however solving it is not possible as it stands.

$$R(x) = \frac{1}{6EI} \left\{ x^3 + \sum_{k=1}^n R_k \langle f(x, k) \rangle^3 + \frac{Ax}{W_0} + \frac{B}{W_0} \right\} \quad (4.6)$$

$$R_k = \frac{1}{W_0} W_k \quad (4.7)$$

$$R_{max} = \frac{1}{W_0} y_{max}$$

Once R_k has been found for each case the maximum supported load, at a given distance, can be determined simply by inserting the highest tolerable displacement. The loads, $W_1 \rightarrow W_n$, can be applied to the hydrostatic bearing equations to give required flow-rates, for a given clearance, or clearances for a given flow-rate, and power required to support said load. From (2.43);

$$W_n = L_H \frac{Q_n}{h_n^3} \quad (4.8)$$

and from(2.46);

$$H_{P_n} = \frac{W_n^2 h_n^3}{A_e L_H} \quad (4.9)$$

where the bearing design, including A_e and L , is fixed. The total losses for the machine should be;

$$P_L = \sum_{n=1}^k H_{P_n} \quad (4.10)$$

For an example beam supported on different numbers of bearings the following table gives the reaction forces from the supports for a 10kN load placed at a distance of 6m from the first bearing. The dimensions and loads chosen for this

example are arbitrary and intended to demonstrate the method.

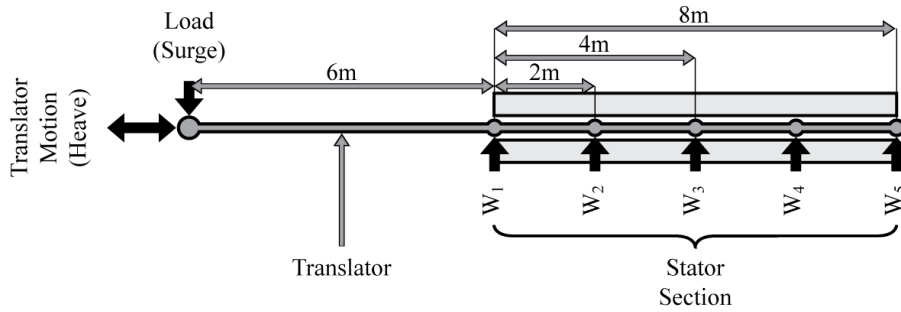


Figure 4.2: Test Beam Layout

Bearings	Spacing	W_1	W_2	W_3	W_4	W_5
2	8m	17.5 kN				-7.55 kN
3	4m	28.9 kN		-22.7 kN		3.79 kN
5	2m	48.2 kN	-48.5 kN	12.9 kN	-3.22 N	0.54 kN

Table 4.1: Support Reaction Forces

Figure 4.3 is derived from FEA results, from Solidworks Simulation, and shows the comparative deflection of a loaded beam supported on different numbers of bearings. The scale for each set of results is the same but has not been included since it is the comparison which is important. In the case of a rigid linear device the deviation needs to be very small and therefore to tolerate larger forces a greater number of bearings is required within the generator.

As the number of bearings increase, and therefore the bearing spacing decreases, the reaction forces increase. This is due to the reduction in the flexibility of the beam. Since the force in the bearing is directly related to the power consumption/losses, using fewer bearings reduces the power consumption overall.

As is clear from Figure 4.3 the greater the number of bearings included in a design the more rigidly the translator is held. Therefore the force on the leading bearings

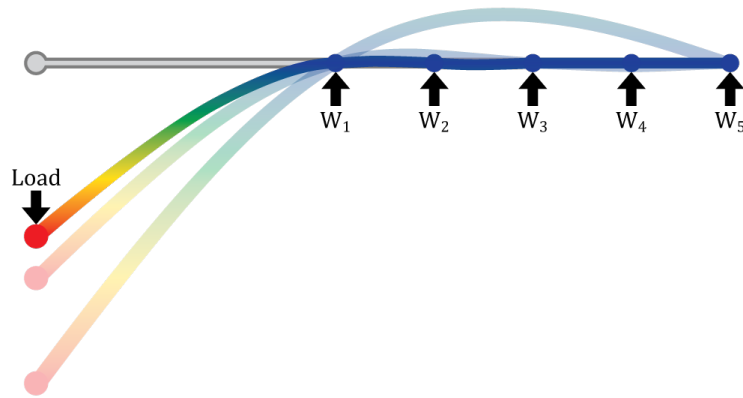


Figure 4.3: Deflection of an Arbitrary Beam Supported at 2, 3 and 5 Points

also increases as the number of bearings increases.

From Table 4.1 it can be seen that the total force supported by the lead bearings of a generator can be several times that applied to the translator. The total power consumption of the bearings, assuming constant flow-rate, will be;

$$P_L = \frac{Q}{A_e} \sum_{i=0}^n |W_n| \quad (4.11)$$

Figure 4.4 shows a cross section through the magnets and translator in the generating stage of a variable reluctance generator. The separation (h) of the magnets and translator is small, and since it will be subject to deviation if an external forces is applied to the translator the separation will be a tolerable range rather than a value. This operational range determines the maximum deviation that can be tolerated by the generator. The operational range is determined by the interaction between the bearings and the magnets.

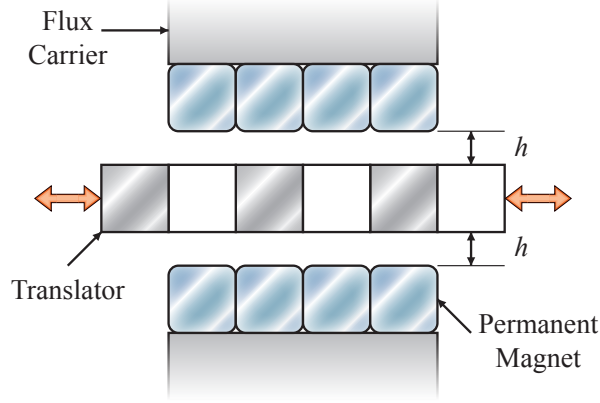


Figure 4.4: Variable Reluctance Generator Cross-Section

$$\begin{aligned}
 F &= L_H Q \left(\frac{1}{(h + \Delta h)^3} - \frac{1}{(h - \Delta h)^3} \right) + M_m \left(\frac{1}{(h - \Delta h)^2} - \frac{1}{(h + \Delta h)^2} \right) \\
 F &= M_m \frac{4\Delta h h}{(h^2 - \Delta h^2)^2} - L_H Q \frac{6h^2 \Delta h + 2\Delta h^3}{(h^2 - \Delta h^2)^3} \\
 \therefore (h + \Delta h)^3 (h - \Delta h)^3 &= (h^2 - \Delta h^2)^3 \quad (4.12)
 \end{aligned}$$

from an analytical perspective the range is dictated by the balance point between the magnetic forces and hydrostatic bearings, where $F = 0$.

Where M_m is the collected magnetic constants, see (2.23), and h is the land clearance of the hydrostatic bearings in designs where magnets and bearings have the same separation from the translator. The balance point occurs at;

$$\begin{aligned}
 \Delta h &= h \sqrt{\frac{2M_m h - 3L_H Q}{2M_m h + L_H Q}} \\
 &= h \sqrt{1 - \frac{4L_H Q}{2M_m h + L_H Q}} \quad (4.13)
 \end{aligned}$$

therefore, since Δh must be a real number.

$$4LQ \leq 2M_m h + L_H Q$$

$$\frac{3}{2}L_H Q \leq M_m h \quad (4.14)$$

therefore the minimum value for M_m is;

$$M_m = \frac{3L_H Q}{2h} \quad (4.15)$$

At this value of M_m and values below it the balance point is central. As the value of M increases the balance point moves outward. From (4.10) it is possible to derive a relationship for the value of Q to give a specific balance point;

$$Q = 2 \frac{Mh \left(1 - \left(\frac{\Delta h}{h}\right)^2\right)}{L_H \left(\left(\frac{\Delta h}{h}\right)^2 + 3\right)} \quad (4.16)$$

The balance point can be chosen to give a margin of safety for the device during operation, as such the Δh value chosen is essentially a safety factor.

If the bearings are closer to the translator surface than the magnets then this problem is largely obviated since the force generated by the magnets does not build as rapidly as that from the bearings.

Although magnetic circuit theory says that as long as the total air-gap within a circuit remains constant the flux will also stay constant, the forces are not so obliging. As the translator moves off-centre the lateral forces on increase dragging it further off centre. As a result the bearing loads increase.

4.3 Defects

If a defect is introduced into the translator or one of the bearings is out of position then it will affect the losses in the bearings and the stresses caused. The effect is different depending on the type of bearings used.

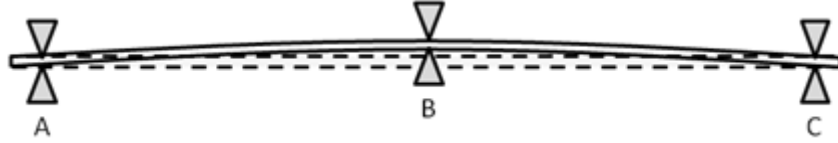


Figure 4.5: Flawed Bearing Arrangement (B displaced from ideal position)

If it is assumed that the translator is held rigidly then it is possible to estimate the resultant clearance in the bearing and the additional power used to maintain it.

If a bar is mounted on two points and forced to deform by a given distance then the force (W) can be estimated. For such a bar the displacement caused by a centrally applied force is;

$$y = \frac{1}{EI} \left\{ \frac{W}{12}x^3 - \frac{W}{6} \left\langle x - \frac{l}{2} \right\rangle^3 - \frac{Wl^2}{16}x \right\} \quad (4.17)$$

The maximum displacement is in the centre, therefore;

$$y_{max} = -\frac{Wl^3}{48EI} \quad (4.18)$$

The additional load applied would be;

$$W = -48EI \frac{y_{max}}{l^3} \quad (4.19)$$

Obviously, the greater the distance between the supports the easier it will be to cause a given deflection. The way this increase in load affects the performance of the machine will depend on the type of bearing used.

4.3.1 Hydrostatic Bearings

In the case of hydrostatic bearings if a defect is present it will increase the load on the bearing and the clearance of the bearing. If the defect is larger than the clearance of the bearing then the force is even higher. The net force generated by a pair of opposing hydrostatic bearings for a given offset, Δh , is;

$$\frac{F_{net}}{L_H Q} = \frac{6h^2 \Delta h + 2\Delta h^3}{(h^2 - \Delta h^2)^3} \quad (4.20)$$

The net load/displacement curve is;

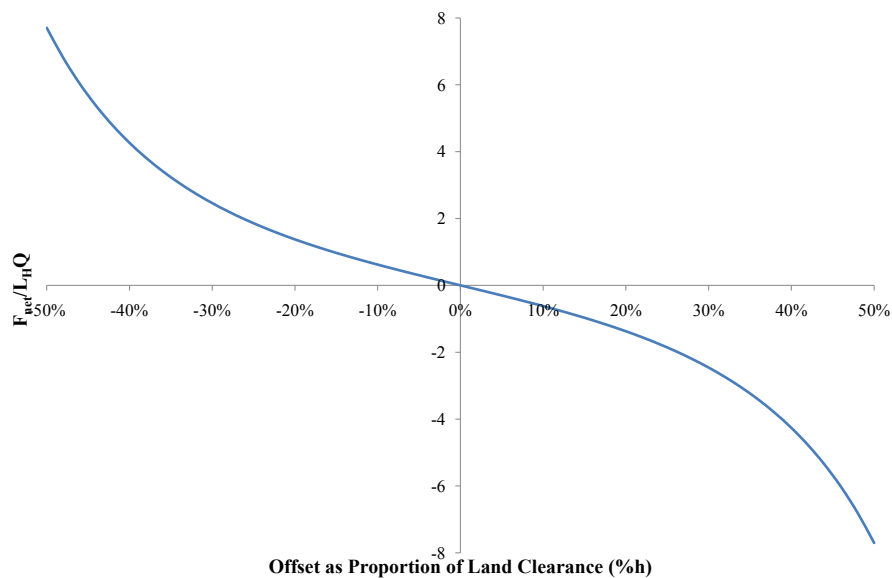


Figure 4.6: Load/Displacement Plot

Chapter 4: Evaluation of Rigidly Structured Generators

The load can then be matched with the land clearance of the hydrostatic bearings to find the clearance change that would result. This is done by equating the net force, F_{net} , to the load, W . Although this yields the change in position caused by a given force it does not give the stresses in the underlying members. These must be determined separately for each of the pair of bearings.

The change in the required power can be calculated from;

$$\begin{aligned}
 H_{P_0} &= pQ = \frac{L_H Q^2}{A_e h^3} \\
 H_{P_{1a}} &= pQ = \frac{L_H Q^2}{A_e (h + \Delta h)^3} \\
 H_{P_{1b}} &= pQ = \frac{L_H Q^2}{A_e (h - \Delta h)^3}
 \end{aligned} \tag{4.21}$$

Therefore the total power required to operate the bearings in the offset position is;

$$\begin{aligned}
 \sum H_P = H_{P_{1a}} + H_{P_{1b}} &= \frac{L_H Q^2}{A_e} \left(\frac{1}{(h + \Delta h)^3} + \frac{1}{(h - \Delta h)^3} \right) \\
 &= \frac{L_H Q^2}{A_e} \frac{6\Delta h^2 h + 2h^3}{(h^2 - \Delta h^2)^3}
 \end{aligned} \tag{4.22}$$

As the translator is forced away from the equilibrium position the power consumption increases. The power consumption for the support arrangement is the sum total of all the bearings in it. Expanding on Table 4.1;

The specific parameters used to generate the information in Table 4.2 are listed in 4.3. The fluid has been chosen to be sea water as is reflected in the value for dynamic viscosity. A 2mm clearance is desirable for a high efficiency generator.

Chapter 4: Evaluation of Rigidly Structured Generators

	Bearing	Spacing	W_1	W_2	W_3	W_4	W_5	Total Power
FEA	2	8m	17.5 kN				-7.55 kN	
Analytical			17.5 kN				-7.5 kN	
		Δh	1.57 mm				-1.44 mm	
		H_P	20.7 W				9.0 W	29.6 W
FEA	3	4m	28.9 kN		-22.7 kN		3.79 kN	
Analytical			28.75 kN		-22.7 kN		3.75 kN	
		Δh	1.64mm		-1.61mm		1.29mm	
		H_P	33.8 W		26.7 W		4.5 W	65.1 W
FEA	5	2m	48.2 kN	-48.5 kN	12.9 kN	-3.22 kN	0.54 kN	
Analytical			48.0 kN	-48.2 kN	12.9 kN	-3.21 kN	0.54 kN	
		Δh	1.70 mm	-1.70 mm	1.53 mm	-1.25 mm	0.70 mm	
		H_P	56.6 W	56.6 W	15.3 W	3.9 W	0.8 W	133.2 W

Table 4.2: Extension to Table 4.1 including power and offset

The rest are arbitrary and included for the sake of completeness.

Parameter	Value
L_H	$1.69 \times 10^{-4} N_s$
Q	$80 cm^3 s^{-1}$
A_e	$6.80 \times 10^{-2} m^2$
h	$2 \times 10^{-3} m$
μ_h	$1.88 \times 10^{-3} Pas$

Table 4.3: Additional parameters required for Table 4.2

From this it is clear that increasing the number of bearings not only increases base power consumption, because there are more bearings involved, but as the number of bearings increases so do the loads and in turn the individual power consumption. Therefore a machine with few bearings will be more energy efficient than one with many.

4.3.2 Non-fluid Bearings

Whereas the power lost in hydrostatic bearings can be considered to be the power required to operate them at a given load and flow-rate, the power loss in normal continuous contact bearings can be considered to be a function of the friction within them. As the load on a mechanical bearing increases the friction coefficient will vary, however there is usually a given range of loads where the bearings coefficient will change very little. Therefore;

$$F_f = C_f W \quad (4.23)$$

Where W is the load applied to the bearing, as in the previous sections. In this case the friction force is directly proportional to the bearing load. As such the power loss is the product of the frictional force and the translator velocity;

$$H_P = F_f v_t \quad (4.24)$$

Therefore the power loss through each n^{th} bearing is;

$$H_{P_n} = C_f W_n v_t \quad (4.25)$$

since all the bearings are subject to the same translation velocity.

The deflection in such bearings is a different matter. For the sake of this analysis they can be considered to be solid blocks of metal, as such;

Chapter 4: Evaluation of Rigidly Structured Generators

$$E = \frac{\sigma}{\epsilon} \quad (4.26)$$

Therefore the deflection is described as;

$$h = h_o \frac{W}{AE} \quad (4.27)$$

Where A is the cross-sectional area of the bearing, E is the young's modulus and h_o is the original thickness of the bearing. In the case of ball or roller based bearings the area should be reduced to match the contact area in the bearings.

Since the distribution of the loads will be the same regardless of the bearing type being used, the deflections and the power consumptions can be calculated for the same scenario as was used previously;

	Bearings	Spacing	W_1	W_2	W_3	W_4	W_5	Total Power
FEA	2	8m	17.5 kN				-7.55 kN	
Analytical			17.5 kN				-7.5 kN	
		F_f	26.25 N				11.25 N	
		H_P	42 W				18 W	60 W
FEA	3	4m	28.9 kN		-22.7 kN		3.79 kN	
Analytical			28.75 kN		-22.5 kN		3.75 kN	
		F_f	43.13 N		33.8 N		5.6 N	
		H_P	69 W		54 W		9 W	132 W
FEA	5	2m	48.2 kN	-48.5 kN	12.9 kN	-3.22 kN	0.54 kN	
Analytical			48 kN	-48.2 kN	12.9 kN	-3.21 kN	0.54 kN	
		F_f	72.0 N	72.3 N	19.4 N	4.8 N	0.8 N	
		H_P	115 W	115 W	31 W	7.7 W	1.3 W	270 W

Table 4.4: Mechanical Bearing Data Table

A coefficient of friction of 1.5×10^{-3} has been assumed^[41]. For the power calculations an average velocity of $1.6ms^{-1}$ has been assumed (average velocity for a 5m

sinusoidal oscillation over 10 seconds). Deflections have been omitted from this table since they will be very small for most bearing materials.

The coefficient of friction of bearings is generally stated in air or oil, the effect of being submerged in water can change the performance of the bearing drastically.

4.4 Performance & Losses

The key factors to creating a working generator will be to create the greatest output for the smallest losses. From (2.60) the power consumed by a hydrostatic bearing (ignoring the supply mechanism) is;

$$H_{P_n} = \frac{W_n^2 h_n^3}{A_e L_H} \quad (4.28)$$

Therefore it is important, for a given A_e and L_H , to either reduce the load (W), the land clearance (h) or both. Reducing the land clearance may work well in theory but in practice it may well be problematic. In ideal cases the land clearances might be sub-millimetre however it is difficult to maintain the necessary accuracy during construction, which leads to attempting to reduce the loads and the land clearance simultaneously. Care must be taken when designing the bearings. If possible high values for A_e must be sought. L_H is related to the bearing dimensions too and therefore will vary, to some degree, with A_e .

Since some of the force that is applied will be due to the magnets this force should be minimized too, however reducing the magnetic force requires that the B-field be reduced and doing this will reduce the power output. As a result an attempt to

Chapter 4: Evaluation of Rigidly Structured Generators

reduce the losses would also reduce the output. Additionally the power output of the generator is load dependant. The maximum power it could produce is limited by its own internal resistance. From (2.32) and (2.33);

$$P \approx f_A \frac{A_C}{L_P \rho_r} (\varphi')^2 \quad (4.29)$$

This equation could be applied for the total AC for the generator if the flux variations were synchronized but if this were the case there would be large cogging forces on the generator components. Therefore the flux changes are slightly out of sync for each set of magnets in the generator.

The φ' is dependant on the maximum flux within a circuit. This is determined, in part, by the air-gap between the magnets and the translator. This in turn is related to the spacing of the bearings since that affects the maximum deviation in the translator. To reduce the number of bearings, the maximum allowable deviation in the translator must increase, this in-turn increases the air-gap for the magnets and decreases the flux in the magnetic circuit. If it is assumed that φ is represented as a triangle wave related to displacement, approximated by a fourier series;

$$\varphi = \varphi_0 \frac{8}{\pi^2} \sum_{k=0}^{\infty} (-1)^k \frac{\sin((2k+1)\omega_2 s)}{(2k+1)^2} \quad (4.30)$$

$$\varphi' = \varphi_0 \omega_2 \frac{ds}{dt} \frac{8}{\pi^2} \sum_{k=0}^{\infty} (-1)^k \frac{\cos((2k+1)\omega_2 s)}{2k+1} \quad (4.31)$$

where;

Chapter 4: Evaluation of Rigidly Structured Generators

$$s = A_t \cos \omega_1 t \quad (4.32)$$

Then it is directly proportional to φ_0 which represents the maximum flux within the magnetic circuit. As is explained in section 2.5.2 this is not completely accurate because of the interaction between flux and current, but for the purposes of this evaluation it will serve as a first approximation. Since the form of this is a square wave the φ'_{max} is;

$$\varphi'_{max} = \varphi_0 \omega_2 s'_{max} \quad (4.33)$$

where s is the displacement of the translator and ω_2 is the slot frequency.

$$s'_{max} = A_t \omega_1 \quad (4.34)$$

By using φ'_{max} in place of φ' in (2.32) an indication of the maximum power can be determined. Since φ' for the purposes of this evaluation is a square wave $(\varphi')^2$ is more or less a constant therefore using φ'_{max} will give a maximum achievable power. This does assume that the current is in phase with the driving EMF and that the inductance of the coil is zero. Therefore;

$$P_{max} \approx f_A \frac{A_C}{L_P \rho_r} (\varphi_0 A_t \omega_1 \omega_2)^2$$

From Figure 2.19 it can be seen that the waveform for the power output is similar enough that a sawtooth wave can be used as a first approximation. As such the RMS power output would be;

$$P_{rms} \approx \frac{1}{\sqrt{3}} f_A \frac{A_C}{L_P \rho_r} (\varphi_0 A_t \omega_1 \omega_2)^2 \quad (4.35)$$

since for a sawtooth wave^[28];

$$P_{rms} = \frac{1}{\sqrt{3}} P_{max}$$

From (2.39);

$$\varphi(t) = \varphi_m f(t) + \varphi_c I(t)$$

Since φ_0 represents the maximum, positive flux that can be achieved in the generator and current depends on the loading, for this comparison;

$$\varphi_0 = \varphi_m$$

Since $f'(t)$ represents the Fourier series in (4.31), from (2.38);

$$\varphi_0 = \varphi_m = \frac{AB_{rem} l_{magnet}}{l_{air-gap} + l_{magnet}}$$

4.5 Scaling

The basis for the scaling analysis is based of the dimensional analysis of the various governing equations once the embedded constants have been removed. For

example;

$$m = \mathbf{M} \quad (4.36)$$

$$m = \rho v \quad = (ML^{-3}) (L^3) \quad (4.37)$$

If ρ is assumed to be a constant then;

$$m \propto L^3 \quad (4.38)$$

and therefore, for a uniform scale factor of G , will scale by G^3 .

The key relationships for determining the effect of direct scaling of a machine are as follows;

4.5.1 Hydrostatic Bearing Scaling

$$F_1 = L_H \frac{Q}{h^3} \Rightarrow F_2 = \frac{1}{G} F_1 \quad (4.39)$$

Assuming that the flow-rate remains unchanged.

From this is it clear that to maintain the force on the translator at the new clearance the flow-rate must be increased by a factor of G . Since the mass of the translator has also increased, to create the same effective stiffness the force would need to be increased by a factor of G^3 . In order to do this the flow-rate would have to be increased far more. Therefore to maintain the same characteristics in the new circumstances the flow-rate in the bearing would need to be increased by a factor of G^4 . Doubling the size of each component in the machine would result in a 16 fold increase in the power drawn from the bearings. This suggests

that the bearings and clearances need to be specified for each design of machine individually.

$$H_{P_1} = \frac{L_H Q^2}{A_e h^3} \Rightarrow H_{P_2} = \frac{1}{G^3} H_{P_1} \quad (4.40)$$

If the flow-rate in the bearings needs to increase by a factor of G^4 then the power drawn will increase by a factor of G^5 .

4.5.2 Permanent Magnet Scaling

$$P_{rms_1} \approx \frac{1}{\sqrt{3}} f_A \frac{A_C}{\overline{L_P} \rho_r} (\varphi_0 A_t \omega_1 \omega_2)^2 \Rightarrow P_{rms_2} = G^3 P_{rms_1} \quad (4.41)$$

A_T and ω_1 are unchanged by the scaling since they relate to the wave motion itself. φ_0 is related to the active area of the magnets and the clearance, and therefore scales accordingly. ω_2 is derived from the magnet size and as such goes varies inversely to the scaling. A_C & $\overline{L_P}$ both scale with the machine resulting in the increased power generating potential. As in (4.35) the P_{rms} is based on approximating the power curve with a sawtooth wave. The scale factor in (4.41) assumes that the clearances have not been adjusted and that the magnets have been scaled up in line with the rest of the generator.

4.5.3 Effect on Efficiency

If a generator design is assumed to have an average efficiency of $\overline{\eta}$ then as the design is scaled up;

$$\bar{\eta}_2 = 1 - G(1 - \bar{\eta}_1) \quad (4.42)$$

For a generator with an original average efficiency of 99%, scaling the design up by a factor of 2 would reduce its efficiency to 98%. Therefore as the generators get larger alterations must be made to the design to ensure that efficiency is maintained. In the case of hydrostatic bearings this relates directly to the clearances in the bearings. In order to overcome this, the power loss from the bearings must be reduced by a factor G . This could be done by reducing the flow-rate, however reducing the clearance would allow flow-rates to be maintained, or at least not be increased as much, reducing the need to use very large pumps. Therefore as a generator is scaled up by a factor of G , the bearings must be scaled up by $\sqrt[3]{G}$, or the area must be scaled up by $G^{(3/2)}$ to maintain a given efficiency.

$$\begin{aligned} \bar{\eta} &= \frac{P_{in} - P_{loss}}{P_{in}} \\ &= 1 - \frac{P_{loss}}{P_{in}} \\ P_{loss} &= (1 - \bar{\eta}) P_{in} \end{aligned} \quad (4.43)$$

4.5.4 Summary

Scaling of generators has implications for both the power generation and fluid bearing components. If a generator with an arbitrary set of dimensions is directly scaled, by a factor of G , then the following will happen;

Chapter 4: Evaluation of Rigidly Structured Generators

- Mechanical:
 - The mass of all components increases by a factor of G^3
 - The stiffness of all components will increase by a factor of G^4

- Hydrostatic Bearings:
 - The L_H value for the hydrostatic bearings increases by a factor of G^2
 - The h value increases by a factor of G
 - Power loss in the bearings, for the new land clearance in a vertically aligned machine, decreases by a factor of G^3
 - Overall load support for a bearing running on the same flow-rate is reduced by a factor of G

- Permanent Magnets:
 - The flux generation increases by a factor of G^2
 - The slot frequency is reduced by a factor of G
 - The power generation capacity of the coils increases by G^3

4.6 Test Case

4.6.1 Parameters

The basic structure of the machine can be seen in Figure 4.7.

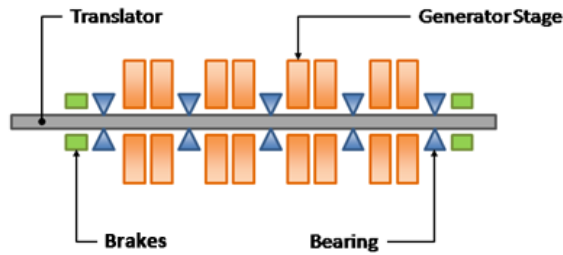


Figure 4.7: Layout of Test Case Generator

4.6.2 Assumptions

- The flux carrier is rigid and does not bend due to the attractive forces of the magnets.
- A maximum flux density of 1T occurs in the flux carrier
- The grid the device is attached to is an infinite grid of parallel connected devices
- The parameters are as set out in Table 4.5

The arrangement of equally spaced bearings is described by the matrix (4.44);

Chapter 4: Evaluation of Rigidly Structured Generators

Parameter	Value
Length	$2m$
Load Distance (l_1)	$1m$
Bearing Spacing (l_2)	$0.5m$
No. Bearings	5
Load (W_0)	$100N$
Second Moment of Area (Translator) (I)	$80,000mm^4$
Youngs Modulus (E)	$200GPa$
Bearing/Magnetic Clearance (h)	$2mm$
Fluid Viscosity (μ_h)	$1.88 \times 10^{-3}Pas$
Bearing Constant (L_H)	$1.69 \times 10^{-6}Ns$
Flow-Rate (Q)	$235cm^3s^{-1}$
Deflection Factor (%)	50%
Coil Turns (N)	1000
Coil Area (A_C)	$13500mm^2$
Area Factor (f_A)	0.907(<i>Hexagonal</i>)
Average Path Length ($\overline{L_P}$)	$421mm$
Coil Length	$300mm$
No. Coils	32
Flux Carrier Area	$8 \times 10^{-4}m^2$
Max. Flux (φ_0)	$8 \times 10^{-4}Wb$
Oscillation Frequency (ω_1)	$0.1Hz$
Slot Frequency (ω_2)	$50m^{-1}$
Oscillation Amplitude (A_T)	$1m$
Effective Area (A_e)	$6.80 \times 10^{-4}m^2$
Resistivity of Copper (ρ_r)	$1.70 \times 10^{-8}\Omega m$

Table 4.5: Test Case Parameters

$$\begin{bmatrix} 0 & l_2 & 2l_2 & 3l_2 & 4l_2 & W_0(l_1 + 0l_2) \\ -l_2 & 0 & l_2 & 2l_2 & 3l_2 & W_0(l_1 + 1l_2) \\ -2l_2 & -l_2 & 0 & l_2 & 2l_2 & W_0(l_1 + 2l_2) \\ -3l_2 & -2l_2 & -l_2 & 0 & l_2 & W_0(l_1 + 3l_2) \\ -4l_2 & -3l_2 & -2l_2 & -l_2 & 0 & W_0(l_1 + 4l_2) \end{bmatrix} = \begin{bmatrix} W_1 \\ W_2 \\ W_3 \\ W_4 \\ W_5 \end{bmatrix} \quad (4.44)$$

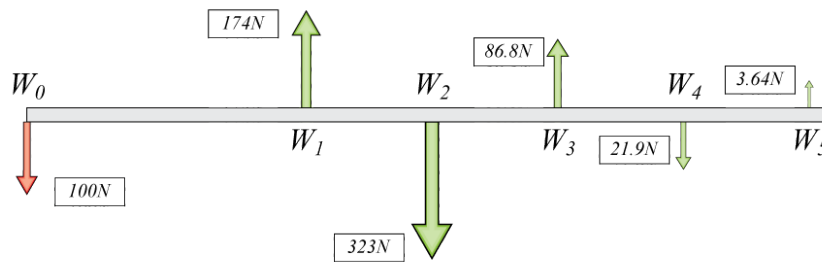


Figure 4.8: Loaded Beam

From the parameters in Table 4.5 the FEA from Solidworks Simulation produced the results shown in Figure 4.8 and Table 4.6. Figure 4.9 shows how a loaded beam deforms when supported on 5 bearings.

Parameter	Value
W_1	174 N
W_2	-323 N
W_3	86.8 N
W_4	-21.9 N
W_5	3.64 N
Maximum Deflection	0.0753 mm
Total Power Consumed (@ $Q = 500cm^3s^{-1}$)	168 W

Table 4.6: Loads, Deflections and Total Power Consumption

The maximum deflection show in Table 4.6 assumes that the bearings around it have not moved, if the bearings have shifted under load that value may well

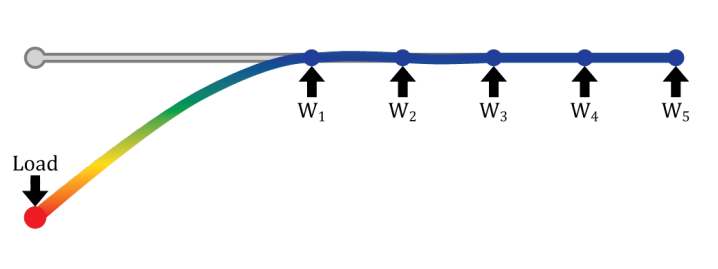


Figure 4.9: Deflection of a 5-point supported beam due to an external load.

increase. The flow-rate will be chosen to best account for these forces.

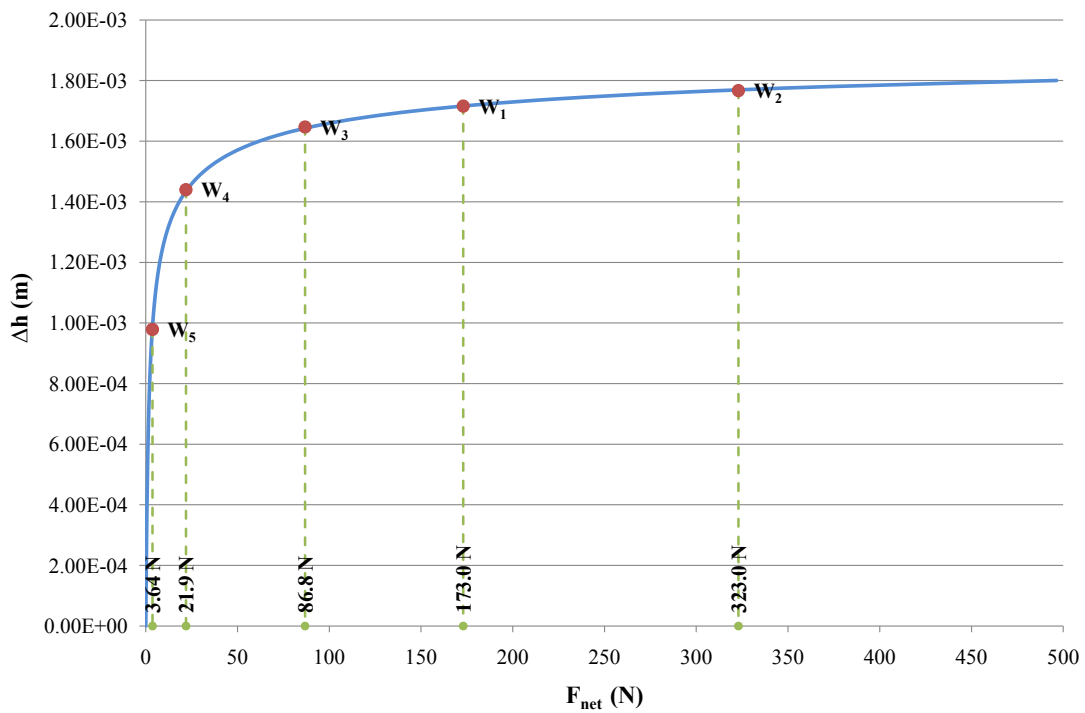


Figure 4.10: Net Force/Displacement Plot

Figure 4.10 shows how the net force on a set of bearings relates to displacement of the translator. The red dots relate to the individual bearings for the test case. Only one of the offsets is within the deflection factor, therefore to make this generator viable either;

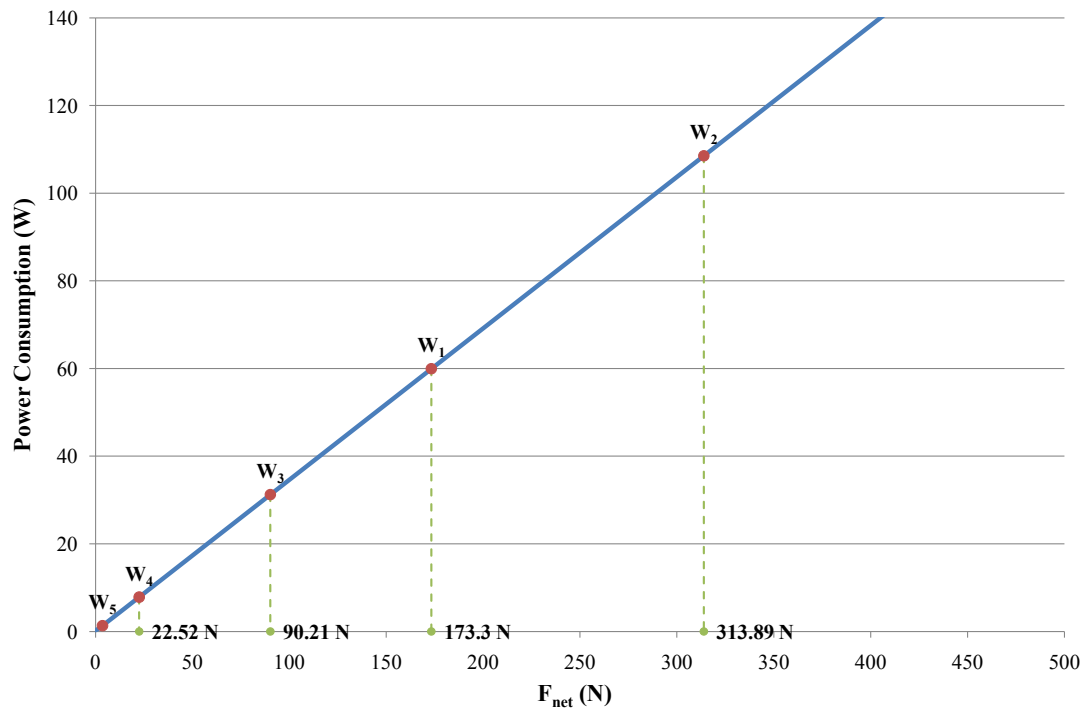


Figure 4.11: Net Force/Power Plot

- The flow-rate needs to increase
- The bearing size needs to increase
- The magnet clearance needs to increase

Bearing	Load	Offset
W_1	174 N	1.716 mm
W_2	-323 N	-1.767 mm
W_3	86.8 N	1.647 mm
W_4	-21.9 N	-1.44 mm
W_5	3.64 N	0.979 mm

Table 4.7: Loads and Hydrostatic Offsets

The increase in the magnet clearance is simply to avoid a collision. Unfortunately increasing the magnet clearance also reduces the generators output potential, unless the change is anticipated and corrected by changing the dimensions of the magnets.

4.6.3 Performance & Losses

From (4.35);

$$P_{RMS} \approx \frac{1}{\sqrt{3}} f_A \frac{A_c}{L_P \rho_r} (\varphi_0 A_t \omega_1 \omega_2)^2$$

From this the RMS power output from the coils can be estimated. The total output of the machine depends on the number of coils. Using the parameters in Table 4.5, the maximum power output from a single coil is approximately 0.5kW, resulting in a total theoretical power output for the machine of 16kW.

In the conditions stated the power consumption from the bearings is approximately 168W making the overall efficiency 99%. In unloaded conditions, where the net force on each bearing pair is zero, the power consumption is approximately 1.6W making the machine as a whole 99.99% efficient.

This does not account for the pipe losses in the fluid supply chain, losses due to eddy currents in the translator or numerous other losses that can occur within the generator but simply the power output and the bearing operational power consumption. It also only applies to a vertically mounted generator. A horizontally mounted device will have to contend with the weight of the translator too.

As shown in Figure 4.11 power consumption is directly related to the force applied.

Therefore the greater the external force applied the lower the efficiency. As well as a maximum allowable deflection the minimum allowable efficiency would need to be set as a design constraint. They both have a bearing on the maximum force that can be tolerated during operation.

4.7 Additional Concerns

During this section of the research additional concerns arose as to the composition of the lubricating fluid, in this case sea water. Sea water in general contains large quantities of particulate matter, especially around the sea floor. Some of this is organic matter, such as plankton or algae, which is generally soft and will generally only be a concern for its ability to clog intakes, as shown in Figure 4.12, and bearings.

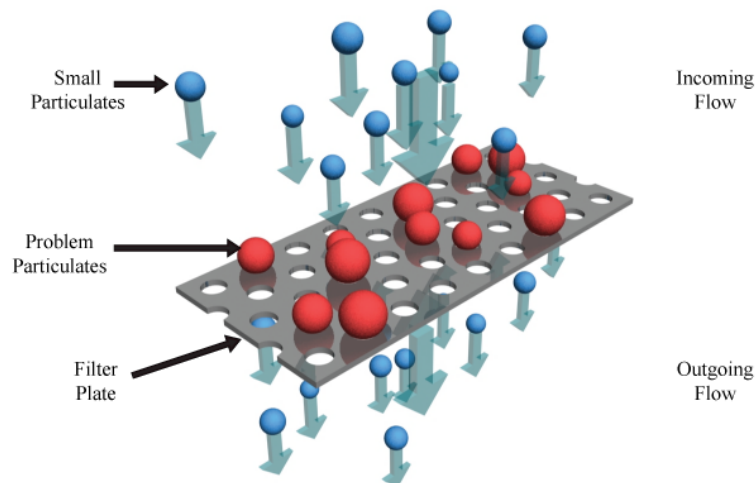


Figure 4.12: Partially Clogged Filter Plate with Fluid-Flow

The non-organic particulates are more of a problem, these include sand and grit.

Chapter 4: Evaluation of Rigidly Structured Generators

These particulates can still clog components but also may cause additional wear and damage to the machine parts. Bearings in general, but hydrostatics especially, operate best when working on smooth surfaces, additional wear, pitting or scarring on the surfaces changes the behaviour of the bearings and will affect the machines longevity and performance. In addition cracks/pits that form in the coatings on steel components, assuming coatings were used, promote corrosion which is a major issue.

In the case of hydrostatic bearings, the uni-directional nature of the fluid flow means that if the particulates are filtered out at the intake point then no particulates will be carried into or through the bearings. However the inclusion of filters will significantly increase the power consumption of the fluid supply system.

In mechanical bearing systems the inclusion of sand and grit presents even greater problems because of its effect on the smooth running of the bearing. As is well known, the presence of particulates in many oils or lubricants, with the exception of graphite particulates, can cause bearings to grind and jump and will cause additional wear reducing their overall lifespan. Therefore it would be very important to implement seals to protect the bearings.

A possible solution to this problem overall was to flood the generator with clean sea water and use labyrinth seals around the translator at either end to allow for the movement of the translator whilst maintaining the integrity of the internal environment.

Chapter 5:

Moving to Non-Rigidly Structured Generators

Rigidly structured generators work well on paper, where everything is perfect, however with large moving devices the smallest of changes and cause large losses or potentially cause the generator to fail. The concept of Non-Rigid construction allows those parts which do not need to be rigidly constrained to move by small degrees, reducing the load in the generators members and on the bearings.

5.1 Theory

The non-rigid design is based on the concept that an impulse force is applied to a rigid structure that structure will be subject to larger internal stresses than a structure mounted on a flexible substrate. Therefore, by mounting the bearings on a flexible substrate the maximum forces are reduced. This reduces the losses in any form of bearing and in the case of hydrostatic bearings it affects the design of the pump and the required operating pressures and flow-rates.

Key to all of the non-rigid designs explored in this work is modularity. Modular design has implications for manufacture and maintenance. These implications will be explored on a case by case basis.

5.2 2-Stage Bearings

The 2-stage bearing design is intended to provide the movement necessary to overcome fabrication errors and damage caused during operation. The 2-stage bearings need to be mounted on a flexible mounting, such as springs or rubber.

The amount the 2-Stage bearing will move will depend on the force applied to it

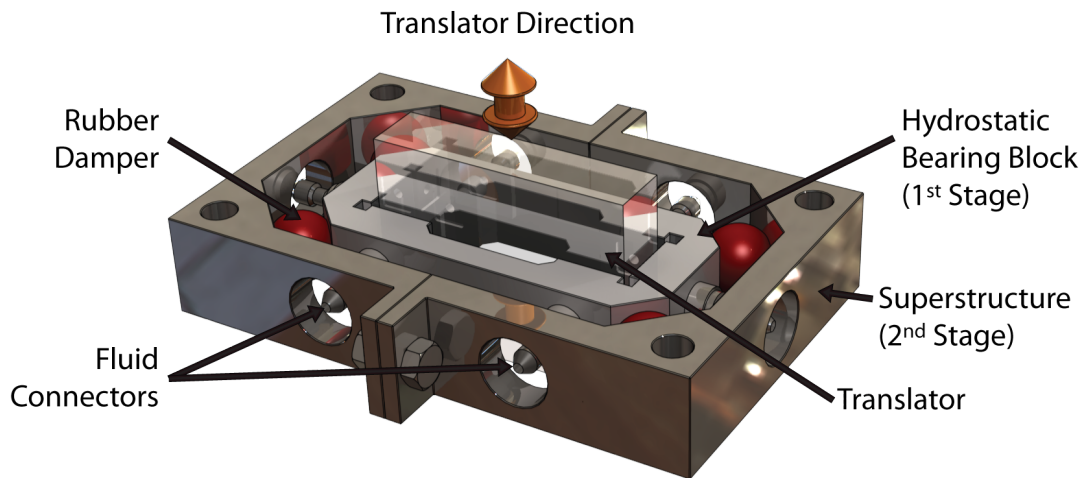


Figure 5.1: 2-Stage Bearing

and with any constant external force, the final force experienced by the bearings will be equal. However in circumstances where the force is rapidly changing, the addition of the soft materials lowers the forces experienced by the bearings by extending the time over which the force acts. As a result the maximum stress in any component and the losses of any bearings is reduced.

The additional bonus is that the increased loading and losses caused by damage or manufacturing errors is greatly reduced, allowing for devices to be created more easily and cheaply.

The 2-Stage bearing concept was originally intended to supply additional damping whilst reducing peak loads, however the damping properties of hydrostatic bearings themselves proved to provide greater damping than the 2-Stage bearing was capable of in its original forms. However the realization that the use of this design could potentially have other benefits meant that it warranted further study. The original designs used rubber spring dampers akin to squash balls, intended to give the

support of rubber but, as with squash balls, they would damp any sudden/large movements reducing the overall loads on the machine structure.

5.2.1 Theory

The basis for the work on the 2-stage device is the principle of reducing impulse forces. Impulse is defined as;

$$Impulse = \frac{dF}{dt} \quad (5.1)$$

From the spring equation;

$$\frac{dF}{dt} = k \frac{dx}{dt} \quad (5.2)$$

Since dF/dt is the instantaneous impulse, the higher this value is the more likely that damage will be caused to generator components and the greater the losses in the supporting bearings. As the k value decreases, the spring gets softer and for a given dx/dt the impulse is reduced. If dx/dt is taken to be the velocity of the object as it compresses the spring with the constant k , then it can be a function of transferred momentum after a collision.

$$\begin{aligned} m_1 \frac{dx}{dt}_1 &= m_2 \frac{dx}{dt}_2 \\ \frac{dx}{dt}_2 &= \frac{m_1}{m_2} \frac{dx}{dt}_1 \end{aligned} \quad (5.3)$$

Chapter 5: Moving to Non-Rigidly Structured Generators

For a perfectly elastic collision, all the momentum of the incident object would be transferred; therefore the dx/dt is the velocity of the supported object after the momentum has been transferred. By extending the time over which loads are applied, and therefore reducing the impulse forces, the losses to the bearings and the maximum loads on each supporting member is also reduced.

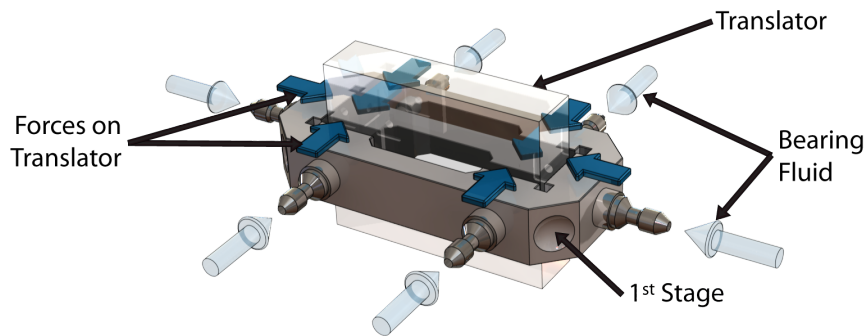


Figure 5.2: 1st Stage System

The easiest way to think of such a bearing would be in 2-stages, hence the name. The first stage is a system containing hydrostatic (or other) bearings and the translator, see Figure 5.2.

The second is a system containing the bearings as a block but inheriting the net force.

As a displacement or load displaces the translator the imbalance in F_1 & F_2 produces a net retarding force on the translator. However an equal and opposite force is experienced by the bearings. The retarding force should be;

$$F_T = F_2 - F_1 \quad (5.4)$$

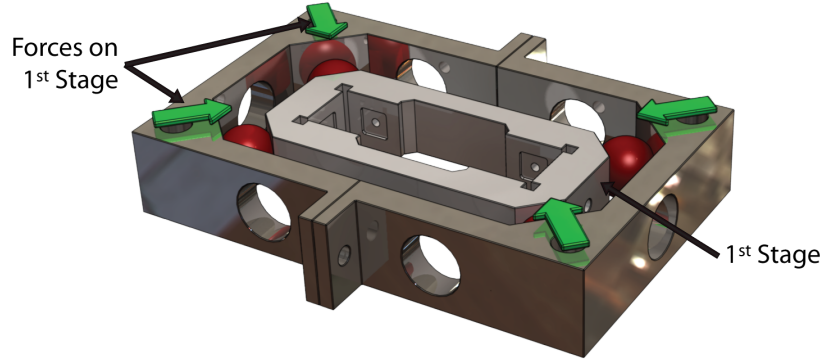


Figure 5.3: Second Stage System

Note: If the system were rigid this force would result only in additional tension and strain in the supporting structure.

The force applied to the bearings causes a displacement of the bearing stage which, in turn, causes an imbalance in forces F_3 & F_4 , resulting in a net retarding force on the bearing stage. That force would be;

$$F_B = F_3 - F_4 + F_T \quad (5.5)$$

If the external influence is short lived, such as an impact, this method is capable of reducing the maximum forces experienced by the system.

A complete model for the system requires two 2nd order differential equations to describe it, the first of which applies to the force on the translator;

$$m_T \frac{d^2 x_t}{dt^2} = F_T = L_H \left[\frac{Q_2}{(h_0 - \Delta h)^3} - \frac{Q_1}{(h_0 + \Delta h)^3} \right] \quad (5.6)$$

where Δh is;

$$\Delta h = x_T - x_B \quad (5.7)$$

The second equation applies to the force on the bearings themselves;

$$m_B \frac{d^2 x_b}{dt^2} = F_B = -k_3(x_0 - x_B) - k_3(x_0 + x_B) - F_T = -2k_3 x_B - F_T \quad (5.8)$$

For both differential equations require that at the equilibrium position both x_T and x_B are zero. These equations are interdependent and as such are tricky to solve on their own.

5.2.2 Conclusion

A 2-Stage bearing system will not reduce the maximum force experienced by the bearings for any sustained external force or permanent displacement, however it does offer greater tolerance for rapid dynamic loading such as impacts. As a secondary concern the implementation of the 2-Stage bearings will offer a release from some design constraints and may allow for the use of lighter/weaker materials in some areas. As a result of the relaxation of the design constraints the price of production and quality of production can be reduced for a number of parts without it compromising the operation of the device.

Power Usage

Using the 2-stage bearings in a generator reduces the peak loads on the hydrostatics or other bearings and therefore would reduce the power loss for whatever bearing technology has been employed in the design. Inline with (3.1) the reduction in the bearing loads will provide an energy saving, however it will not provide an energy saving with a sustained external load because it will reach equilibrium.

Economic Impacts

Since the peak loads are reduced, the maximum required strength of the materials used in the generators construction, particularly in the load bearing members, can be reduced, lowering material costs and potentially weight. Additionally, by relaxing the tolerances, manufacturing costs are reduced.

The introduction of the 2-stage bearings should deliver a lower $m_{structural}$ value as a result of lower peak loads, however the necessary inclusion of sufficient pumping equipment to operate the hydrostatic bearings would introduce a higher $m_{support}$ value. An overall transport cost saving can be achieved if there is sufficient reducing in structural mass to offset the additional support hardware.

The key benefit will be the relaxed tolerances and their impact on manufacturing costs.

5.3 Multi-Machine Architecture

The Multi-Machine architecture (MMA) expands on the principles of the 2-Stage designs by creating a modular structure to the machine with two types of modules. An MMA machine uses modules using 2-stage construction at the ends and in the middle. The rest of the machine is made of MMA modules. An MMA module has its generator components supported longitudinally but they are free to move laterally.

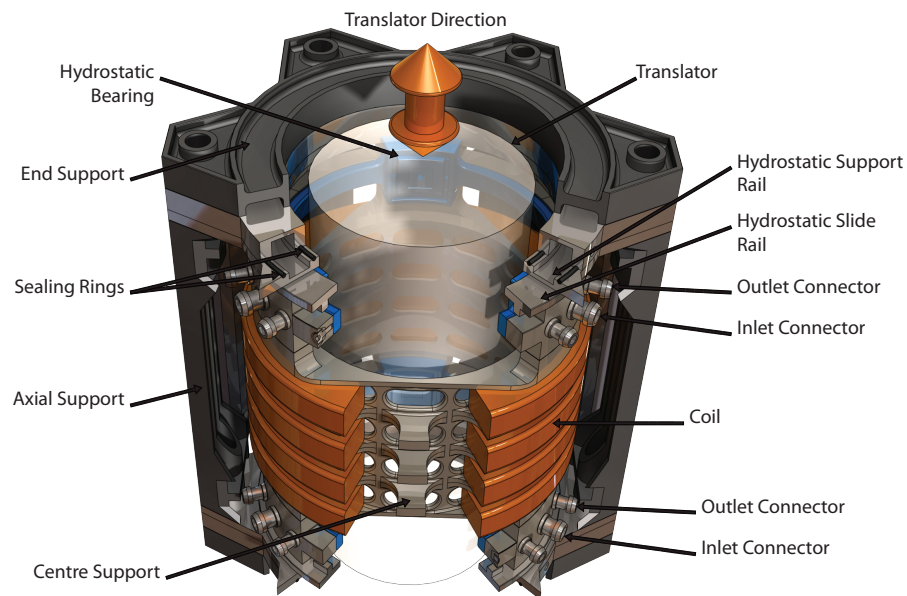


Figure 5.4: MMA System

The increased lateral movement in the generator modules allows for an even greater reduction in the losses from bearings and the complete removal of the supporting members reduces the overall weight of the device.

5.3.1 Theory

The theory for the MMA is quite simple. In essence it is a 2-Stage bearing without the second stage supports. Therefore the only force acting upon the bearing stage is that of the bearings within it.

Therefore, for the MMA, the differential equation for the bearing stage would look like this;

$$m_B \frac{d^2 x_B}{dt^2} = F_B = -F_T \quad (5.9)$$

As a result there is a small phase difference between the movement of the bearing stage and movement of the translator but the bearings will essentially move with the translator. The retarding force on the translator is minimal, but the MMA modules are not intended to restrain the motion of the translator, that job is done by the 2-Stage Bearings. In essence the MMA modules act like an additional mass added to the translator during lateral motions. The pressure in the bearings (for hydrostatic bearings) will determine the degree of lag between the motion of the translator and the motion of the bearings. The higher the pressure, the higher the stiffness and the less lag there should be. The position of the MMA module is effectively;

$$x_B(t) = x_T(t - \tau)$$

Where τ is related to the stiffness and the mass of the bearing being used. The stiffer the bearings the smaller the value of τ will be and the faster the module

will respond.

Since the MMA modules are free to move the translator must be restrained to a degree at other points within the modular structure of the machine. In order to restrain it sufficiently the translator should be restrained in three places. This will be referred to as 3-point pinning. The theory behind 3-point pinning is explained in more detail in 5.10.2.

5.3.2 Conclusion

The MMA designs should offer a substantially improved performance of both 2-stage supported modules and rigidly structured machines. It is also important to note that the capacity of the MMA modules to move allows for much larger flex and lateral movement in the translator than can be permitted in a rigidly structured generator. The total power consumed by the bearings to support MMA modules should, in general, be less than that of a rigidly structured generator.

Power Usage

The power consumption for an MMA design should remain relatively constant even while the translator moves and flexes, depending on the operating pressure. The higher the pressure the faster the module will correct its position and lower the variation in the power consumption but the higher the average power consumption. Given the mobile nature of the MMA modules even a sustained external force will not cause an increased power consumption once the module has moved, delivering a significant saving over the 2-stage.

Economic Impacts

The concept for the MMA should reduce the weight to the bare minimum required in order to construct the generator. The support materials used in the external structure can be made of lighter materials since the majority of the force is now carried by the generators core resulting in a lower $m_{structural}$ value. Hydrostatic support equipment would be required introducing a $m_{support}$ value, however due to the lack of mobile nature of the MMA modules they and the machine's superstructure do not necessarily need to be transported together, however the effect of this on transport costs is not speculated on in this work.

5.4 Fast Replace MMA (FR-MMA)

Fast Replace MMA modules extend on the MMA principles by making it possible to exchange modules, for maintenance & testing purposes, while the parent machine is in operation. Ideally these machines would be self-positioning and would regulate their own operational air gap. The capability to swap components in-situ coupled with the modular nature of the machine should substantially reduce the operation and maintenance costs for this type of machine, further improving commercial viability.

5.4.1 Theory

The theory behind these designs is quite simple, the force provided by the bearings balances that of the magnets and the closing force of whatever mechanism is being

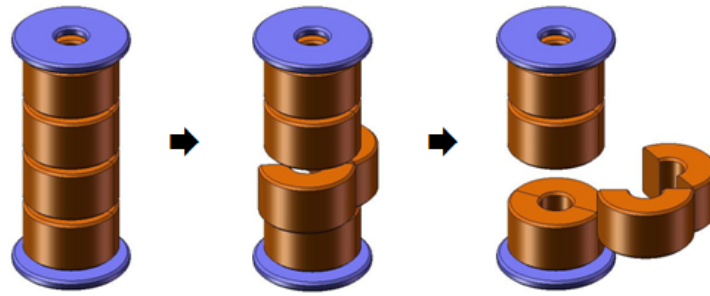


Figure 5.5: Principle of FR-MMA

used to hold the module in place. The use of hydrostatic bearings can provide an option for varying the clearance by altering the bearing flow-rate.

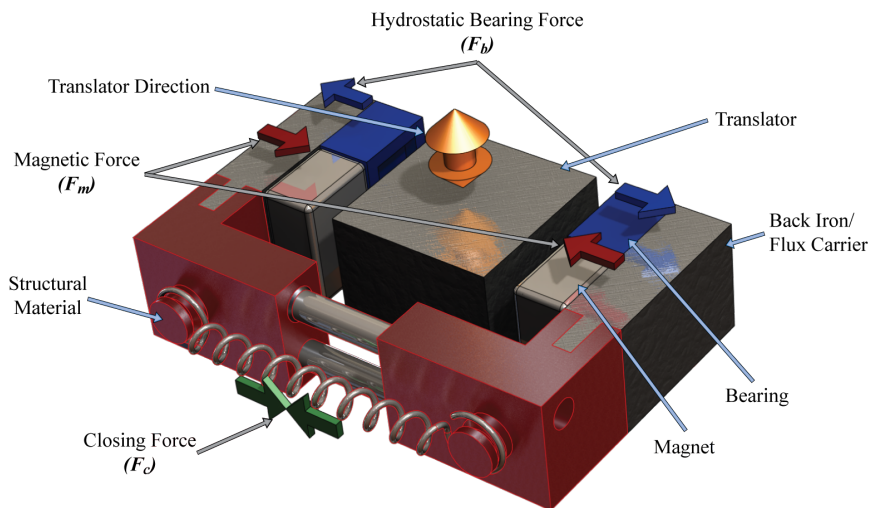


Figure 5.6: An Example of Self-Supporting FR-MMA

Figure 5.6 shows an example FR-MMA layout including all the required forces. It should be noted that the structural material shown in red is not intended to be a flux carrier. In an equilibrium state the forces on each bearing would be identical, therefore;

$$F_b = F_c + F_m \quad (5.10)$$

Since all three forces are in some way related to distance, assuming the closing force is a simple spring, it follows that;

$$F_b(s) = F_c(s) + F_m(s) \quad (5.11)$$

It should be noted that each function of s will likely operate with a different offset based on the design geometry. Since the magnets and bearings no longer have fixed positions with the module design it is vital that their possible movements be accounted for during the design stages.

The option of hydrostatic bearings offers a potential mechanism for varying the clearance of both the magnets and bearings by varying the flowrates through them.

$$F_b(s, Q) = F_c(s) + F_m(s) \quad (5.12)$$

By varying the flow-rate, Q , the force from the bearings can be varied. Using (2.59), the equivalent pumping power can be calculated from the pressure and flow-rate in the bearings.

If designed correctly the closing mechanism on a module would move the bearings and power generation components into their ideal positions, however by having a sprung mechanism to manoeuvre these components the module would have an additional capacity to compensate for more extreme loads than MMA.

A complete generator would consist of multiple modules, both of the 2-Stage and

FR-MMA type. At least 3 2-Stage modules would be required to undertake the 3-point pinning strategy, see Section 5.10.2, and all the remaining modules would be FR-MMA. Ideally 6 2-Stage modules would be included for the sake of redundancy. The advantage of designing the generators in this fashion is that the basic construction doesn't include the installation of the units. They can be fitted once the generator's main structure has been anchored, reducing costs and complexity of installations.

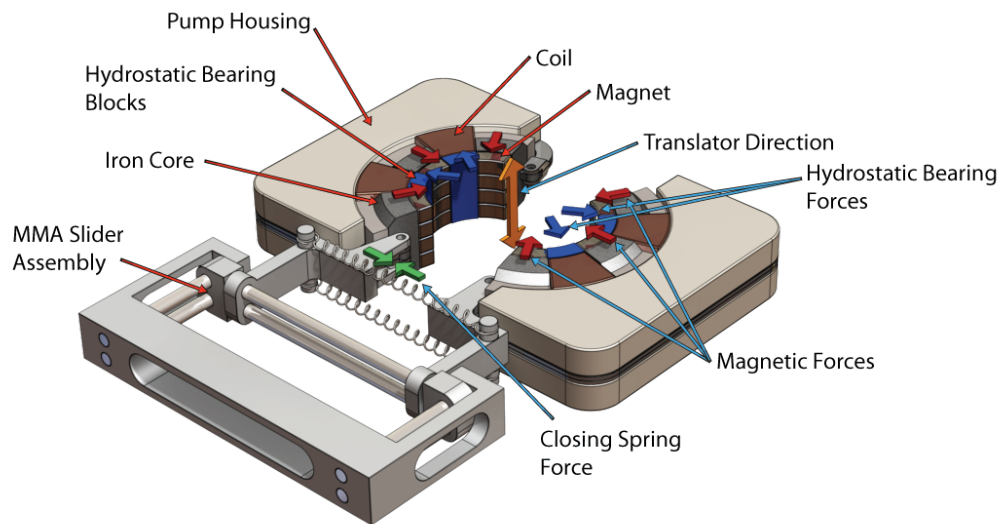


Figure 5.7: Example FR-MMA Module

Figure 5.7 shows how a potential Variable-Reluctance FR-MMA module might be constructed for a circular translator. During insertion and extraction the two halves would be forcefully separated and then allowed to close once in place or clear of the translator.

5.4.2 Complexities of FR-MMA

The FR-MMA concept introduces additional complexities in certain topologies of linear machines. In the case of air-cored linear generators the arrangement of the coils is critical and the majority of designs for tubular machines have the axis of the coil aligned with the direction of the translator.

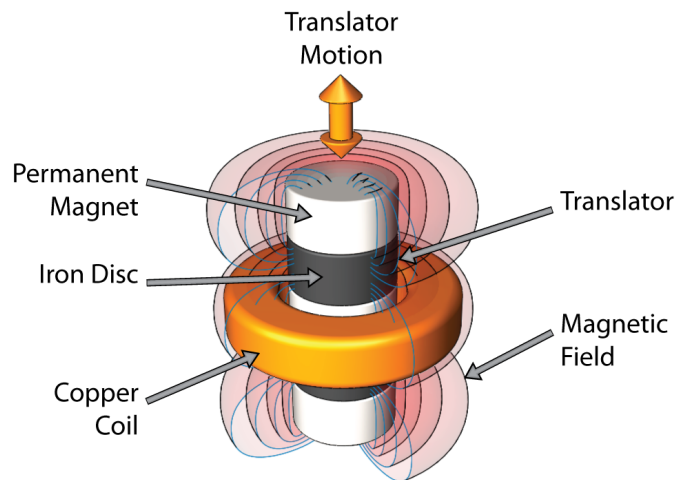


Figure 5.8: Classic Tubular Air-Cored Arrangement

In order to make this generator a Fast-Replace version the coil would need to be split. No matter what method is used, the amount of copper required to make the generator is increased by this. The following shows a few possible arrangements that could be used for FR-MMA.

The third arrangement shown in Figure 5.9 has similarities to the method used in the AWS^[27], however in that case the magnets were arranged in rows on a flat bed rather than in a tubular arrangement, however it was still an air-cored linear generator.

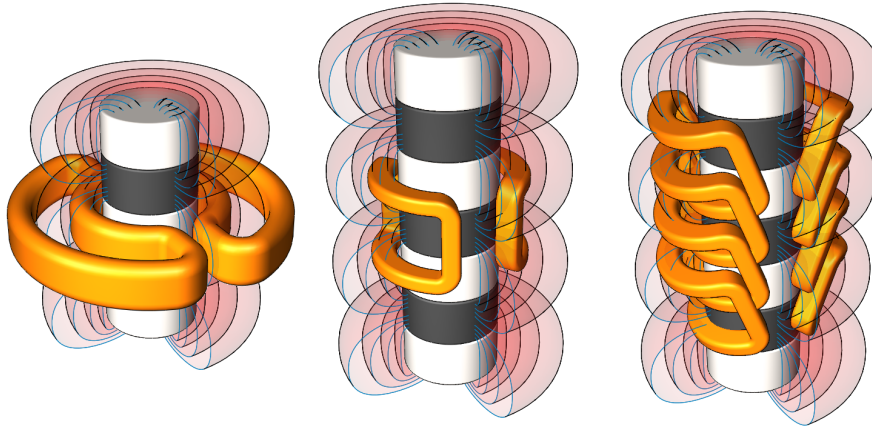


Figure 5.9: Collection of Alternative Coil Arrangements

Figures 5.10 and 5.11 show the translator and stator sections of the AWS prior to installation in the prototype.

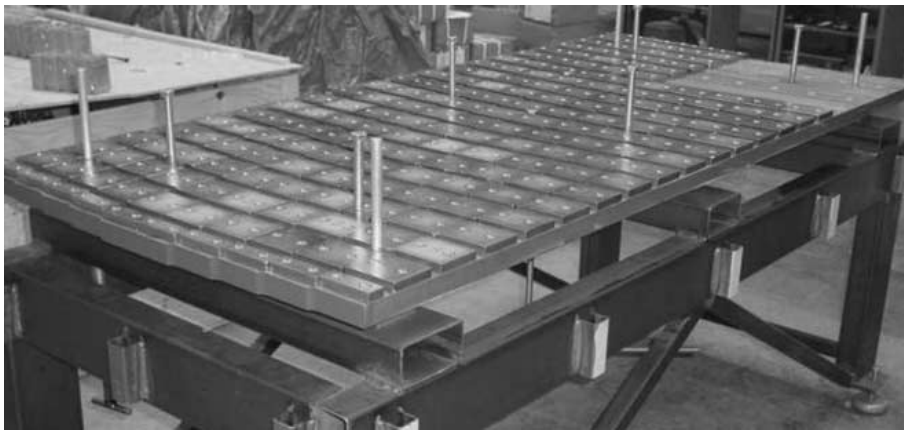


Figure 5.10: AWS Translator with Bed of Magnets During Construction^[27]

5.4.3 Conclusion

After careful consideration the self-supporting mechanism for these designs of device turned out not to be viable due to the additional energy requirements required to maintain the dimensional stability of the module and increased consumption if

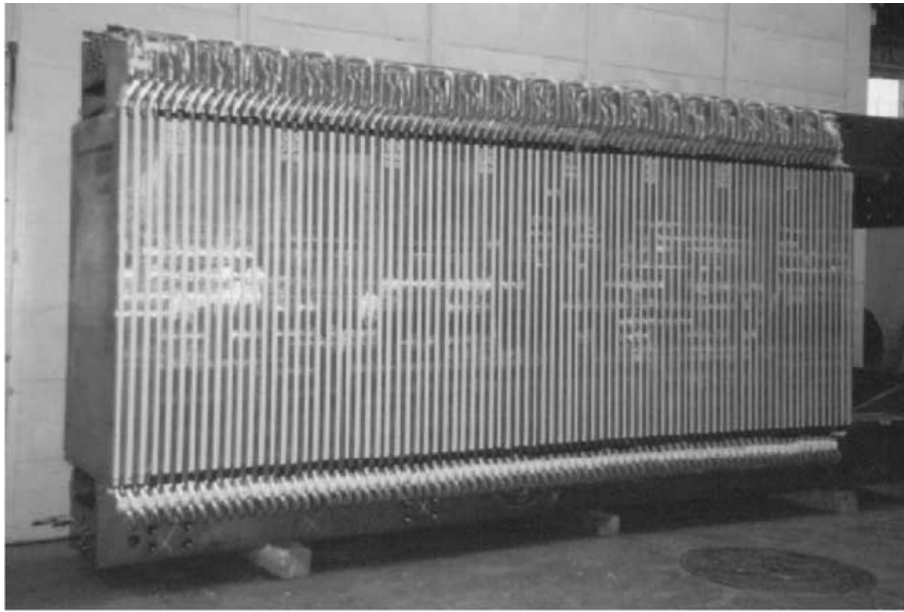


Figure 5.11: AWS Stator Section with Coils Visible^[27]

the module is unable to completely close. If the device was able to fully close then it would not be a problem, but only under those circumstances. This eliminates one of the primary reasons for this section of the research by reintroducing the tolerances that would have been avoided. However the swappable nature of the devices presents an incentive to continue looking at variations of these designs.

It should be noted that although the FR-MMA concept could potentially save a lot on O&M costs it does effectively negate the point made in 4.7 about using labyrinth seals to trap a volume of clean water within the machine. The swapping of modules would continually be introducing more particulates into the main column of the machine making these seals effectively useless. With additional research a mechanism could be devised that could more effectively seal a machine using FR-MMA modules, however, by design, the modules themselves would carry particulates into the machine during insertion operations.

Power Usage

The power usage when operating as a self-supporting device would be higher than other MMA designs if the device is unable to completely close. If the sections are allowed to fully close around the translator then the power requirements would be similar to other MMA designs. Unclosed the bearings would need to support the force from the magnets and the closing mechanism, where as, if closed the forces should balance as in other MMA modules. The increased forces in the unclosed position will translate into a higher power usage in (3.1).

Economic Impacts

The possibility of creating modules that can be inserted and extracted whilst the parent device is in operation could potentially have a big impact on the O&M costs by reducing the $Cost_{equipment}$, $Cost_{personnel}$, t_{repair} and $t_{downtime}$ values. It also introduces a non-zero $Income_{reduced}$ value because the whole machine does not need to be shut down for the sake of single faulty module. At the same time the modular approach will likely affect and the original construction and transport costs.

5.5 Segmented FR-MMA - SFR-MMA

The segmented FR-MMA machine extends the idea of the FR-MMA module by breaking the module into cells. Previously where each stage required a module no each stage requires a number of cells. These cells are spaced evenly around the translator in order to make up the tower.

The cells do different jobs, but the basic structure of the machine follows the MMA principles. The difference, as with FR-MMA, is that there are two sets of the 2-stage bearings as opposed to one. In this case that is a minimum of six modules per support stage. Twin sets are required for redundancy purposes. Should one fail then its counterpart is activated.

In the end a basic tower should resemble something like Figure 5.12.

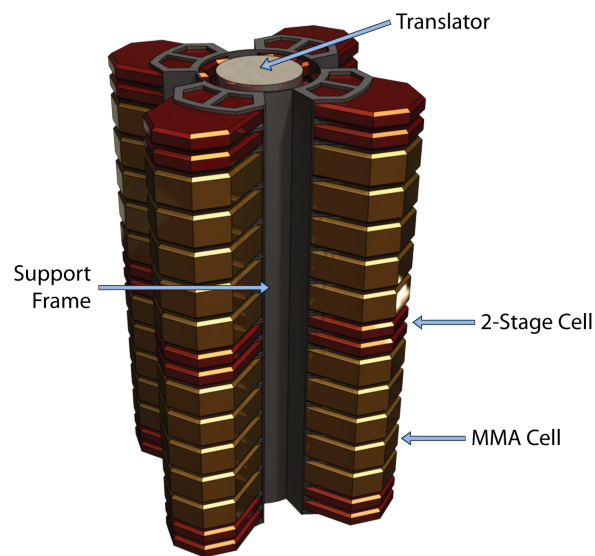


Figure 5.12: SFR-MMA Machine Schematic

One advantage of this type of design is that the internal components of each cell, 2-stage & MMA alike, need only move in one direction and may be fixed in all others. In addition there is little or no rotation to worry about.

5.5.1 2-Stage Cell Operation

Structurally, the 2-stage cell is essentially just a Head, containing the bearings and, in hydrostatically supported devices, a pumping stage. The head contains a

bearing of some description to support the translator, supported on a spring or rubber support. It is mounted as to allow for a single direction of motion, pressing onto the support. The 2-stage cell has to be locked or bolted into place in order to operate properly, since it is intended to lock the translator in place laterally.

5.5.2 MMA Cell Operation

Structural each cell is essentially a Head, like the 2-stage, containing the magnets and bearings, a generator section with the coils & cooling, etc., and in the case of hydrostatically supported versions a pump section. The pump could potentially be fixed to the cell casing however the Head and the generator parts would slide within it.

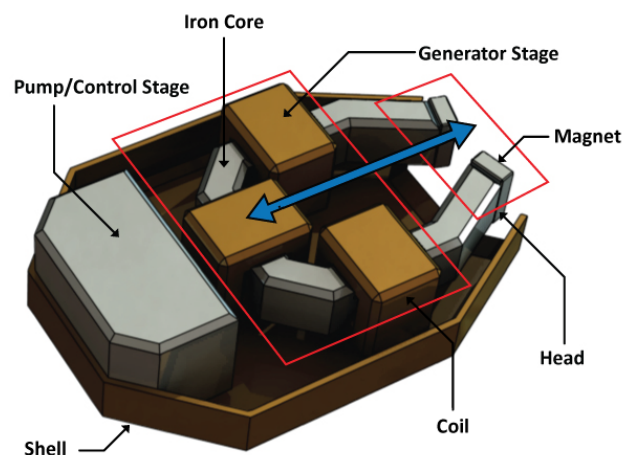


Figure 5.13: SFR-MMA MMA Cell

The position of the head relative to the translator is maintained by the bearings, no matter what kind. If the cell was designed with the head fixed in place then

Chapter 5: Moving to Non-Rigidly Structured Generators

enormous forces would be applied to the bearings if there were structural imperfections or the translator was forced to move externally. In all circumstances the forces applied by the head on the translator and vice versa sum to zero¹, therefore removing a module from the system should have no net effect of the position or motion of the translator.

An MMA cell does not require bolting into place like the 2-stage cells do because they are not subject to the same forces. In an MMA cell the forces are the balance between the magnets and the bearings, and therefore, ideally, the net force applied to the module would be zero. A 2-stage module will be under a constant load since there is only a repelling force applied.

In the event that the cell needs to be removed from the machine, mechanisms to separate the head from the translator need to be in place. This is to take care of the imbalance between the magnetic forces and bearing forces during removal. The most likely problem that would cause a module to fail would be a failure in the bearings. If the safety mechanisms were missing, this would either cause an increased friction force on the translator or cause the head to impact and attach to the translator.

In hydrostatic cases increased pressure in the bearings could force the head back however it is likely that in both cases a secondary mechanism would be required to ensure that the head is properly retracted before removal.

¹In hydrostatic systems this requires additional control

5.5.3 Theory

The force required to support a cell is calculated as;

$$B_{rem} \frac{l_{magnet}}{\mu_0} = \frac{\varphi}{A_m \mu_0} (l_{magnet} + l_{air-gap})$$

$$B = \frac{\varphi}{A}$$

$$F = \frac{B^2 A_m}{2\mu_0}$$

Since the head of the cell applies force on only one side the complete force must be balanced by the hydrostatic bearings, and the power consumption or the bearings can be calculated from (2.4), (2.22) and (2.57);

$$F = \frac{B^2 A_m}{2\mu_0} = L_H \frac{Q}{h^3}$$

$$H_p = \left(\frac{B^2 A_m}{2\mu_0} \right)^2 \frac{h^3}{L_H A_e}$$

This shows that the power consumption is directly related to the land clearance. For a given design of bearing (specified by L_H and A_e) and a given B-field, the power required to support the cell can be calculated.

5.5.4 Conclusion

As a result of the self-positioning nature of the modules they should offer exceptional dimensional stability and the operation & maintenance costs for the machine as a whole would be reduced because of the size and weight of each module. Un-

fortunately these modules, in their original form will require cause greater power losses than previous designs because they do not take advantage of opposing magnets, see 2.2.4 This is a major disadvantage to the machine as a whole because it will reduce efficiency substantially.

Power Usage

Since the cells need to provide a force equal and opposite to the direct magnetic forces generated by the modules a substantial amount of power is required in order to keep the generator in operation in accordance with (3.1). This would reduce the efficiency of the complete generator essentially making it less desirable than other variations.

Economic Impacts

Although originally these designs were intended to expand on the FR-MMA modules and further decrease construction costs, there would be no net benefit to this if the power consumption were increased. As such this particular design would show a negative economic impact. The primary advantage of the cell structure was its capacity for easy maintenance, however this is not likely to offset to the efficiency loss. It could be viewed as a permanently decreased $Income_{max}$ value for the sake of reduced repair costs.

5.6 Ring Supported Segmented FR-MMA

The Ring Supported SFR-MMA is an attempt to make the SFR-MMA concepts viable by overcoming the force issues. It essentially requires that as the cells are inserted into the generator their heads are aligned with a ring (or similar structure) which makes supports them and ensure that their positions relative to one another are constrained. By doing this the heads would essentially be in an opposing-force situation, greatly reducing the power required to support them.

5.6.1 Theory

In theory if the cells in the SFR-MMA designs were inserted into a ring structure it would give them the referential integrity that the cells alone are missing. Such a structure would need to be constructed such that as a cell is added it rests into or is attached to the ring and from that point on moves with it. For the sake of maintenance this would require that the ring be designed to move the cells away from the translator before a cell could be inserted or removed, otherwise the unbalanced forces would drag the whole mechanism off centre.

Such a mechanism is complex to construct especially taking into account the forces involved in supporting the magnetic forces required for the operation of the generator. A bayonet style mechanism would likely be the best option, a single ring in the mechanism moves the cells towards and away from the translator. If a single module is missing then the ring must be kept open and cannot be used. In the case of the support used in Figure 5.14 of a single module fails 4 modules will be out of service. It should also be noted that the ring itself must be able to move

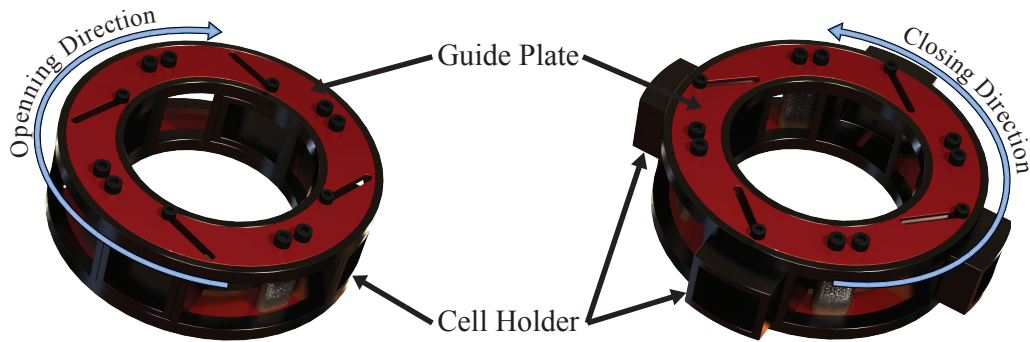


Figure 5.14: Bayonet Ring Support

with the translator in accordance with the MMA principle otherwise its use would be essentially pointless.

5.6.2 Conclusion

The complexity require in order to create the ring support mechanism coupled with the difficulty of making it reliable make this particular arrangement problematic and generally more trouble than can be justified. The Segmented FR-MMA concept essentially would not function without this mechanism, essentially ruling both concepts out.

Power Usage

Compared to the SFR-MMA the ring supported version would save a significant amount of power compared to the cells on their own simply through the reduction of load (3.1)

Economic Impacts

The ring support adds mass, cost and complexity to the SFR-MMA system. The parts need to be accurately produced adding expense to the manufacturing. Compared to the SFR-MMA alone it would be more expensive as a result of increased transport costs due to increasing $mass_{structural}$ and the general higher specification of the parts.

5.7 Simplified FR-MMA

Due to the problems with the SFR-MMA concepts, the Simplified FR-MMA is a return to the original FR-MMA concept but without the self supporting nature. The simplified FR-MMA design distributes the majority of the force through the iron-core of generators.

5.7.1 Theory

As with the original MMA designs, 2-stage modules restrict the motion of the translator whilst MMA modules extract the power. The difference is the design of the MMA modules.

The 2-stage modules are fixed in place to provide support and restrain the translator. The generator modules, MMA design, are intended to not restrict the motion of the translator but to move with it maintaining its operational clearances. The generator modules will allow motion of the translator in two-directions without restraint, and will hold its relative position to the translator in the third. The

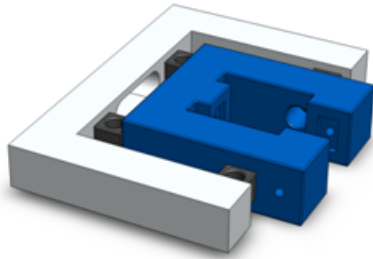


Figure 5.15: Basic Concept SiFR-MMA 2-Stage Module

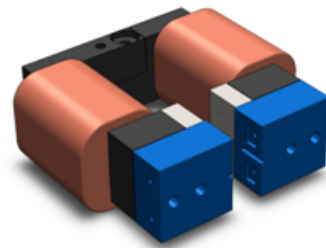


Figure 5.16: Basic Concept SiFR-MMA Generator Module

positional modules restrain position in two directions and rotation in three axes.

A complete generator would be arranged in a similar fashion to Figure 5.17.

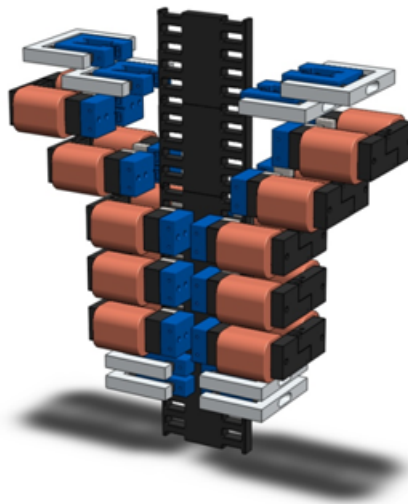


Figure 5.17: Exploded View of Complete Generator

A number of positional modules are arranged in pairs on either side of the translator and at three equidistant points along its length. Between each pair of positional modules would be sets of generator modules. The framework that holds them in place is designed such that modules can be removed from the machine if they fail

in operation. The reason for pairing up the positional modules is so that there is redundancy. Under normal operation only half the positional modules would be in use and given their relative positions within the machine even if some were to fail the staggering of the forces they produce would be negligible.

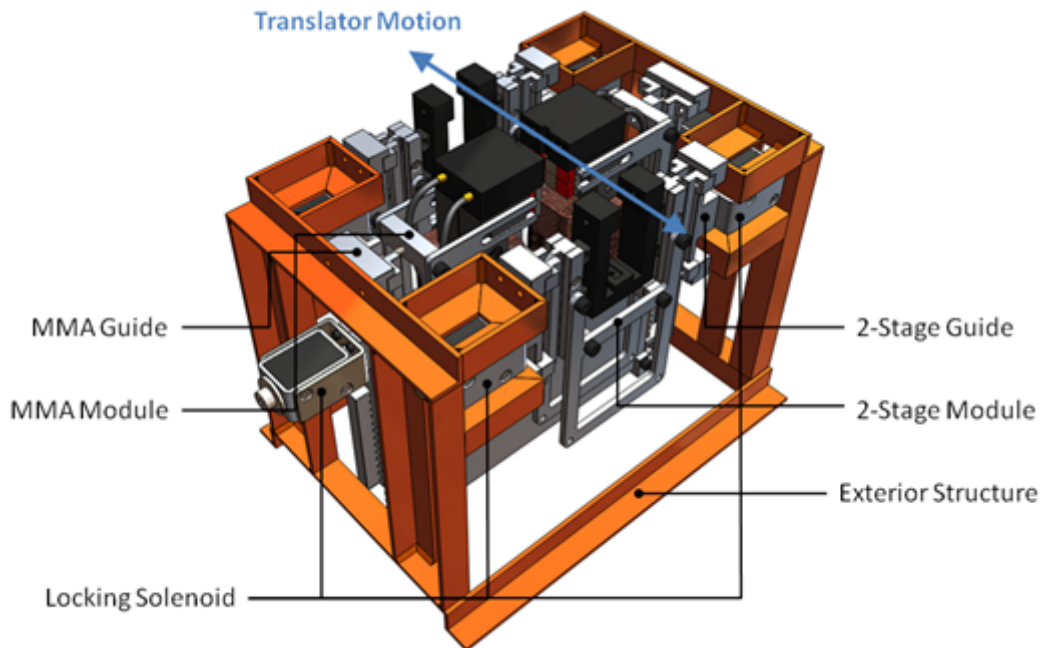


Figure 5.18: Modules inserted into welded support frame

The framework shown in Figure 5.18 is an example of how the modules might be supported. Within the framework would be a locking mechanism that the modules lock into when inserted. In the event of a failure in the module locking mechanism will disengage and the module will be ejected. Additional information on the control strategy can be found in 5.10.1.

5.7.2 Conclusion

The simplified FR-MMA modules probably represent the form that practical FR-MMA modules will take in future designs. The simplicity of the structure does not reduce its generating potential compared to previous designs and its opposing magnet structure allows it to use less materials in its construction, reducing $Cost_{material}$, $Cost_{equipment}$ and $Cost_{labour}$, and reducing $f_{failure-rate}$ as well.

The key issue to the construction of this kind of module is being able to include enough copper in the coils to give the desired power output. From the first approximation in Section 2 it can be seen that the maximum potential power is limited by the total cross-sectional area of copper conductors in the module.

Power Usage

Power usage in these designs would be similar to other MMA modules depending on the type of bearing being used. They will be subject to the same forces as the original MMA designs and therefore will incur similar power consumption characteristics.

The locking mechanisms and failure response electronics will not add a substantial additional power usage since the locking mechanism only draw power when they are activated and the failure response electronics are relatively simple.

Economic Impacts

In keeping with the FR-MMA principles the economic impact of this design of module is mostly related to the operation and maintenance costs of the generator

as a whole. However the simplified structure allows the modular generators to be constructed more easily and without complex mechanical mechanisms that would otherwise need to be employed.

The proper implementation of the FR-MMA principle in this concept will help to reduce construction and transport costs, by reducing;

- $m_{structural}$
- $Cost_{material}$
- $Cost_{labour}$
- $f_{failure-rate}$
- $Cost_{equipment}$

and O&M costs by reducing;

- $Cost_{equipment-hire}$
- $Cost_{personnel}$
- t_{repair} and $t_{downtime}$

while increasing $Income_{reduced}$.

5.8 Multi-Purpose Modules

All the previous topologies were intended to be used for linear machines; however the concepts behind the MMA modules should allow them to be applied to rotational machines as well. By doing this it would change the way devices such as large wind turbines or tidal turbines were constructed, allowing the generator

plants to be constructed in-situ simply by installing the modules. Making a module which is universal may not produce the best result since modules tailored for each situation would likely give better results, however it may be useful purely from a design perspective.

5.8.1 Theory

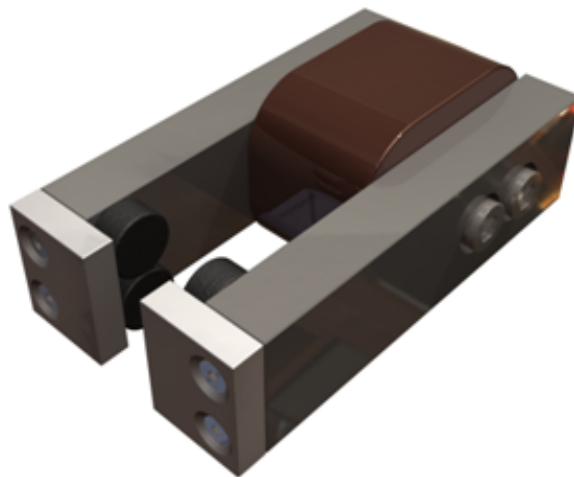


Figure 5.19: Simple Multi-Purpose Module

Figure 5.19 shows a module that could be used for either a linear or rotational device. The magnets used within the device are round, rather than rectangular, allowing the module to work equally well on a slotted linear translator or a slotted rotor.

A basic arrangement of the modules for a rotational device might be similar to Figure 5.20. Each module is slid into the machine radially aligning with the central rotor as they reach their final position. The rotor is supported on its own bearings (much like the overall MMA) and the modules simply align to it to maintain their



Figure 5.20: Simple Multi-Purpose Modules Used for Rotational Generator

own clearances.

Due to the reduction in the active areas of the magnets it is likely that such a module would not be viable, however later designs may not suffer from this issue.

5.8.2 Conclusion

Multi-purpose modules would likely not lead to anything significant in their own right simply because they have a reduced generating capacity for the same weight of materials. Although interesting from a theoretical standpoint to discuss the potential for a module to be interchangeable between machine topologies it is more likely that modules for each design of machine would be preferable. For testing purposes a prototype modules was constructed, as shown in Figure 5.21, however this module was never successfully tested.

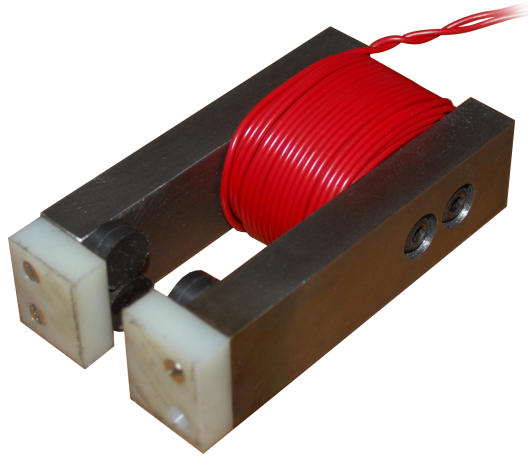


Figure 5.21: Constructed Multi-Purpose Module

Power Usage

In essence the Multi-Purpose version of the module is still a simplified FR-MMA module and as such would have very similar characteristics. Its power usage would likely be marginally lower simply because it has less active area of magnets and therefore a reduced attractive force to overcome.

Economic Impacts

The original reason for exploring a Multi-Purpose module was to see if a module could be designed that would work with all machine topologies allowing for a manufacturer to simply make one module, saving on moulds, dies and specialised manufacturing technology. It is true that the multi-purpose module could conceivably be used in this way but with the push for higher outputs and greater efficiencies it is likely that unless a better design can be presented that having different modules for different machines would still be the way forward.

5.9 Lateral FR-MMA Module

The Lateral modules are intended to pack additional generating capacity into the same volume by increasing the number of magnets that fit within the machines. They extend on the original MMA concepts and may even have applications as multi-purpose modules thanks to their magnet arrangement.

5.9.1 Theory

The arrangement of the magnets in the modules has a great bearing on the number of modules that can be packed into a given space. By arranging the magnets laterally rather than longitudinally it is possible to place more modules in the machine.

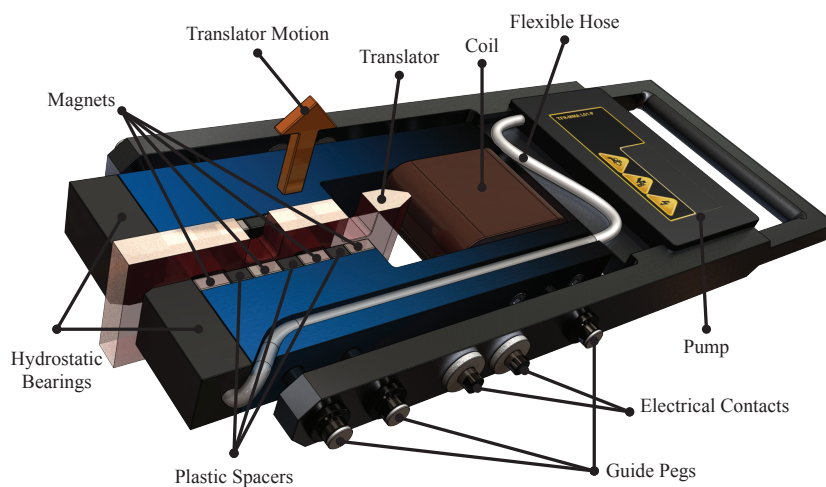


Figure 5.22: Lateral FR-MMA Concept Module

The translator differs substantially from those previously shown in order to work with the new placement of the magnets. In addition the amount of field lost

Chapter 5: Moving to Non-Rigidly Structured Generators

to magnetic short circuits should be greatly reduced by the space that has been added between the magnets. By creating what is essentially an air-gap between the magnets, the fields between the magnets are greatly reduced and with the air-gap between the magnets and the translator being substantially less than the gap between the magnets a much greater proportion of the flux should be carried into the translator.

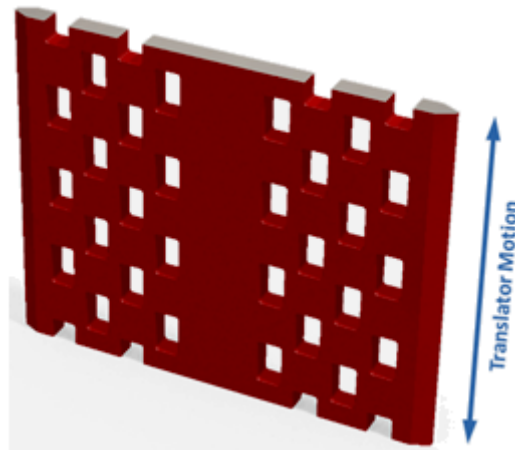


Figure 5.23: Lateral Module Translator

The diagonal slotting of the translator has a similar effect on the module to that of an iron bar moving laterally. The magnets are alternately strengthened and weakened in the same way as in other variable reluctance designs and should perform in a very similar way.

When compared to a module with the magnets stacked along the direction of motion of the translator, the operational frequency of the module will be the same provided that the magnets are of the same height, despite the difference in the translator design. Since the magnets are no longer stacked in the direction of the translator these modules should be readily transferrable to rotating devices such

as large wind turbine generators.



Figure 5.24: Example of Lateral Modules in a Rotational Device

5.9.2 Conclusion

The lateral module is potentially a big step forward in the design of variable reluctance based module design. It has several key advantages over previous FR-MMA modules;

- It halves the mass of back iron required for a given number of magnets, reduced m_{iron}
- It is substantially smaller than previous designs, reduced $m_{structural}$
- MMA principles still apply, meaning low power consumption/losses

Chapter 5: Moving to Non-Rigidly Structured Generators

- Lighter than previous designs reducing handling and transport costs
- Increased energy density of final generator

These points potentially make the module superior to its predecessors whilst still operating at the same generating frequencies. In theory these modules could approximately double the active area of magnets within a machine and reduce the operation and maintenance costs.

The lateral module does not suffer from the reduced magnet area that the multi-purpose module does when applied to different tasks such as a rotational topology. As a result it can be used as a true multi-purpose module, without modification.

Its main drawback is that the translator is harder to manufacture, however, thanks to the spacing between the magnets, the size and spacing of the slots in the translator can be increased. By expanding the holes just a little there is an increased flux change and therefore an increased output EMF

Power Usage

Since the module is still a Simplified FR-MMA module its power usage will be similar to previous designs. The bearings will need to be redesigned to allow for the reduction in the size of the modules, potentially requiring more power to support the same number of magnets, however introducing a second set of bearings at the opposite end of the magnet stack should overcome this.

Economic Impacts

The potential economic impacts of this design are high. The reduction in the requirement of iron per area of magnets reduces the material costs of manufacturing and the cost of transporting modules during maintenance operations. The reduction in the height of the modules allows more to be applied to the same length of machine effectively increasing the energy density of the generator, effectively increasing the $Income_{max}$ from any given generator.

The multi-purpose capability of the modules may make that concept of a single module for all applications viable resulting in vastly reduced manufacturing costs over a range of generators.

The lateral module has great economic potential compared with its predecessors and is likely the module of choice for future developments.

5.10 Additional Work on FR-MMA Modules

5.10.1 Failure Response Mechanism

The locking solenoids, in a design such as 5.18, would be linked to the failure detection mechanisms and in the event of a failure the solenoids would retract and the module would be ejected.

It would be important to disable the module once it has been ejected to reduce the chance of an impact within the module. In the case that a back-up module is not present it is necessary that the system be able to determine what measure of stability exists with the remaining modules, if necessary a module may have

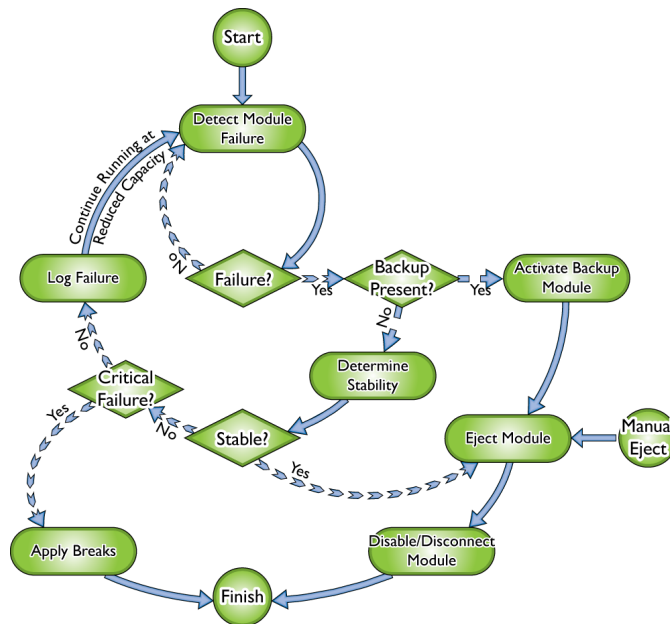


Figure 5.25: Overall Operation of Positional Modules & Complete Generator

to be sacrificed in order to operate the generator at a slightly lower efficiency. This would necessitate that the bearings be made from material softer than the translator and would only be a temporary measure. In the case of the positional modules periodic cleaning would be required to ensure functionality.

The stability function assesses the ability for the generator to continue operating in a stable fashion after it has suffered damage. The ideal case is that the generator will continue to operate unless the level of damage suffered could cause a catastrophic failure to the generator as a whole. In most cases this would mean risking significant damage to the superstructure or the translator since these are the parts that cannot be replaced without dry-docking the device.

It is likely that such results would also be force related since the loss of certain parts of the machine may not compromise its function under normal circumstances but might reduced its overall force carrying capacity. The stability function relates

directly to the survivability of the device as a whole.

The basic layout of a flexible linear generator is as shown in Figure 5.26;

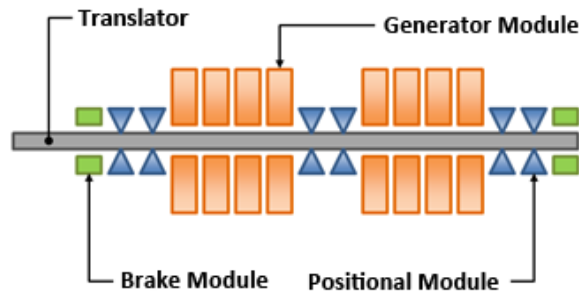


Figure 5.26: Generator Schematic

The positional modules, as mentioned before, restrain the translator and reduce the amount by which it can deflect when an external load is applied. The break modules are the last resort should a problem occur within the generator, locking the translator in place when activated. In order for the generator to be stable, enough of the positional modules must be functioning to maintain the position of the translator.

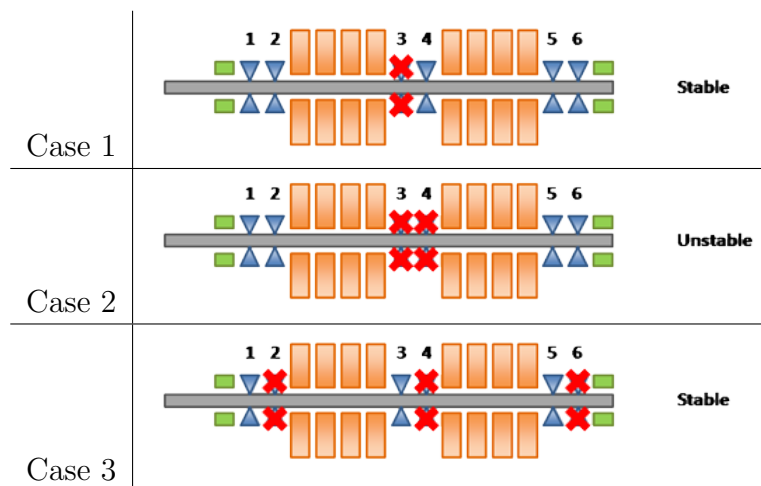


Table 5.1: Cases 1-3

Chapter 5: Moving to Non-Rigidly Structured Generators

Each set of bearings is paired with its neighbour. Should one fail, during operation, its neighbour should take over. In case 3 in Table 5.1, all the primary bearings had failed and the secondary bearings have taken over. If proper maintenance is carried out then this scenario should never happen. In case 2 it is unstable because of the bowing of the translator is now unrestricted and would likely impact the non-functional bearings. In this case it would be an option to sacrifice the bearing and allow the translator to hit it in order to maintain the stability of the machine at a slightly reduced operating capacity.

This cannot be an after-thought as the bearing must be softer than the translator material in order to be sacrificial. A ceramic bearing, for example, could be hard enough to cause damage to the translator. Most likely, after a failure such as case 2, a bearing would be sacrificed in order to maintain stability until replacements can be installed. In the intervening time the bearing would wear away under the motion of the translator. Such a bearing would likely be made of a rigid plastic.

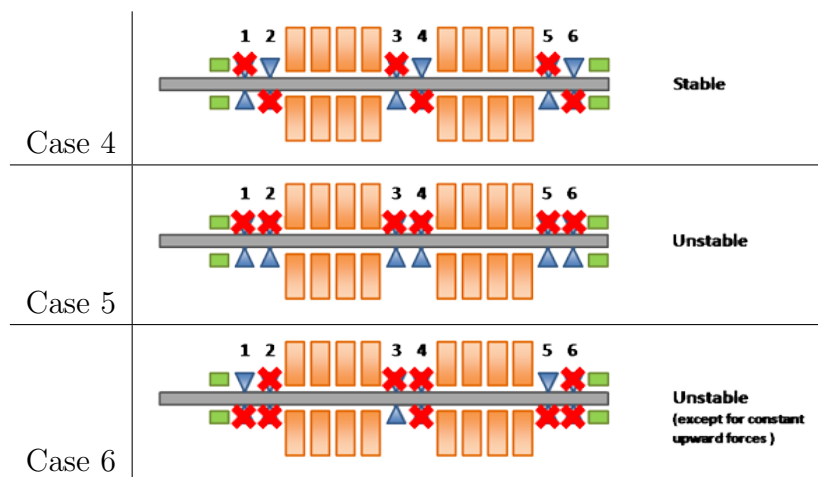


Table 5.2: Cases 4-6

Case 6 would only be stable if a constant upward load were applied. If the load were

Chapter 5: Moving to Non-Rigidly Structured Generators

variable or reversible then the opposing bearings would have to become sacrificial. This is because in one direction the bending of the translator is accounted for by the position of the bearings, if this force was reversed then the beam would bend away from the functioning bearings and likely impact the non-functional ones. Case 5 is not stable since an external load, even against the functional supporting bearings, would cause the translator to flex too greatly and cause damage to the opposing bearings.

This demonstrates that the stability function is a function of the device geometry rather than simply the number of bearings in play at a given time. Also as the number of bearings is reduced the maximum supported load increases. The exact function would be context specific, however in general the function would have to obey certain criteria;

- That each bearing group contains a working bearing in either direction.
- That sacrificial bearings are in place and not worn beyond the point where they are useful
- That if one bearing group fails the stability test then the test as a whole fails

$$f_{st}(a) = (w_{a_1} + w_{a_2})(w_{a_3} + w_{a_4}) \quad (5.13)$$

$$f_s = \prod_{a=1}^n f_{st}(a) \quad (5.14)$$

The values for w_a are weightings given to the state of each bearing in a group, where a is the group number.

Condition	w_{a_k} Value
Functional	1
Sacrificial	0.5
Failed	0

Table 5.3: Weighting values for stability function

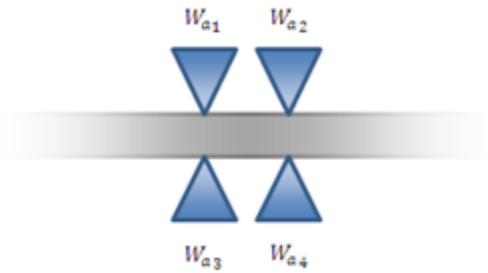


Figure 5.27: Close-up of bearing group

If the overall result, f_s , is zero then the stability of the machine is also considered to be zero and the breaks should be engaged. Any other value will give an overall stability for the machine with the higher the number the better. The stability values in Table 5.4 are generated using the numbers in Table 5.3 and the schematic for the machine previously shown;

Faults	Stability Value
Zero Faults	64
1 Sacrificial in one group	48
2 Sacrificial on one side in one group	32
2 Sacrificial on opposite sides in one group	36
1 Sacrificial on each side in each group	11
2 Failed on one side in any group	0

Table 5.4: Example Stability Values

Any values less than 1 but greater than 0 indicate that all the bearings are sacrificial and that some but not a catastrophic number have failed. Any bearing group suffers a complete failure, where 2 bearings on one side have failed in any group

Chapter 5: Moving to Non-Rigidly Structured Generators

then a zero value is generated and the machine is shut down. By monitoring the stability function externally it should be possible to determine when and where maintenance is necessary. This applies to the positional bearings only; a separate method is applied to the generator modules.

The stability function could be applied in one of two ways, it could either be done periodically, or by way of interrupts depending on the hardware utilised. If it is done periodically then it is simple to do but risks incurring additional damage to components if the check interval is too high. For example if a wave device is placed in an environment with predominantly 10 second waves and the period for checks is also 10 seconds then it is possible that high force from one of these waves could occur within the check period and do serious damage to the device. It is however unlikely that such a time period would be chosen especially in those conditions. Doing interrupt checking would entail that the sensors present to detect failures be attached such that they directly trigger events within control mechanism, this way responses are almost instantaneous, and it reduces the workload on the control hardware.

Care must be given to the design and construction of sacrificial bearings. Although constructed from plastic it is important, from a control aspect, to be able to measure the rate of wear on the bearing surface. During manufacture conductors must be inlaid in the material, which wears down with the block. The length of these wires could be measured directly or they could form breakable paths or connections using the translator itself to complete the circuit. These depend on the materials in use for the translator and whether it has been coated with any other materials. In any case a mechanism must be in place to measure the wear

Chapter 5: Moving to Non-Rigidly Structured Generators

on the bearings in order to determine the eventual failure of a sacrificial bearing.

Coatings on the translator affect the ratio of hydrostatic clearance to magnetic clearance and therefore change the dynamic of the generator this is important, as the magnets coming into contact with the translator would be a worst case for this type of generator. The coating, provided it is non-magnetic, reduces the magnetic forces even at the point of contact and allow the hydrostatic forces to exceed those of that magnets.

The break modules will need to be designed to very rugged and hard wearing since they are required to function as a last resort. If anything impedes their function then it could lead to the machine failing as a whole. Ideally each break module or pair of break modules should be capable of stopping the translator completely. As such a 50% failure rate of the breaks when activated is permissible further ensuring that the generator as a whole will survive. They can also be designed to be sacrificial to a degree since they will not be disengaged until the generator has been fitted with replacement components or removed in its entirety from its location. Since this is the case, when the breaks have been applied, they can be removed from the machine and replaced after they have been released to replace whatever material has worn away from being used. Any number of mechanisms could be used to control the break blocks, which would be best suited would depend on the circumstances. The superstructure of the generator must be reinforced around the breaking modules to ensure that no damage is done when the breaks are applied, additionally part of the control mechanism might attempt to stop the machine when the translator is in a position where force on it will be minimal. This should reduce the chances of causing additional damage to the

superstructure.

5.10.2 3-Point Pinning Strategy

The 3 point pinning strategy is referred to earlier with regard to maintaining positional stability of the translator. In essence restraining the translator at 3 points gives a reasonable level of stability without using too many bearings.

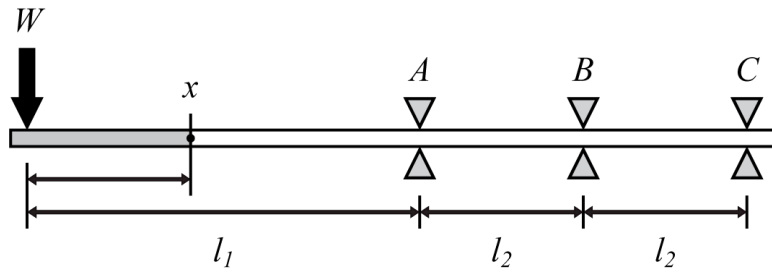


Figure 5.28: Close-up of bearing group

The loads in the 3 supports are;

$$A = \left(1 + \frac{5l_1}{4l_2}\right)W \quad B = -\frac{3l_1}{2l_2}W \quad C = \frac{l_1}{4l_2}W \quad (5.15)$$

The displacement can be found from;

$$6EIy = -Wx^3 + D_1 \langle x - l_1 \rangle^3 + D_2 \langle x - l_1 - l_2 \rangle^3 + D_3x - D_4 \quad (5.16)$$

Where;

$$D_3 = W \left(3l_1^2 + \frac{7}{4}l_1l_2\right) \quad (5.17)$$

$$D_4 = -W \left(2l_1^3 + \frac{7}{4}l_1^2l_2 \right) \quad (5.18)$$

The slope is given by;

$$6EI \frac{dy}{dx} = -3Wx^2 + 3D_1 \langle x - l_1 \rangle^2 + 3D_2 \langle x - l_1 - l_2 \rangle^2 + D_3 \quad (5.19)$$

When compared to an arrangement using 2 bearings the maximum displacement per unit applied force is substantially lower. The slope is also key because too great a slope may cause the translator to impinge on the modules.

As can be seen from section 4, the analytical results tie up quite well with the FEA results and that by allowing the extra flex in the translator, compensated for by the movement in the 2-stage and MMA modules, the force on the 3 bearings, and therefore the power required to restrain the translator, is greatly reduced.

Both the slope and maximum deflection can be predicted using the analytical approach allowing the specific maxima to be calculated that are required to correctly design the machine modules. Since, under normal operating circumstances, the machines construction is symmetrical, a maximum displacement can be calculated in either direction.

The displacement of the translator obeys the same rules as the one in section 4.2, therefore;

$$y = R(x)W \quad (5.20)$$

5.11 Designing a Working Generator Module

This section will explore the issues to do with constructing a generator module similar to that in 5.29;

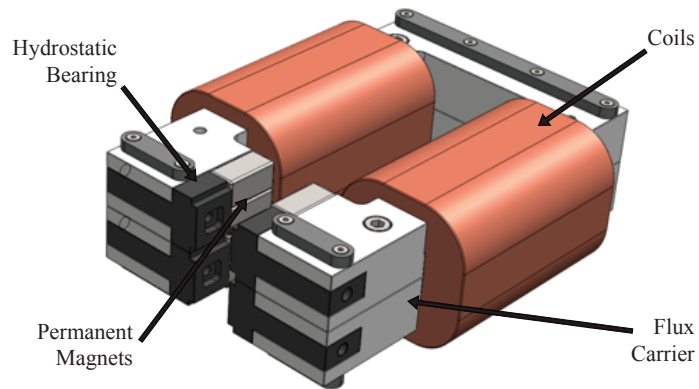


Figure 5.29: Concept Generator Module

It is primarily designed to be used with a rectangular linear translator; however it has potential applications in other areas as well. It is designed to move in 1 degree of freedom, offering 3 degrees of freedom to the translator.

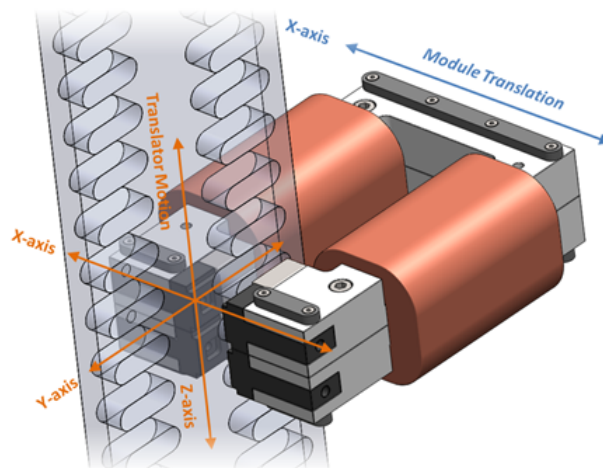


Figure 5.30: Module and Translator Showing Motions

Due to the lack of restriction perpendicular to the modules translation direction the translator can rotate on that plane but is otherwise restrained. Rotation in either Y or Z axes would potentially cause a failure. These rotations should be restricted by the positional bearings at other points in the machine.

5.11.1 Basic Requirements

This module will require;

- 8 Neodymium Magnets
- 4 Bearing Inserts
- 2 Half Flux-Carrier Sections
- 6 Plastic Runners
- 2 Coils

Note: The flux carrier is composed of 2 pieces which are bolted back to back. This is to make the pieces easier to manufacture. The coils would be wound after the flux carrier had been assembled.

The runners are to allow the modules to slide within the support frame. The support frame (See Figure 5.34) would be constructed of Aluminium so as to not interfere or bind with the magnets.

5.11.2 Structural Implications

Magnet Choice

The choice of the magnets used in the design affects the air-gap used in the generator components. The dimensions and class of magnets used has a direct impact on the maximum operable air-gap.

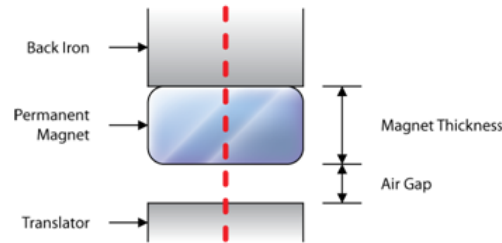


Figure 5.31: Close-up of magnet air-gap

Although it is not shown the back iron and the translator in Figure 5.32 form a closed loop of some form therefore completing the magnetic circuit. The κ -Value in Table 5.5 is defined as;

$$\kappa = \frac{l_{air-gap}}{l_{magnet-thickness}} = \frac{B_{rem} - B_{target}}{B_{target}} \quad (5.21)$$

For a range of;

$$B_{rem} \geq B_{target} \geq 0$$

The stronger the magnet the larger the sustainable air-gap, for example if a magnet $\frac{1}{2}$ " thick is used then the maximum sustainable air-gap would be 4mm for a N42 class magnet. This method works to predict the maximum air-gap to maintain a chosen B_{target} or greater in the flux carrier.

Class	B_{rem}	κ -Value ($B_{target} = 1.0$ T)
N40	1.29 T	29%
N42	1.32 T	32%
N45	1.37 T	37%
N48	1.42 T	42%
N50	1.45 T	45%
N52	1.48 T	48%

Table 5.5: Magnet Classifications

Stiffness of Back Iron

The strength of the magnets chosen for the design has a direct effect on the stiffness of the back iron since it needs to support the attractive force of the magnets.

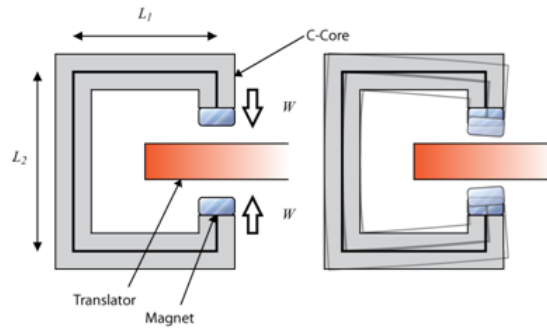


Figure 5.32: Basic C-Core Arrangement & Onion Skin Image of Deformed Shape

The magnetic forces can potentially be very large as such the stiffness of the back iron needs to be high enough to stop the back iron bending so much that the magnets make contact with the translator. The bearings will apply an opposing force which may reduce the effect of the magnets.

An Analytical Approximation:

$$\frac{d^2y}{dx^2} = \frac{M(x)}{EI} \quad (5.22)$$

Chapter 5: Moving to Non-Rigidly Structured Generators

$$M(x) = Wx$$
$$\frac{dy}{dx} = \frac{Wx^2}{2EI} + D_1 \quad (5.23)$$

The slope at $x = 0$ is zero therefore;

$$D_1 = 0$$
$$y = \frac{Wx^3}{6EI} + D_2 \quad (5.24)$$

The displacement at $x = 0$ is zero therefore;

$$D_2 = 0$$
$$y = \frac{Wx^3}{6EI} \quad (5.25)$$

At the corners there will be an applied moment due to the magnet forces. As a result M is a constant. The equation describing the back of the C-Core is;

$$\frac{d^2x}{dy^2} = \frac{M}{EI} \quad (5.26)$$

Where;

$$M = Wl_1$$
$$x = \frac{M}{2EI} \left(y^2 - l_2y + \frac{l_2^2}{4} \right)$$

As a result the maximum x displacement for the length l_2 is;

$$x = \frac{Wl_1l_2^2}{8EI_2} \quad (5.27)$$

And the maximum y displacement at the magnets is;

$$y = \frac{Wl_1^3}{6EI_1} \quad (5.28)$$

Example:

If the C-Core material is made from a low-carbon steel then;

Variable	Value
l_1	60mm
l_2	69mm
I_{l_1}	13,333mm ⁴
I_{l_2}	26,666mm ⁴
E	200kNmm ⁻²

Table 5.6: Example Variables

W is found by taking a target B-Field of 1.0T and using (2.22). Because of the design of the translator only half the magnets are effectively active at any one time. This dictates the active area. In this case $A = 200mm^2$ per magnet, and each head has 4 magnets, 2 of which are active, therefore total area is $400mm^2$.

$$\begin{aligned} W &= \frac{B^2A}{2\mu_0} \\ &= \frac{1.0^2 \times 400 \times 10^{-6}}{2 \times 4\pi \times 10^{-7}} \\ &= 160N \text{ 2sf} \end{aligned}$$

Therefore the maximum displacements are;

$$\begin{aligned}
 x_{max} &= \frac{Wl_1l_2^2}{8EI_{l_2}} \\
 &= \frac{160 \times 60 \times 69^2}{8 \times 2 \times 10^5 \times 26,666} \\
 &= 0.00107mm \\
 &= 1.07\mu m \\
 y_{max} &= \frac{Wl_1^3}{6EI_{l_1}} \\
 &= \frac{160 \times 60^3}{6 \times 2 \times 10^5 \times 13,333} \\
 &= 0.00328mm \\
 &= 3.28\mu m
 \end{aligned}$$

These displacements are minimal and since the cross-section of the back iron is in part dictated by the size of the magnets used it is likely that the stiffness of the metal will always be high enough to only have minimal displacements.

Translator & Bearing Design

The translator must be designed so that it has smooth continuous surfaces to interact with the bearings, be they hydrostatic or not. Since it needs to have numerous slots cut in it in order to work as a variable reluctance machine this surface will not be continuous unless filled with a secondary material. A continuous surface is important for use with any of the Fast-Replace module designs since they need to self-align as they are inserted into the machines. A broken surface, such as

the open slots could be a disaster if the bearings were to encounter the slot during alignment. In the case of the MMA modules if this were to happen it is likely that the magnets would impact the translator locking it in place and causing the machine to fail.

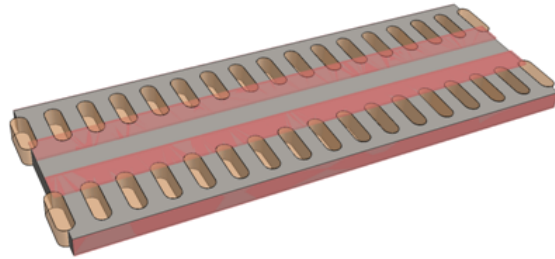


Figure 5.33: Translator Section with Bearing Paths

The red tracks in Figure 5.33 show the paths that the bearings will take along the translator. In this case the filler material is required in order to give the inner bearings a smooth track to run along.

Support Frame

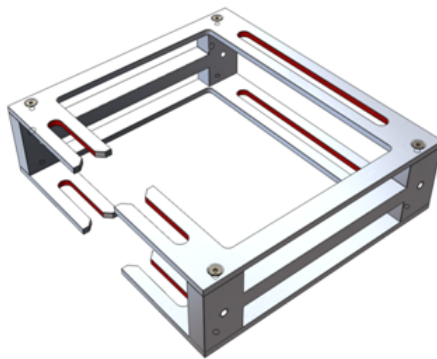


Figure 5.34: Support Frame

The support frame for the machine is intended to serve a dual role. It acts as a

container to house the generator components and also as part of the slide mechanism for the module. The sections that are intended to be used as runners are highlighted in red. The casing should not need to be overly strong as the largest force it will have to withstand is a portion of the force applied to the translator as it moves. There will be a maximum limit but as mentioned in 2.3.1, that force depends on the current load on the machine, which may limit the maximum current that the machine can operate with.

5.11.3 Pump Choice

There are a number of pumps that could be used to supply fluid to hydrostatic bearings in generator modules. From a control point of view a positive displacement pump would likely be the best suited to the application since controlling the flow-rate is critical. With a volumetric pump the volume of fluid that passes through the pump is directly proportional to the rate of rotation of the drive shaft. There are a number of different positive displacement pumps that could be used, the simplest, conceptually, would be a gear pump. They are durable and capable of delivering high pressures but deliver generally low flow-rates. If a higher volumetric flow-rate is required then migration to other pump designs may be necessary, such as swash-plate, vane or piston pumps, see 2.6.4

From (2.57) the following can be derived;

$$Q = \frac{Wh^3}{L_H} \quad (5.29)$$

Where W is substituted for F . From this the necessary Q can be calculated to

support the load on a bearing defined by L_H . It is important to remember that a degree of pre-loading of bearings will be necessary. Pre-loading in the case of hydrostatic bearings is determined by the base flow-rate in the bearings. This will apply a force to the translator even if it is in the equilibrium position.

The preloading requires some power even in the equilibrium position, however the only way to avoid preloading the bearings is to have no flow passing through, therefore there will always be a degree of preloading.

5.11.4 Material Selection

Magnetic Flux Carrier (Back Iron)

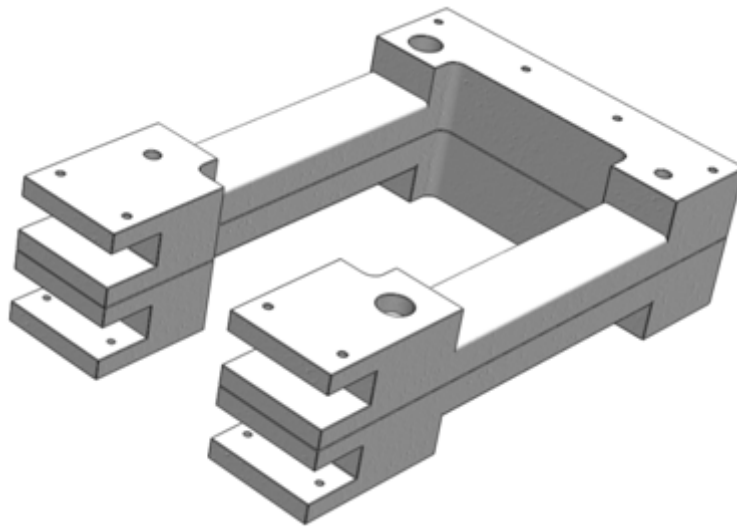


Figure 5.35: Back Iron/Flux Carrier

Ideally the flux carrier should be iron or magnetically soft steel. The key issue is the fact of lamination. Making the flux carrier out of steel laminates encourages the

magnetic fields to flow in certain directions and discourage propagation through the layers of the laminate.

In this design the structural properties of the flux carrier are key since they will be the most highly loaded parts of the generator.

Hydrostatic Bearings

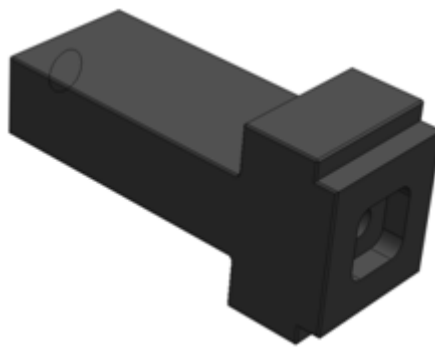


Figure 5.36: Hydrostatic Bearing Insert

The hydrostatic bearings require a smooth surface and should be relatively hard in order to make them durable. In industry the vast majority of hydrostatic bearings are manufactured in metal. However, for the pressures and flow-rates involved in these designs it is quite possible to use some lighter materials such as plastic.

Ideally the hydrostatic bearings would be manufactured about of a ceramic material because of its weight, surface finish and strength, however this would likely also end up being more expensive than plastic or metal bearings. In this example plastic will be used in order to test viability and because something non-metallic is preferred so as to avoid eddy currents being generated during operation.

Note: Long term plastics may prove too soft for use with sea water due to the

amount of particulates and sediment that may be passing over them.

Note: Designing the bearings as inserts that are added to the design, rather than as an integral part of the structure should allow for other materials to be substituted at a later date.

Translator Materials

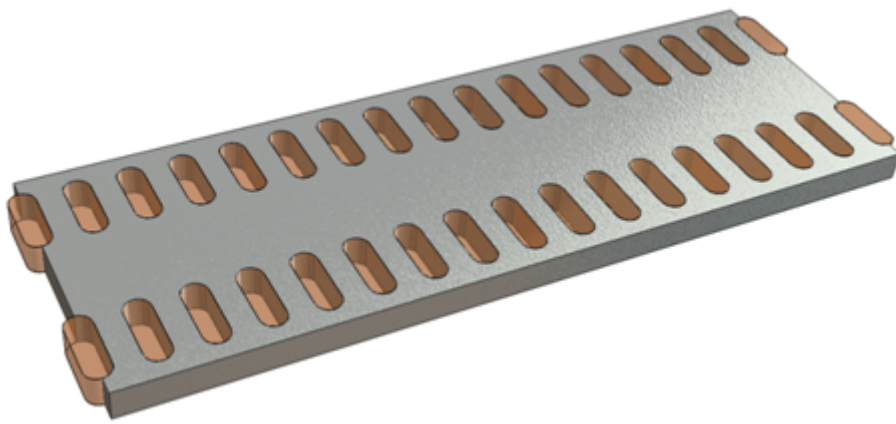


Figure 5.37: Translator Section

The translator would ideally be an iron/soft steel sheet. Due to the direction of magnetization laminations would not work as they would weaken the translator and potentially cause it to break under the required loads. Also, making a laminate translator would take an extended period of time and as such cutting it from a single piece of steel appears to be the best option currently available.

The slots can either open to the air/water, depending on environment, or could be filled with a secondary material. The latter might be preferable if the material was able to give additional strength to the translator, however it is unlikely that any non-metallic material could serve this purpose and any metallic material would

suffer from issues arising from eddy currents. If the translator were thick enough it would be possible to do make it so that the slots did not go all the way through the material, giving additional strength but sacrificing some of the machines efficiency, but this would increase the mass of the translator substantially.

Filling the slots with plastic may prove to be the best compromise due to the issue of eddy currents and those of the bearings raised previously. (See 5.11.2) Depending on the conditions where the device will be placed some additional work may need to be done as to the effects of temperature.

Support Frame Materials

The support frame would most likely be constructed from Aluminium. It is required to be non-magnetic but still relatively stiff and strong. From a magnetic standpoint the use of steel screws and bolts in the frame isnt an issue provided they are a good distance from the magnets since Aluminium has similar magnetic properties to air, from a corrosion standpoint it is important that any non-aluminium components are coated or otherwise insulated from the frame to avoid issues of galvanic corrosion.

Although most aluminium alloys are not suited to use in sea water and suffer from problems of de-alloying there are a number of alloys available for use in ship building which would be suitable for use in flooded devices^[15].

Given the direction of the magnetic fields being generated any eddy currents should be minimal.

5.11.5 Predicting Performance

The following is an approximation of the behaviour of a single generator module. It assumes that there is no loss due to magnetic short circuits, and that the driving motion is purely sinusoidal.

$$s = A \cos \omega_1 t$$

$$\frac{ds}{dt} = -A\omega_1 \sin \omega_1 t \quad (5.30)$$

The flux is approximated by the comparing the overlapping areas from the magnets and the translator.

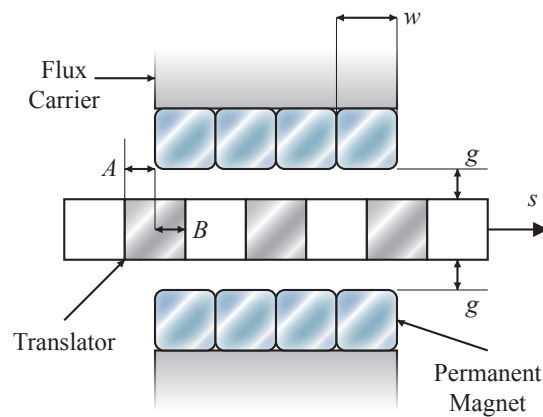


Figure 5.38: Cross-section of a Variable Reluctance Generator Head

The active area of one pair of magnets will be represented by the dimension A multiplied by the depth of the magnet and the other by the dimension B. As the translator moves these dimensions change, A increasing as B decreases and vice versa. This is represented by the following piece-wise expression;

Chapter 5: Moving to Non-Rigidly Structured Generators

$$\varphi = \begin{cases} \varphi_0 h(w - 2s), & 0 \leq s \leq w \\ \varphi_0 h(2s - 3w), & 2 \leq s \leq 2w \end{cases} \quad (5.31)$$

This can be approximated by the Fourier Series shown below giving a triangle wave output.

$$\varphi = \varphi_0 \frac{8}{\pi^2} \sum_{k=0}^n (-1)^k \frac{\sin((2k+1)\omega_2 s)}{(2k+1)^2}$$

$$\frac{d\varphi}{dt} = \varphi_0 \omega_2 \frac{ds}{dt} \frac{8}{\pi^2} \sum_{k=0}^n (-1)^k \frac{\cos((2k+1)\omega_2 s)}{2k+1} \quad (5.32)$$

The maximum $d\varphi/dt$ value would occur at the maximum velocity and as such can be expressed as;

$$\begin{aligned} \left[\frac{d\varphi}{dt} \right]_{max} &= \varphi_0 \omega_2 \left[\frac{ds}{dt} \right]_{max} \\ &= \varphi_0 A \omega_1 \omega_2 \end{aligned} \quad (5.33)$$

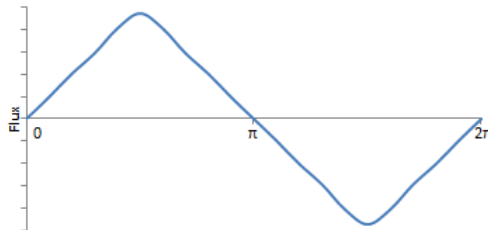


Figure 5.39: Triangle wave Approximated with a 4-term Fourier Series

Since both the EMF and the frequency are variable power electronics will be re-

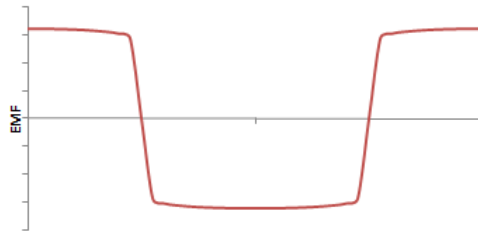


Figure 5.40: Characteristic EMF Output Profile

Parameter	Value	Parameter	Value
Turns	1000	Air-Gap	4mm
B_{rem}	1.42T	Wave Period	10s
Range	2m	Max Flux	$3.23 \times 10^{-4} Wb$
Magnet	$1'' \times \frac{1}{2}'' \times \frac{1}{2}''$	Slot Width	$\frac{1}{2}''$

Table 5.7: Output Profile Parameters

quired in order to convert them to the necessary grid standards. The power output would most likely need to be converted to DC and converted to AC conforming to the grid. Although not a focus of this research, an array of devices such as this might produce a more even power output.

The EMF shown in Figure 5.42 is the unloaded EMF, or more precisely the EMF due to just the magnets with no current effects. From Figure 2.19 in Section 2 it can be seen that the actual EMF would be different when the module was under load because of the influence of the current on the magnetic circuit and the induction effects of the coil. However the effect of the current in the coils is substantially less than that of the magnets. This can be seen in the shape of plots in Figure 5.42.

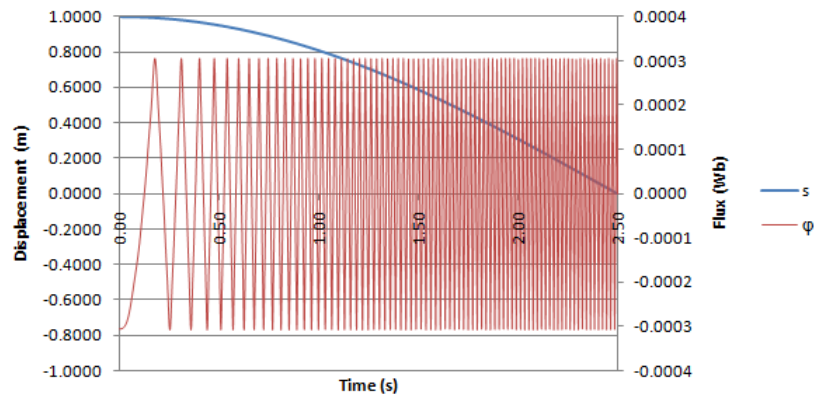


Figure 5.41: Translator Position and Instantaneous Flux

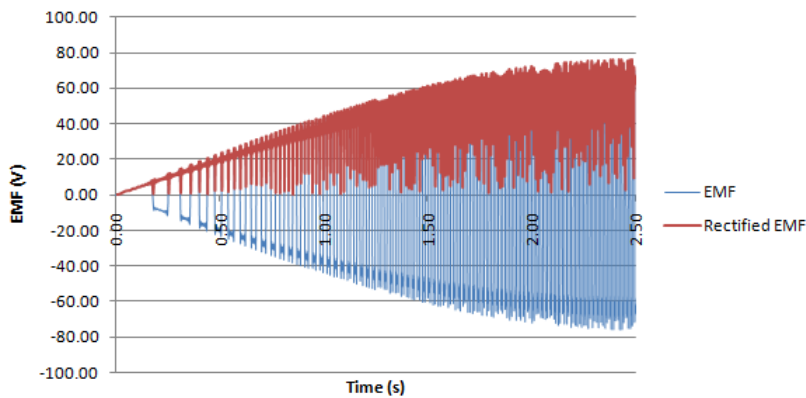


Figure 5.42: Generated EMF

5.12 Other Areas of Research

5.12.1 Re-circulating Bearings

A key issue for the design of hydrostatic bearings submerged generators is the fluid supply. Ideally the sea-water (or surrounding fluid) would be used, however that can lead to problems if the level of particulates is too high, given the clearance required in hydrostatic bearings. Since the issue is the amount of particulate

Chapter 5: Moving to Non-Rigidly Structured Generators

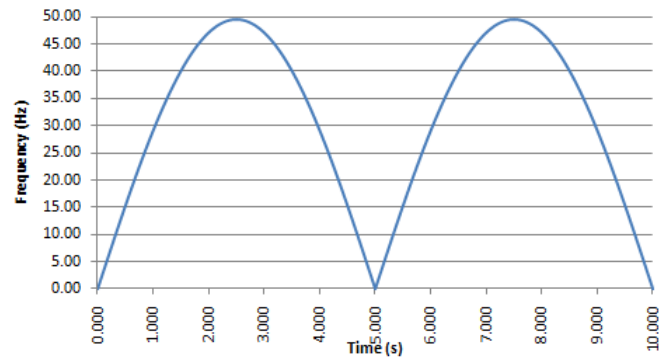


Figure 5.43: Output Frequency

matter passing through the fluid supply systems it would make sense to seal the generator in one way or another but that approach may not always be practical for large linear devices.

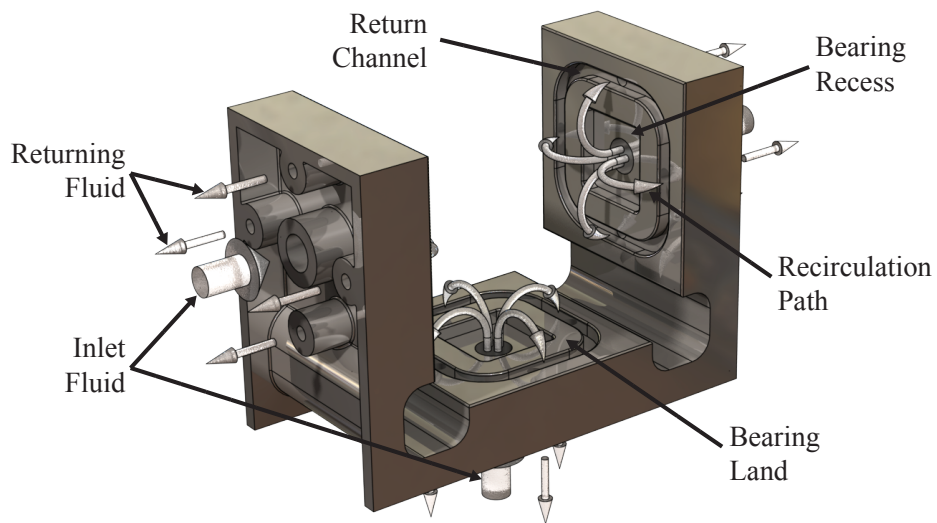


Figure 5.44: Concept Re-Circulating Bearing

A re-circulating bearing is designed to recover and reuse a proportion of the fluid passing through the bearing. When the fluid is expelled by the bearing it radiates sideways, by adding a second channel around the bearing, it may be possible to

capture some of the escaping fluid by drawing the volume flow back into the return side of the pump.

Since there is a substantial head-loss across the land of the bearing the fluid being returned can be captured at the same flow-rate as it entered the bearing without having a massive effect on the bearings power usage and since the fluid that has already passed through the bearing should be cleaner than that of its surrounding environment, it should help with reliability.

A number of designs of recirculating bearing were tested using CFD to see just what proportion of the fluid was recovered, however due to the high pressures present in the centre of the bearing the exit velocity of the fluid across the land proved to be high resulting in an effect not unlike a hydraulic jump^[11] where a sheet of fast moving fluid expands outwards until its Reynolds number reaches a critical point. In this case this point occurred outside the simulation space and only a small proportion of the exiting fluid could be recovered. Although it may be possible to produce more effective designs of this bearing, for example ones that trip the flow early by increasing the Reynolds number to increase the recapture rate, they would most likely incur greater losses in the process, therefore this concept will only have limited effectiveness.

5.12.2 Jet Bearing

The jet bearing is an evolved form of the recirculating bearing designed entirely from the standpoint of recirculation rather than traditional hydrostatic bearing design.

The concept is simple, rather than being fed into a recess the fluid is injected

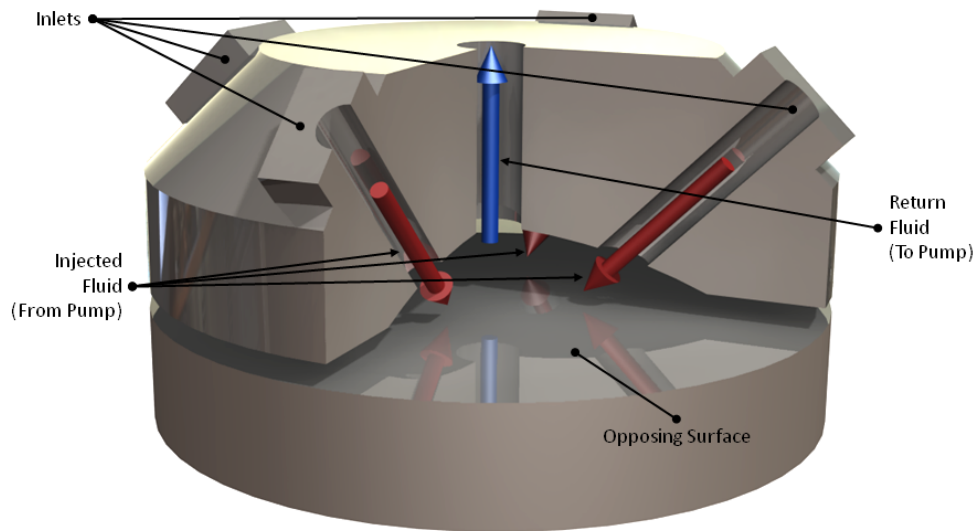


Figure 5.45: Jet Bearing Concept

into a cavity as multiple small jets. These jets are angled towards the opposing surface and they provide the force to support it. There is momentum transfer to the surface, depending on the angle of the inlets as well as an increased pressure in the cavity. The resultant force of these two components works to separate the bearing and the surface.

It should be noted that, unlike in hydrostatic bearings, fluid will continue to flow through a jet bearing if there is not clearance due to the need for the cavity.

CFD Tests

Figure 5.46 shows the results of a simulation using a total flow-rate of 80mls^{-1} . The pressures are absolute and, for ease, atmospheric pressure is taken to 100kPa . For the given bearing an average pressure of $100,543\text{kPa}$ is recorded across the

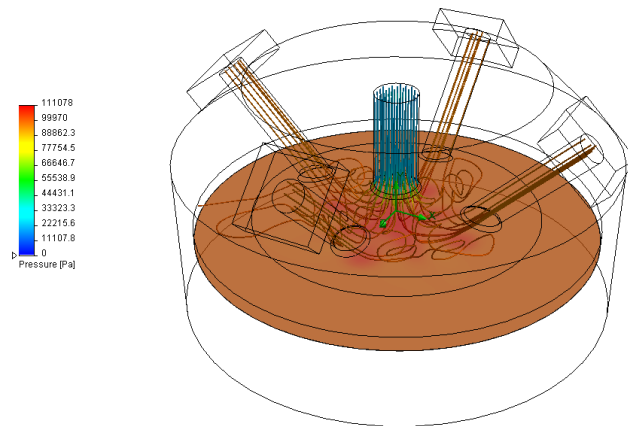


Figure 5.46: Jet Bearing inc. CFD modelled flows

land area, resulting in a normal force of $0.461N$ due to the size of the bearing ($30mm\varnothing$).

Strangely a greater force is generated when using two jets with twice the flow compared to four. The average pressure is lower but the maximum pressure increases significantly. Unfortunately the increased force comes at a price since it promotes more mixing with the surrounding fluid compared to the four jet version. This can be seen in Figures 5.47 - 5.50.

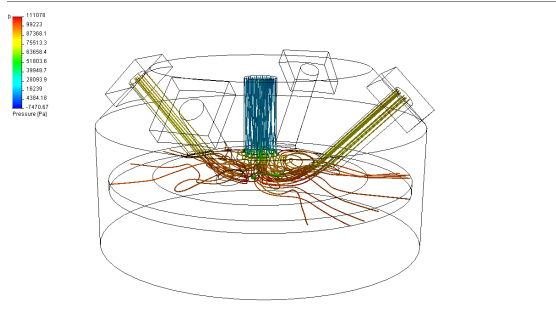


Figure 5.47: 2-Jet Recirculating Flow

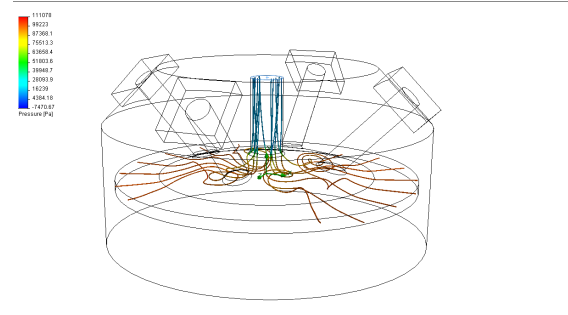


Figure 5.48: 2-Jet Additional Flow

The 4-Jet arrangement has far less mixing, evident from the lack of paths leading up the outlet shaft in Figure 5.50 compared to the number in Figure 5.48. Cross

Chapter 5: Moving to Non-Rigidly Structured Generators

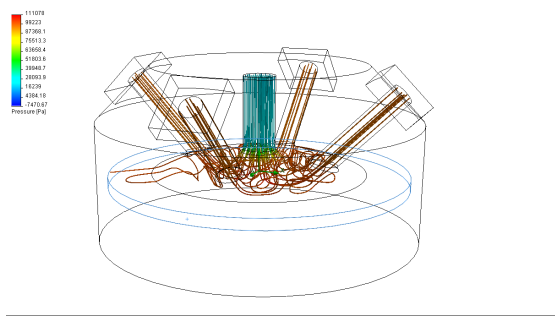


Figure 5.49: 4-Jet Recirculating Flow

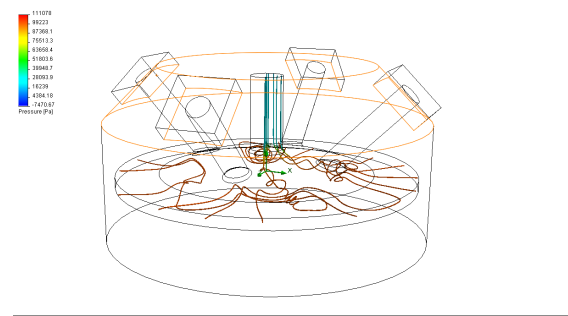


Figure 5.50: 4-Jet Additional Flow

sections, taken through the flows, show the increased maximum pressure present in the 2-Jet flow compared to the 4-jet but also how localised that maximum pressure is.

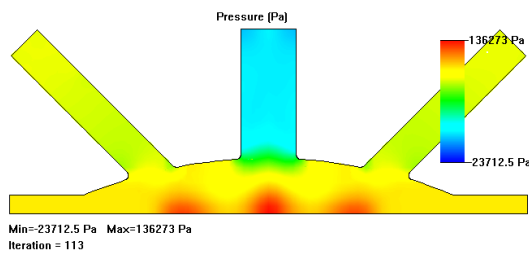


Figure 5.51: 2-Jet Pressure Distribution

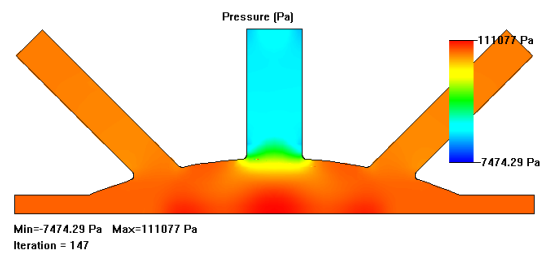


Figure 5.52: 4-Jet Pressure Distribution

In both of the velocity vector cross sections the amount of leakage is extremely low but as would be expected the velocities in the 2-Jet plot are substantially higher on the inlet.

Although unable to generate the same amount of force as a hydrostatic bearing for the same size the lack of mixing and the ability of the jet bearing to recirculate the majority of the fluid passed through it may make it an alternative technology for lubrication in flooded applications where mixing of lubricant and surrounding fluid must be kept to a minimum.

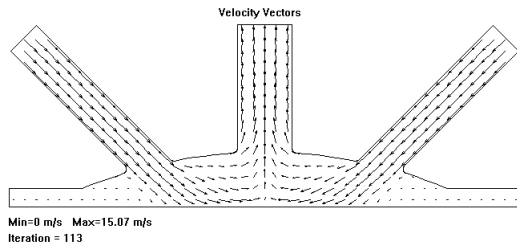


Figure 5.53: 2-Jet Velocity Vectors

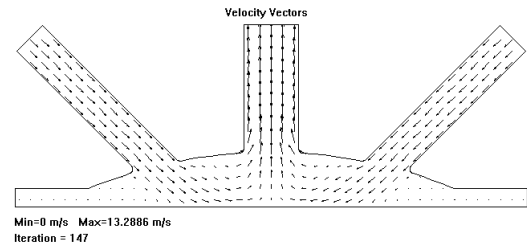


Figure 5.54: 4-Jet Velocity Vectors

5.12.3 Hybrid Ball-Fluid Bearing

One of the key issues with using fluid bearings is that of flow control. Adding restrictors and intelligent flow control systems increases losses and weight in fluid bearing devices, not to mention increase the complexity of the system giving greater scope for errors. The Hybrid Ball-Fluid Bearing is designed to act not only as a bearing but as a flow regulator as well.

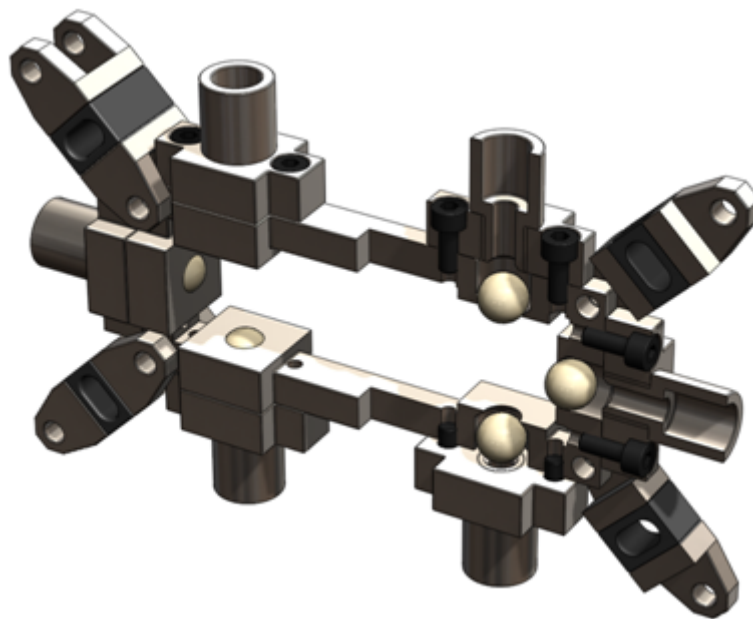


Figure 5.55: Hybrid Bearing Frame

Chapter 5: Moving to Non-Rigidly Structured Generators

If the clearances are properly calculated in the first instance then there should be no circumstance where every bearing is closed (except after wear and tear) reducing the chance of water hammer occurrences, that being when the valves shut suddenly and it causes a shockwave to propagate back through the system.

In this circumstance, the balls should be composed of a smooth hard substance such as engineering ceramics. Since they will be operating in a completely fluid environment and essentially suspended they should have excellent longevity. All the bearings should be fed from the same source, that way as soon as a displacement occurs the supporting balls apply a force to correct it.

Theory

The model behind this mechanism is different for the standard hydrostatic mechanism and therefore does not display the same displacement characteristics. The displacement/force function for this will be represented as $Z(s_r)$. Since in its closed position the bearing may have no contact with the translator there will be a range of motion through which it will operate. As such it will be described as a singularity function. If it is assumed that in the perfect equilibrium position all the bearings are closed then;

$$Z(s_r) = z(s_r) \langle s_r \rangle^0 \quad (5.34)$$

In this equation the singularity function could be replaced with the Heaviside step function;

$$Z(s_r) = z(s_r)H(s_r) \quad (5.35)$$

In either case this means that when the relative displacement, s_r , drops below zero the value of $Z(s_r)$ becomes zero rather than implying a negative force on the translator where none exists. $z(s_r)$ represents the function describing how the force varies irrespective of valve effects of the bearings. s_r is the displacement relative to the bearing, a displacement towards the bearing is seen as positive. In the case of opposing bearings;

$$s_{r_a} = -s_{r_b} \quad (5.36)$$

for any displacement between them.

Operation

From a standpoint of positioning, the same concepts apply to these bearings as to the normal hydrostatics. Offsetting the plane of the bearing from that of the magnet should allow the bearings to function more effectively and more efficiently. The longevity of this type of bearing should be lower than that of a normal hydrostatic bearing; however its self-regulating nature may afford power savings in the long run.

Conclusions

The hybrid bearing offers an interesting alternative to either the mechanical or fluid bearings and with the right lubricant and proper design could potentially be

quite promising, however there are a few potential problems. Due to the need for the bearings to completely seal when not in use the inclusion of particulates could potentially wedge bearings open leading to fluid losses and additional power loss. Likewise particulates could damage the ball of the bearing or indeed the channels resulting the same problem of power loss.

5.12.4 Sacrificial Bearings

Rather than being an actual devices sacrificial bearings refers to a survival strategy that can be implemented on hydrostatic bearings to aid reliability. This strategy required a bit of revision of the materials and methods involved in creating these bearings in the first place since the sacrificial characteristic cannot simply be added. The key points about sacrificial bearings have already been outlined to a degree however they are;

- That the bearing be suitable for use as a contact bearing should a failure occur
- That the material the bearing is composed of be softer than that of the translator and unlikely to cause any damage
- That the bearing be inlaid with materials suitable for measuring the wear of the material

These are all design factors and therefore need to be considered during the design stage. When a bearing fails it becomes sacrificial until it is too worn to serve its purpose. This is measured by the materials inserted into the bearing, perhaps metal tracks or fine wires that will be work away with the plastic.

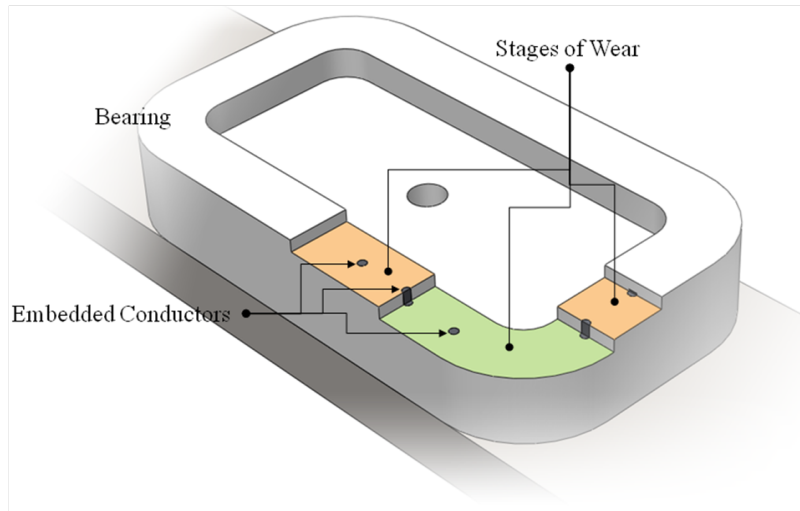


Figure 5.56: Example of Conductors Embedded in Bearing material

Only the top section of a bearing need be composed of the sacrificial material, which means that it is necessary to be able to measure the decay to avoid whatever substrate or support is used being exposed. This ties in directly with the failure-response section.

5.12.5 Protective Measures

During this research the subject of protection needed to be considered. The numerous metal components, including the magnets, would likely result in numerous corrosion problems thanks to the salt water and the galvanic interactions due to the different metals in play. In most applications where metals need to be protected from corrosion by salt water another metal is electrically connected to the one requiring protection. This is termed a sacrificial anode and is allowed to corrode in preference.

The theory is straight forward, by connecting two metals in an ionic solution, in

Chapter 5: Moving to Non-Rigidly Structured Generators

this case water, an electrochemical cell is created. If the metals have two different electric potentials they become charged. The positively charged metal is the anode and will be attacked by corrosion, the cathode will not corrode until the anode is completely degraded or the connection is broken. This is known as galvanic corrosion^[31].

In fresh water Aluminium could be used in galvanic circuits to help protect items such as the iron since the aluminium oxide coating is waterproof but still provides an electric potential, however in salt water the oxide layer will not be enough to protect the aluminium from corrosion resulting in the progressive decay of the components.

Most components could be coated to protect them from the effects of the sea water; this includes most faces of the iron. However coating of some sections would not be feasible because of the small clearances. Adding a coating would also affect the way in which any bearings would function. In such places a sacrificial anode may need to be connected to the components in order to protect them. This is especially true of the magnets since it has been shown that magnets subjected to salt water can corrode quite rapidly. This is one of the reasons that the bearings, and all feasible components should be made from high density plastics or composites. As part of this research the possibility of using the generators structure, in conjunction with a number of extra components, as a salt-water battery was explored. Such batteries have been created and have been used to power ocean floor seismometers. The hope was that enough power could be generated to drive the bearings and help increase the efficiency still further, unfortunately the amount of power that could be captured this way without causing problems was minimal and therefore

Chapter 5: Moving to Non-Rigidly Structured Generators

the concept of using a salt-water battery was shelved.

As an aid to protecting the generator it might be possible to impart a negative electric charge to all the at-risk components with the use of external control electronics. Previous salt water battery work used a carbon brush electrode as part of the battery design to act as the cathode. Carbon has a low electric potential and therefore naturally forms a cathode. At the same time, these carbon filaments are relatively unaffected by corrosion due to salt water and as such it may be possible to engineer a circumstance where a carbon electrode may be forced to become anodic. If this were the case, the corrosive elements would be attracted to the carbon but do very little damage while the other components should be protected. Applying an EMF in opposition to the naturally occurring one generated by the interaction between the electrodes should promote this shift.

Chapter 6:

Real World Impacts

The real world implications of this work extend to most areas of kinetic generator design. Generators based on the MMA structure utilising 2-stage bearing restraints promise to have greater shock tolerances and reduced bearing losses no matter the type of bearing used. In keeping with that, the reliability of the machines is increased and the generators become more durable, reducing downtime and improving profitability.

6.1 Manufacturing Costs

The reduction in the bearing loads thanks to the flexible nature of the machines is key to reducing the manufacturing costs. The reduced number of bearings in the generator reduces the effect of any externally applied load (see section 4.2), this in turn can be seen to either reduce the stresses in any given supporting member or increase the maximum force that can be tolerated by the machine. Either way the cost of tolerating a given force is reduced allowing weaker/cheaper materials to be used in the construction of the generator whilst not compromising its operation or survivability.

The modular construction allows for the bulk production of units for the generators. Since they are composed of multiple identical units the generators are easily manufactured and constructed. This saves time on construction of large and complex generators as well as transport costs since the number of large and bulky components is greatly reduced. In many renewable energy applications this allows for on-site construction of the generators with the actual generator components being added once the superstructure has been assembled. This is especially useful

in the case of wind or wave power.

Given the flexible nature of the generators the overall tolerances for their design can be relaxed. The accuracy of the superstructure becomes a secondary concern since movement in the modules will account for any variations in the superstructure. Likewise the tolerances for the modules themselves are not overly strict provided that the magnet and bearing clearances are well defined and the translator is dimensionally stable. All this means that the cost of production is greatly reduced. Some aspects of construction, such as the sacrificial bearing components would require slightly more complicated manufacturing techniques, however these should not increase the construction cost too much.

6.2 Reliability

The modular design of the generator works in a few ways to improve reliability.

1. The reduction in forces across the machine reduces the chance of components failing, reducing the possibility of a catastrophic failure and increasing the longevity of the whole machine.
2. The motion and self-positioning nature of the modules accounts for variations in construction, deflections from external forces, and damage suffered during operation, at least to a degree. This means that in most circumstances the generator will continue to operate after other designs would have ceased.
3. The replaceable nature of the modules means that, a catastrophic failure of the module is not a catastrophic failure for the machine and that when

such a failure occurs the modules can simply be exchanged. The FR-MMA modules allow for replacement of damaged modules with ceasing generation, resulting in a greatly reduced downtime and therefore a greatly increased reliability. The reduction or elimination of downtime is key to the concept of flexible generation and is the major benefit of this method of design.

The introduction of the 2-stage support bearings improves the generators tolerance to impacts and other sudden forces. They reduce bearing loads and the maximum power drain on the bearings whilst adding tolerances to defects or damage suffered during operation helping to improve the reliability of the machine.

6.3 Operation & Maintenance Costs

The use of fewer support bearings within the generator reduces the bearing losses by reducing the individual bearing loads and total number of bearings, as a result the losses caused by external forces drop dramatically. Since the losses are reduced the generator operates more efficiently and is therefore more profitable.

The key benefit however is the ability of the FR-MMA modules to be swapped during operation, by reducing the generating capacity of the machine rather than stopping it, it will continue to generate revenue and as such is a much more profitable option than stopping the generator for maintenance and in extreme case removing the device from site. The cost of repairs is also reduced thanks to a reduction in the transport costs. If all that is required for a repair is a single module then there is no need for heavy vehicles or servicing gear.

As an example, to service a wave generator that does not use these principles it

is necessary that the generator be removed from site or at least raised onto the deck of a ship. With a modular design, such as the ones discussed, simply the faulty components could be removed and replaced, as such the type of boat used is changed, the number of people involved is reduced and therefore the cost of maintenance is reduced. The aim with the modular designs is that if necessary a single diver could do required maintenance that would otherwise require a barge and a skilled crew.

Since all modules are designed to be swappable in this way, any failed component can be replaced in this manner. If the control architecture, and especially the stability functions (see section 5.10.1), are designed correctly then the generator should operate without interruption continuously and its longevity should be good. If it is possible to eliminate the downtime inherent to maintenance of current designs then it would dramatically improve the economic viability of linear generators in the market place.

6.4 Efficiency

The efficiency of the generator in ideal conditions is dependent on the idle loads of the bearings and the efficiency of the power take of mechanisms. By reducing the loads on the bearings within and decreasing the number of bearings the generator the overall efficiency of the generator is increased.

Although operating at design conditions might allow for very high efficiency a generator will likely be subject to numerous external forces, especially in renewable energy applications, as a result it is likely that there will always be some variable

Chapter 6: Real World Impacts

loading on the bearings which will cause additional losses. Such a variable load might be the drag caused as a buoy is dragged by the waves, or a minor imbalance in the geometry of a wind turbine.

Chapter 7:

Conclusions

7.1 Conclusions

Although, as stated in section 1, the initial focus of this research was the evaluation of hydrostatic bearing technology in linear generators, it expanded to encompass almost the whole of generator design, looking more at the overall costs of generator construction and maintenance. The concepts that were originally conceived to improve the efficiency of hydrostatic bearings, 2-Stage and MMA designs, have lead down paths not considered before.

7.1.1 Hydrostatic Evaluation

Hydrostatic bearings could indeed be used in flooded wave energy applications and at high efficiencies. This can be improved still further using the implementation of the 2-stage and MMA design strategies, as show described in 5.2.2 & 5.3.2. The reduction of the number of bearings within the generator, the reduction of impulse forces and flexible construction all help to improve the efficiency of the generator. The flexible nature of the modules allows the translator more flexibility reducing the loads on the bearings constraining it (See section 4). The mobility of the individual modules allows them to maintain their individual clearances without excessive power consumption.

It is possible to produce a hydrostatically supported generator that will work at high efficiencies and have excellent longevity and damping characteristics. Since no analysis has been done over the course of this research into the power loss in standard bearings when used in water rather than air it is cannot be said as to which solution will be the most efficient, however properly designed hydrostatic

Chapter 7: Conclusions

bearings will have the benefit of a much longer lifespan than traditional bearings. Also, off the shelf bearing solutions are generally not suitable for deployment in salt water, requiring specialist sealing which increases losses.

Overall it appears that hydrostatic bearings would be a viable option for linear generator construction, however the research also flagged potential problems with their operation in marine environments. Initially the idea was to use the surrounding sea water as the lubricating fluid, as time went on it became apparent that the particulate matter in the water could pose a potential problem for the operation of the machine, clogging pumps and bearings. Overcoming this requires either filters be placed over the intakes which introduces additional issues for clogging and power consumption, or the system be designed with a level of tolerance to these particulates, most likely involving increasing the bearing spacing to allow them to pass however either method would increase the power consumption of the support mechanisms as a whole.

A potential solution to this came in the form of the re-circulating fluid bearing which would allow a limited amount of already cleaned fluid to be recycled through the bearing reducing the need for filtering. Although in theory it is possible to recycle 100% of the bearing fluid without invalidating the bearing as a whole, the exit velocity of the fluid proved too high in simulations and only a fraction of the the used fluid was recovered. Different designs of bearings could potentially be used for this task however it is likely that their effectiveness will always be limited.

7.1.2 Additional Benefits

As the research progressed it became apparent that the concepts that have been created to help improve the hydrostatic bearing efficiency had a number of additional benefits;

By reducing impulse forces and increasing bearing mobility with the use of the 2-Stage bearings it became possible to relax the previously very tight design tolerances required to make a linear generator operate. Although this potentially reduced the generating capacity by a small degree it had the benefit of allowing for less precise construction, with the exception of a few parts, reducing the cost of generators as a whole and therefore increasing economic viability.

The inception of the MMA designs further improved on this by reducing the number of bearings required to support the translator within the generator and allowing tolerances to be relaxed still further. As the 2-stage bearings were moved to being positional bearings only, and the MMA designs took over the role of supporting the generating components the theoretical ease of construction increased while the potential costs were reduced still further. In these circumstances lighter, cheaper and weaker materials become ever more viable driving down construction costs.

With the 2-stage and MMA concepts looking to potentially have a large impact on the manufacturing costs of the generators it became apparent that the next great stumbling block to commercial viability was the cost of maintenance. This is especially important for wave energy devices since they are hard to reach and must be designed to be very rugged. Previously attempted linear generators were designed as single units. This makes them difficult to service and, when coupled with the degree of specialisation in the technology and the environments where

these devices are to be deployed, costly to maintain. The next round of concepts attempted to create a generator structure that was easy to service and maintain.

7.1.3 The Next Step

The 2-stage and MMA concepts satisfied the original scope of the project in that they allowed hydrostatic bearings to be used to align and control generation components with relatively low power losses. Consideration of the additional benefits they offered presented new directions in which the research could advance moving beyond the efficient use of hydrostatic bearings and into the areas of operation & maintenance and construction costs.

Fast-Replace Modular construction attempted to create a generator architecture with hot-swappable modules for both positional and generating applications. Such modular construction would allow for failed modules to be replaced without shutting the generator down. If the generator continues to generate whilst maintenance is carried out then there is not loss of revenue normally associated with down-time during maintenance. In the case of oceanic applications it reduces the need for dry-docking or the hiring of expensive barges or equipped ships to handle the technology.

The core concept was that a single diver or ROV² could swap damaged modules quickly, without needing to halt generator operations to do it. All modules would be interchangeable, the only part of the generator which could not be exchanged, without a dry-dock, is the superstructure, the rest would be extractable modules with redundancies especially in the case of the positional modules. An appropri-

²Remote Operated Vehicle

Chapter 7: Conclusions

ately designed control system would be able to compensate for almost any failure during operation and act to remove modules that were potentially threatening continued operation. For such a control system to be truly effective though there must be a method of communicating the condition of the generator to shore. The mechanism for determining overall machine health would offer a measure of warning if such information was used to coordinate repairs.

By enabling generators to run without needing to be shut down for the majority of maintenance and failures that occur, the overall economic viability is increased. By allowing individual modules to fail and disconnect from the machine superstructure the machine is safe-guarded and it continues to operate but at a reduced capacity until replacement modules can be installed. Many of the machines explored during this work contained 20 modules with the understanding that if a single one failed the machine would still operate at 95% output.

It also introduces the possibility of creating the superstructure of a generator without the generating components, installing it and then installing the generating modules at a later stage. This would make the construction of the superstructure easier as well as the installation. This can be expanded beyond the original linear generator applications to include almost any driven electromagnetic device, on or off land. This modularity and expandability in theory means that it can be applied to future applications as they arise.

The final reported concept of the lateral module contains all the concepts explained to date and improves on the material efficiencies in the flux carrier by reducing its size. The amount of steel required to produce the modules is reduced by up to 50% whilst still containing the mass of magnets. The arrangement is superior

to previous designs since, depending on coil sizes and arrangement will allow for more modules to be placed within the same volume. The spacers that have been inserted into the design to separate the magnets reduce the effect of magnetic short circuit for on-design circumstances increasing the modules generating potential and energy density. As a result a machine composed of such modules should also have an increased energy density.

7.1.4 Overall Conclusions

Overall, the implementation of these design concepts should make construction and deployment of large magnetic generators cheaper and easier, with the provision to use a greater range of materials and reducing the reliance on very high accuracy machining/production when creating the machines components. Operation and maintenance costs should be reduced through the use of modular construction increasing reliability, profitability and overall commercial viability. The application of 2-stage & MMA concepts, although originally conceived in conjunction with hydrostatic bearings, is not limited to them. Any kind of bearing can be used in these concepts.

All modules designs will suffer to a degree from high levels of particulates it is therefore important to use appropriate materials for construction and prepare for as many possibilities as possible. However special attentions must be paid to the fluid supply systems for hydrostatic bearings and the sealing of mechanical bearings to prevent the inclusion of too much particulate matter. The additional areas of research, such as the jet and recirculation bearings present intriguing possibilities for these particular problems and may help greatly with the particulate problem

but further research needs to be done.

Although the need for renewable energy is well understood what is less well understood is the timescale for investments. Beginning largescale investment sooner rather than later will ensure that the expense is well spread whilst giving time for the technologies to improve. In essence although waiting would produce a more efficient generator, making a less efficient generator today is likely to be of greater benefit. To this end the drive to create inexpensive and economically viable generator technologies should be very strong in order to encourage early deployment. Investing early on in the development timetable would also help to drive further developments and accelerate the creation of new technologies. Modular generation systems would allow for generators to be created faster at a lower cost and be upgraded with new modules as the power technologies improved.

7.2 Future Work

Potentially, this work could provide a well needed boost to the development of linear generators for use in wave energy and other applications, as such there are many avenues of research that could be followed to extend this work;

1. Research should be conducted to determine the optimum air-gap for magnets with a view to bearing losses.
2. Construction and testing of certain module designs should be conducted to evaluate the 2-Stage and MMA designs effectiveness. Ideally the modules would be tested with differing air-gaps and flow-rates (in the case of hydrostatics).

Chapter 7: Conclusions

3. Testing of the lateral magnet arrangement with regard to comparison with other module designs should be undertaken. Determining whether the design of flux carrier and translator indeed allows for the same performance from a smaller module.
4. Work needs to be done to validate or invalidate the control mechanisms used in the design. Simulations need to be performed to ensure that modules are ejected at the appropriate times and that the system behaves as expected.
5. The power output from the modules needs to be mapped to determine what additional power electronics is required to convert the waveform and supply/absorb whatever reactive power is necessary.
6. Further research into the best topologies and structures should also be pursued to maximise the potential of the modular designs.
7. Further study should be devoted to the jet bearings and their possible hybridisation with hydrostatic bearings.
8. Since the type of bearing is not restricted in this work, further research can be conducted on generators operating in media other than water. Also the affects of water on mechanical bearings needs to be addressed to ensure that in circumstances where mechanical bearings are in use they operate effectively. This should also give a pro's and con's list for each type of mechanical bearing when submerged.
9. Research into coatings for machine components and alternative methods of protection should also be conducted. Tough coatings should also be researched to help maintain components against damage from particulates.

Appendices

Appendix A - Derivations

A.1 Pressure Distribution

This is for the pressure distribution across an annulus of radius r and a thickness dr . Height/clearance is assumed to be constant.

$$dp = \frac{1}{r} dr$$

$$p = \ln r + C$$

In order to calculate the pressure at any radius, the following is necessary. It should be noted that all pressures are relative.

$$\begin{aligned} \frac{p - p_o}{p_i - p_o} &= \frac{\ln r - \ln r_o}{\ln r_i - \ln r_o} \\ &= \frac{\ln \frac{r}{r_o}}{\ln \frac{r_i}{r_o}} \end{aligned}$$

$$p_o = 0$$

$$p = p_i \frac{\ln \frac{r}{r_o}}{\ln \frac{r_i}{r_o}} \tag{A.1}$$

This gives pressure as a function of radius with respect to the inner and outer radius

A.2 Generalised Reynolds Equation

$$\begin{aligned} \frac{\partial}{\partial x} \left(\frac{\rho h^3}{12\eta} \frac{\partial p}{\partial x} \right) + \frac{\partial}{\partial y} \left(\frac{\rho h^3}{12\eta} \frac{\partial p}{\partial y} \right) &= \frac{\partial}{\partial x} \left[\frac{\rho h (u_a + u_b)}{2} \right] + \frac{\partial}{\partial y} \left[\frac{\rho h (v_a + v_b)}{2} \right] \\ &+ \rho \left[(w_a - w_b) - u_a \frac{\partial h}{\partial x} - v_a \frac{\partial h}{\partial y} \right] + h \frac{\partial \rho}{\partial t} \end{aligned} \quad (\text{A.2})$$

Since u_a and u_b represent the speed of the flow at two points. By ignoring the no-slip condition and assuming that there is not relative movements in the plates the fluid flow velocity can be considered to be the average of u_a and u_b , therefore;

$$u = \frac{u_a + u_b}{2} \quad \therefore \quad \frac{\partial}{\partial x} \left[\frac{\rho h (u_a + u_b)}{2} \right] \Rightarrow u \frac{\partial(\rho h)}{\partial x}$$

Flow in the y-direction is assumed to be negligible therefore;

$$v_a = v_b = 0 \quad \therefore \quad \frac{\partial}{\partial y} \left[\frac{\rho h (v_a + v_b)}{2} \right] \Rightarrow 0$$

h is assumed to be constant and w_a & w_b represent movements in the z-direction but in static environments h is constant, therefore;

$$\left. \begin{aligned} \frac{\partial h}{\partial x} = \frac{\partial h}{\partial y} = 0 \\ w_a = w_b = 0 \end{aligned} \right\} \quad \therefore \quad \rho \left[(w_a - w_b) - u_a \frac{\partial h}{\partial x} - v_a \frac{\partial h}{\partial y} \right] \Rightarrow 0$$

The fluid is incompressible therefore;

$$\frac{\partial \rho}{\partial t} = 0 \quad \therefore \quad h \frac{\partial \rho}{\partial t} \Rightarrow 0$$

and since ρ is constant it can be cancelled through for the whole equation. Therefore;

$$\frac{\partial}{\partial x} \left(\frac{h^3}{12\eta} \frac{\partial p}{\partial x} \right) + \frac{\partial}{\partial y} \left(\frac{h^3}{12\eta} \frac{\partial p}{\partial y} \right) = u \frac{\partial h}{\partial x}$$

If $x = r$ and $p = p_i$ then;

$$\frac{\partial}{\partial r} \left(\frac{h^3}{12\eta} \frac{\partial p_i}{\partial r} \right) + \frac{\partial}{\partial y} \left(\frac{h^3}{12\eta} \frac{\partial p_i}{\partial y} \right) = u \frac{\partial h}{\partial r}$$

$$\frac{\partial}{\partial r} \left(h^3 \frac{\partial p_i}{\partial r} \right) + \frac{\partial}{\partial y} \left(h^3 \frac{\partial p_i}{\partial y} \right) = 12\eta u \frac{\partial h}{\partial r}$$

A.3 Hydrostatic Lubrication Equation

Taken from Reynolds equation for hydrostatic lubrication;

$$\frac{\partial}{\partial r} \left(h^3 \frac{\partial p_i}{\partial r} \right) + \frac{\partial}{\partial y} \left(h^3 \frac{\partial p_i}{\partial y} \right) = 12\eta u \frac{\partial h}{\partial r}$$

Assuming there is no variation in the y-direction;

$$\frac{\partial p_i}{\partial y} = 0 \quad \therefore \quad \frac{\partial}{\partial r} \left(h^3 \frac{\partial p_i}{\partial r} \right) = 12\eta u \frac{\partial h}{\partial r}$$

$$h^3 \frac{\partial p_i}{\partial r} = 12\eta u h \tag{A.3}$$

Velocity, u , must be related to volumetric flowrate;

$$Q = 2\pi rhu$$

$$u = \frac{Q}{2\pi rh} \quad (\text{A.4})$$

Substituting A.4 into A.3;

$$h^3 \frac{\partial p_i}{\partial r} = 12\eta \frac{Q}{2\pi rh} h$$

$$\frac{\partial p_i}{\partial r} = \frac{6\eta Q}{\pi r h^3}$$

$$dp_i = \frac{6\eta Q}{\pi r h^3} dr$$

Integrating across the land area yields expression for p_i related to input values.

$$p_i = \frac{6\eta Q}{\pi h^3} \int_{r_i}^{r_o} \frac{1}{r} dr$$

$$p_i = \frac{6\eta Q}{\pi h^3} [\ln r]_{r_i}^{r_o}$$

$$p_i = \frac{6\eta Q}{\pi h^3} \ln \frac{r_o}{r_i}$$

A.4 Polar Hydrostatic Derivation

$$\frac{\partial}{\partial r} \left(\frac{\rho r h^3}{12\eta} \frac{\partial p}{\partial r} \right) + \frac{1}{r} \frac{\partial}{\partial \theta} \left(\frac{\rho h^3}{12\eta} \frac{\partial p}{\partial \theta} \right) = \frac{1}{2} U \frac{\partial(\rho h)}{\partial \theta} - r \rho V_s \quad (\text{A.5})$$

If h and ρ are constant then;

$$\frac{1}{2}U \frac{\partial(\rho h)}{\partial \theta} - r\rho V_s = 0$$

since V_s is the velocity in the h direction.

If it is assumed that the bearing surface is uniform and therefore the same flow occurs at all angles all variation with respect to angle is eliminated, therefore;

$$\frac{\partial p}{\partial \theta} = 0$$

Therefore;

$$\frac{\partial}{\partial r} \left(\frac{\rho r h^3}{12\eta} \frac{\partial p}{\partial r} \right) = 0$$

Divide through by ρ

$$\frac{\partial}{\partial r} \left(\frac{r h^3}{12\eta} \frac{\partial p}{\partial r} \right) = 0$$

From dimensional analysis;

$$\frac{r h^3}{12\eta} \frac{\partial p}{\partial r} = \mathbf{L}^3 \mathbf{T}^{-1} = Q \quad \therefore \quad \frac{r h^3}{12\eta} \frac{\partial p}{\partial r} = f_{rc} Q$$

f_{rc} in this case is $\frac{1}{2\pi}$.

$$\frac{r h^3}{12\eta} \frac{\partial p}{\partial r} = \frac{1}{2\pi} Q$$

$$\partial p = \frac{12\eta Q}{2\pi h^3} \frac{1}{r} \partial r$$

$$p = \frac{6\eta Q}{\pi h^3} \int_{r_i}^{r_o} \frac{1}{r} dr$$

$$p = \frac{6\eta Q}{\pi h^3} \ln \frac{r_o}{r_i}$$

A.5 Effective Area

Effective area is obtained by integrating the pressure function with the derivative area to give the total force;

$$\begin{aligned}
F_{land} &= 2\pi \int_{r_i}^{r_o} pr dr \\
&= \frac{2\pi p_i}{\ln \frac{r_o}{r_i}} \int_{r_i}^{r_o} r \ln \frac{r}{r_o} dr \\
&= \frac{2\pi p_i}{\ln \frac{r_o}{r_i}} \int_{r_i}^{r_o} r \ln r - r \ln r_o dr \\
&= \frac{2\pi p_i}{\ln \frac{r_o}{r_i}} \left\{ \left[\frac{r_o^2}{2} \ln r_o - \frac{r_i^2}{2} \ln r_i - \frac{r_o^2 - r_i^2}{4} \right] - \left[\frac{r_o^2}{2} \ln r_o - \frac{r_i^2}{2} \ln r_o \right] \right\} \\
&= \frac{2\pi p_i}{\ln \frac{r_o}{r_i}} \left\{ \frac{r_i^2}{2} (\ln r_o - \ln r_i) - \frac{r_o^2 - r_i^2}{4} \right\} \\
&= 2\pi p_i \left\{ \frac{r_o^2 - r_i^2}{4 \ln \frac{r_o}{r_i}} - \frac{r_i^2}{2} \right\} \\
F_{land} &= p_i \left\{ \frac{\pi (r_o^2 - r_i^2)}{2 \ln \frac{r_o}{r_i}} - \pi r_i^2 \right\} \tag{A.6}
\end{aligned}$$

This is then equated to the product of the input pressure, p_i , and the effective area;

$$F_{Land} = p_i A_{Land}$$

$$\therefore A_{Land} = \frac{\pi (r_o^2 - r_i^2)}{2 \ln \frac{r_o}{r_i}} - \pi r_i^2 \quad (\text{A.7})$$

To be the effective area the area of the recess must also be added;

$$\begin{aligned} A_{Recess} &= \pi r_i^2 \\ A_e &= A_{Land} + A_{Recess} \\ A_e &= \frac{\pi (r_o^2 - r_i^2)}{2 \ln \frac{r_o}{r_i}} \end{aligned} \quad (\text{A.8})$$

A.6 Dynamic Hydrostatic Force

A.6.1 Pressure

Again, taken from Reynolds equation;

$$\frac{\partial}{\partial r} \left(\frac{\partial p}{\partial r} h^3 \right) = 12\eta u \frac{dh}{dr} \quad (\text{A.9})$$

Substituting u from Q but in this instance replacing Q with the flow caused by the movement of the two surfaces relative to one another.

$$\begin{aligned} u &= \frac{Q}{2\pi r h} \\ u &= \frac{\pi r^2 \frac{dh}{dt}}{2\pi r h} \\ u &= \frac{r}{2h} \frac{dh}{dt} \end{aligned} \quad (\text{A.10})$$

Substituting A.10 into A.9;

$$\begin{aligned}\frac{\partial}{\partial r} \left(\frac{\partial p}{\partial r} h^3 \right) &= 12\eta \frac{r}{2h} \frac{dh}{dt} \frac{dh}{dr} \\ \frac{dp}{dr} h^3 &= 6\eta r \frac{dh}{dt} \\ dp &= \frac{6\eta r}{h^3} \frac{dh}{dt} dr\end{aligned}\tag{A.11}$$

Integrating from 0 to r gives the rpressure caused by the motion at any given radius.

$$\begin{aligned}p &= \int_0^r \frac{6\eta r}{h^3} \frac{dh}{dt} dr \\ p &= \frac{3\eta r^2}{h^3} \frac{dh}{dt}\end{aligned}\tag{A.12}$$

A.6.2 Force

Force is simply the above multiplied by the derivative area and integrated across the land and recess.

$$\begin{aligned}
F &= \int_A p \, dA \\
F &= 2\pi \int_0^{r_o} p(r)r \, dr \\
F &= 2\pi \int_0^{r_o} \frac{3\eta r^2}{h^3} \frac{dh}{dt} r \, dr \\
F &= \frac{6\pi\eta}{h^3} \frac{dh}{dt} \int_0^{r_o} r^3 \, dr \\
F &= \frac{3\pi\eta}{2h^3} r_o^4 \frac{dh}{dt}
\end{aligned} \tag{A.13}$$

A.7 Air-gap Flux Relationship

Working from a standard arrangement of opposing magnets such as the one in Figure 2.5 the following equation for the static arrange is derived.

$$2B_{rem} \frac{l_{magnet}}{\mu_0} = \frac{2\varphi}{\mu_0 A} [l_{magnet} + l_{air-gap}]$$

From 2.4

$$\varphi_{rem} = B_{rem} A$$

By substituting for B_{rem}

$$\begin{aligned}
\frac{2\varphi_{rem}}{\mu_0 A} l_{magnet} &= \frac{2\varphi}{\mu_0 A} [l_{magnet} + l_{air-gap}] \\
\varphi_{rem} l_{magnet} &= \varphi [l_{magnet} + l_{air-gap}] \\
\varphi_{rem} &= \varphi \left[\frac{l_{magnet} + l_{air-gap}}{l_{magnet}} \right]
\end{aligned} \tag{A.14}$$

This yields a coefficient for the ratio between the remnant flux and the circuit flux.

A.8 Maximum Usable Air-Gap Relationship

By replacing the flux value, φ , with a target flux, φ_{target} , the following can be derived;

$$\begin{aligned}
\frac{\varphi_{rem}}{\varphi_{target}} &= 1 + \frac{l_{max-air-gap}}{l_{magnet}} \\
1 + \frac{\varphi_{rem} - \varphi_{target}}{\varphi_{target}} &= 1 + \frac{l_{max-air-gap}}{l_{magnet}} \\
\frac{\varphi_{rem} - \varphi_{target}}{\varphi_{target}} &= \frac{l_{max-air-gap}}{l_{magnet}} \\
\frac{\varphi_{rem} - \varphi_{target}}{\varphi_{target}} &= \frac{B_{rem} - B_{target}}{B_{target}} \\
\therefore \frac{B_{rem} - B_{target}}{B_{target}} &= \frac{l_{max-air-gap}}{l_{magnet}} \\
\frac{B_{rem} - B_{target}}{B_{target}} l_{magnet} &= l_{max-air-gap}
\end{aligned} \tag{A.15}$$

Appendix B - Design Gallery

The following illustrates the numerous devices explored during the research and a few additional notes about each one.

2-Stage Generator

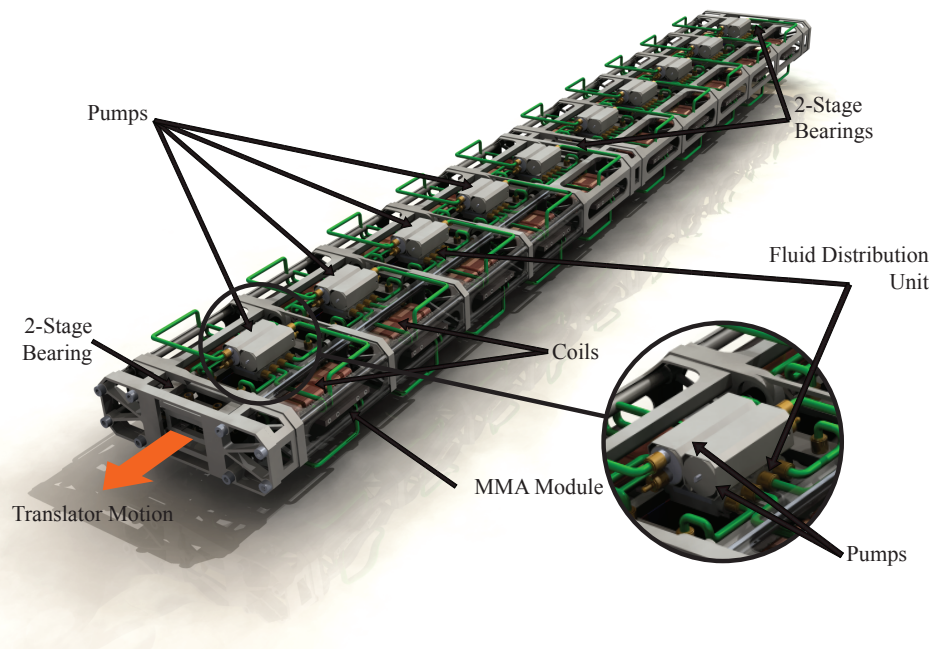


Figure B.1: Complete Concept 2-Stage Generator

The first complete concept generator, the 2-stage system shown had each generator

stage mounted on a single set of hydrostatic bearings mounted on rubber dampers. The pumps were mounted locally and fed each generator stage individually.

Combined 2-Stage & MMA Generator

The most complete version of the MMA module contained numerous additional components that hadnt been included with all the previous designs simply to illustrate what a complete module would need to include.

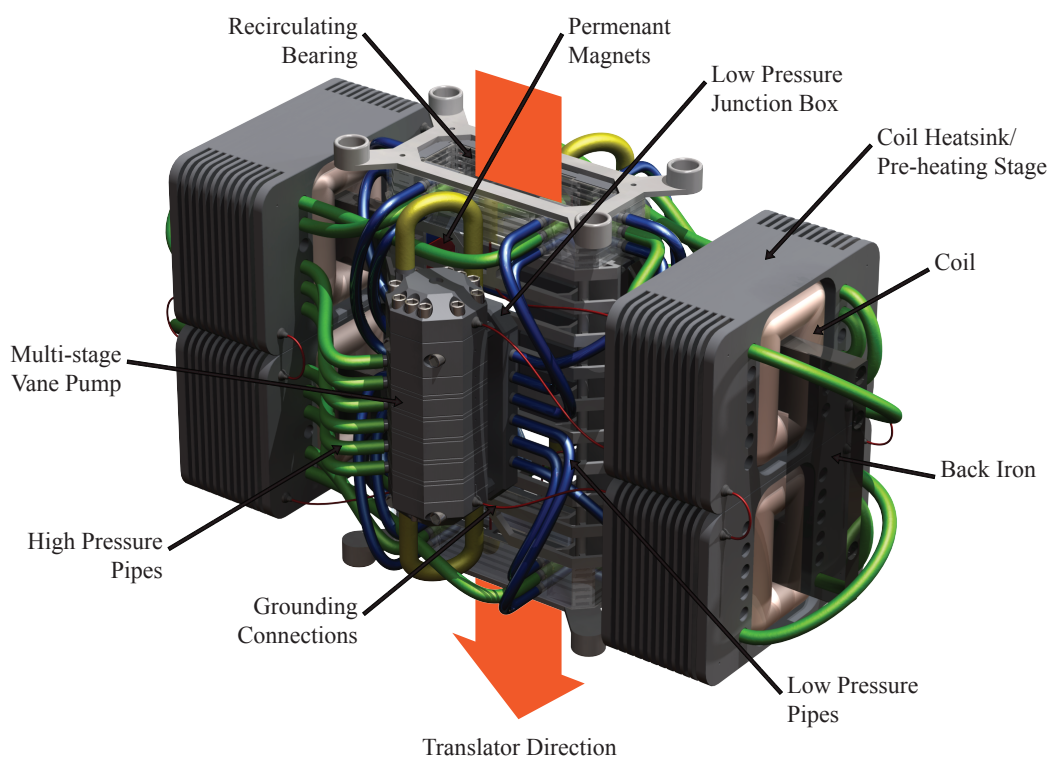


Figure B.2: Complete Concept MMA Module

These included integrated preheating for the lubricant via heatsinks for the coils, the structure of the pumps and motors the electrical connects required to avoid galvanic corrosion and the support structures. It also illustrated the variety of materials that might be used depending on the relative loading of the various

parts.

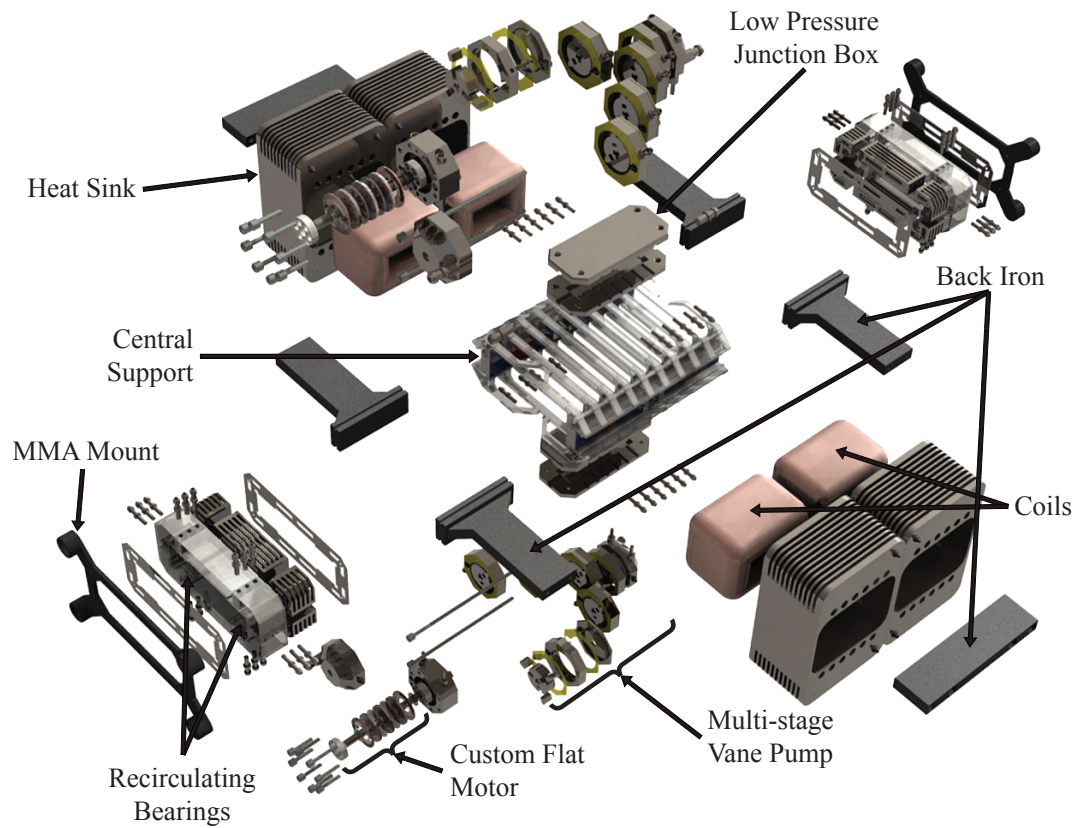


Figure B.3: Exploded View of Concept MMA Module

The exploded view included here shows all the components required for a working MMA generator module except the piping since it was intended to be flexible hosing.

Combined FR 2-Stage & FR MMA Generators

This FR-MMA modules was designed to open when held at specific clamping points allowing it to be separated from the translator/superstructure with ease. Sets of sliding components and levers cause the module to expand whilst held and to close around the translator when release after which it uses hydrostatic bearings to maintain its relative position.

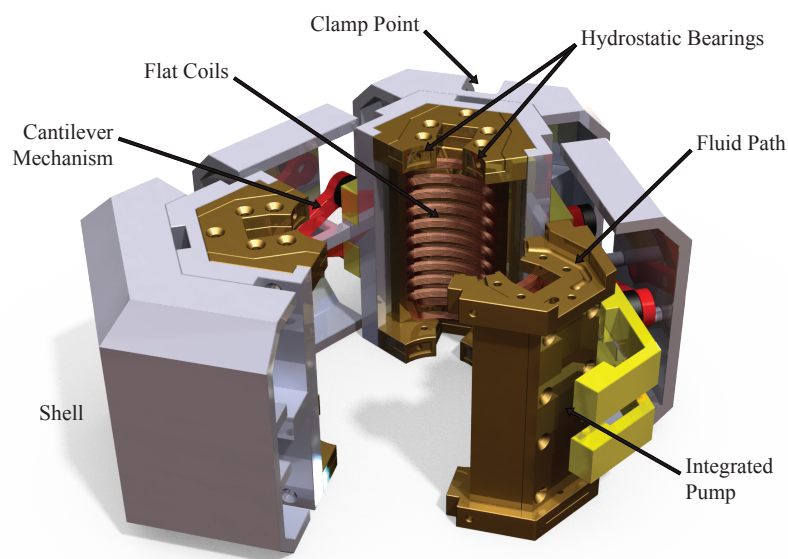


Figure B.4: 3-Section FR-MMA Module in a Partially Expanded State

The arrangement of coils used for this design is one of the more unusual ones mentioned previously however it requires more copper than many of the others without increasing the output, this coupled with a complexity of construction and field interaction problems caused this approach to be abandoned.

Combined SFR 2-Stage & SFR MMA Generators

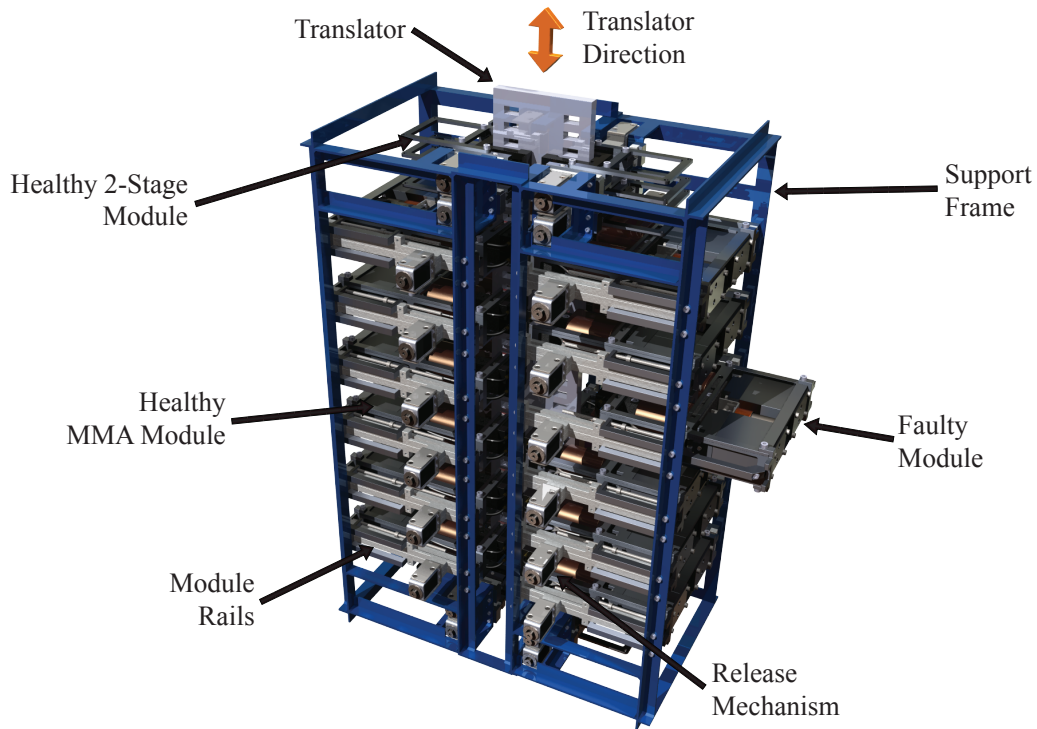


Figure B.5: SFR-MMA Tower with Faulty Module Ejected

The SFR-MMA concept designs were the first designs complete with support frames, module guides and eject mechanisms. The support frame is intended to hold the module guides and support the majority of the load from the translator. Since the module control algorithms were intended to have the capacity to eject damaged or malfunctioning modules it was necessary to have some form of eject mechanism which could be controlled electronically.

As modules are inserted they compress a spring within the mechanism which leaves them primed for ejection. High force solenoids were chosen to overcome the friction

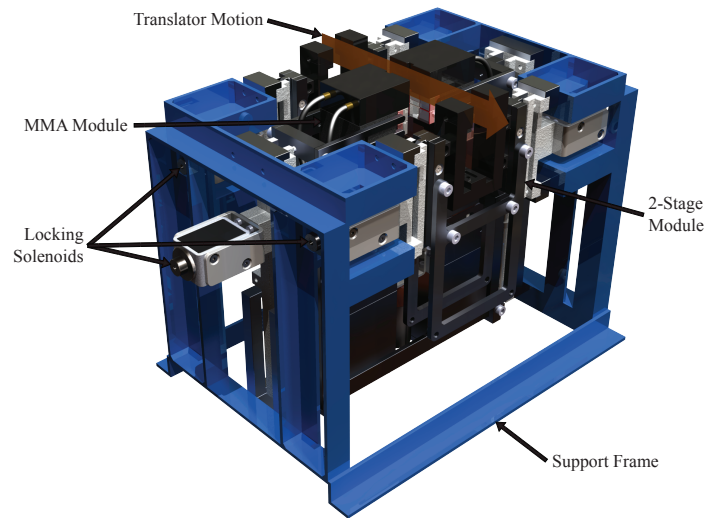


Figure B.6: Concept SFR-MMA & SFR-2Stage Arrangement

caused by the latch and potential build-ups that might clog the mechanisms.

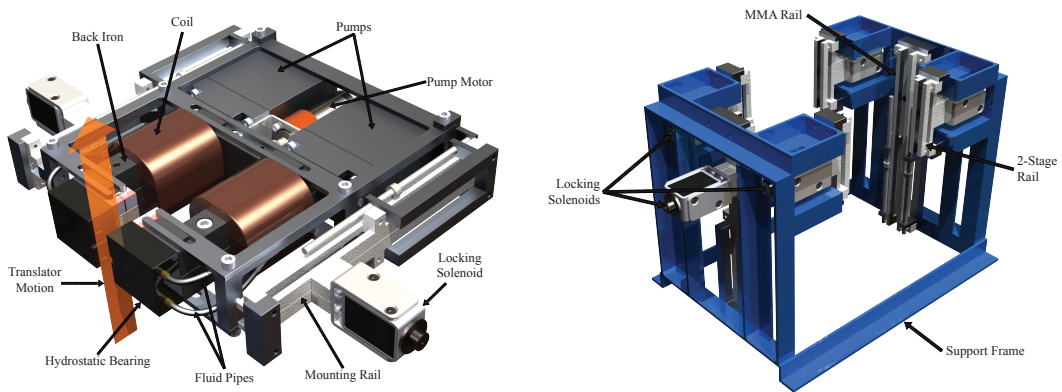


Figure B.7: SFR-MMA Module & Concept Empty Mounting

Each module can therefore be easily inserted into the parent generator without having to worry about alignment. Detecting failed modules during maintenance is also easy since all failed modules should have been ejected from the machine and therefore would be sitting clear of the operational ones.

The modules are design to fit within guide rail slots within the support structure. The notches present in the module rails fits with the latch in the guild rail allowing modules to be replaced manually.

Necessary connections between the superstructure and the modules would be made through contacts in or alongside the slots. These contacts would run at low voltages to prevent major short circuiting through the sea water.

Lateral MMA Generator

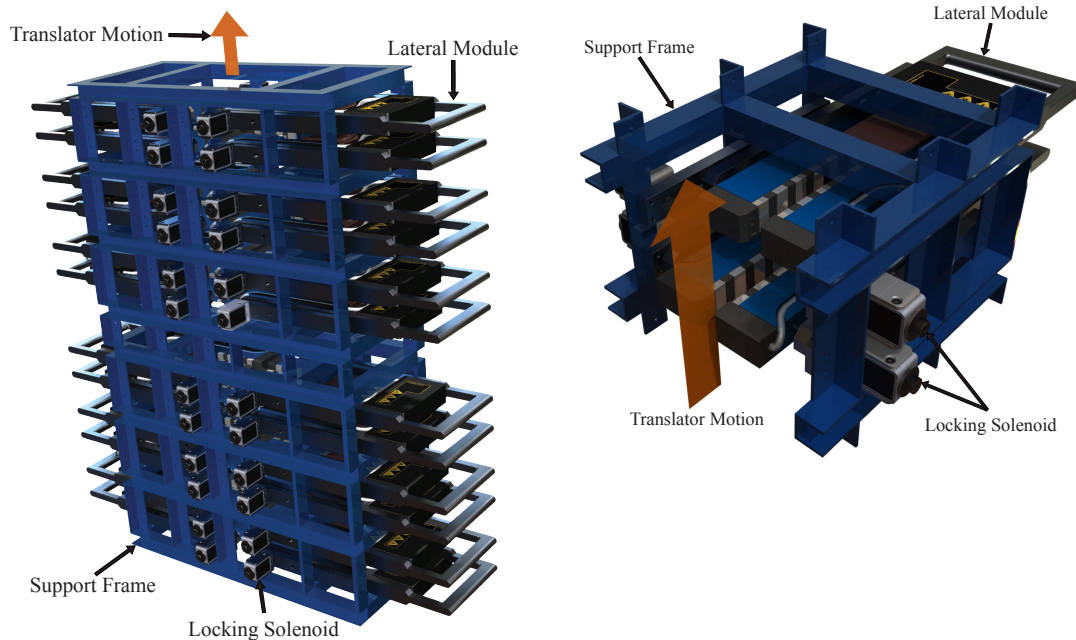


Figure B.8: Lateral Module Superstructure & Shown in Cut-away

The lateral SFR-MMA generator inherits a number of traits from its ancestors however is much more compact for its generating capacity. The limiting factor for deployment of this type of module is the cross sectional area of copper required in the coils to give sufficient power output. However, the key benefit of the lateral design is the capacity for the module to contain greater numbers of magnets

compared to the previous SFR-MMA designs.

As before the failure response mechanisms are the same, ejecting faulty modules so that the generator can continue to operate. Since these modules would be thinner, depending on amounts of copper required, the overall form factor of the generator is potentially decreased and maintenance options are improved thanks to the reduction in weight of the modules.

Proof of Concept Generator

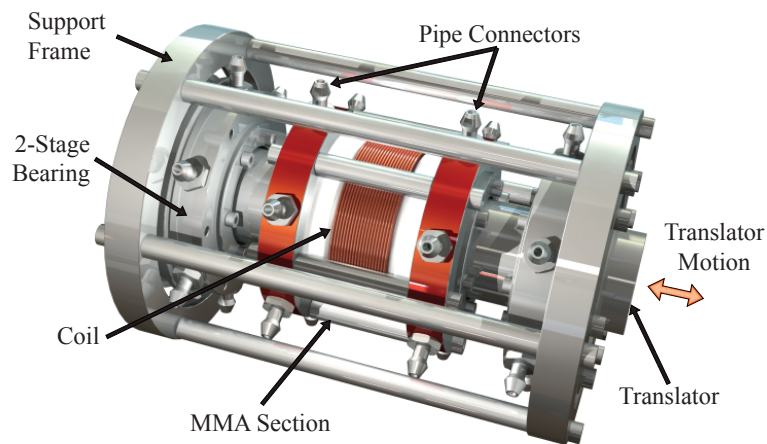


Figure B.9: Final Design for Proof of Concept Generator

This was a concept generator intended to demonstrate various elements of the designs to date. Unlike most of the other designs it was intended to use a tubular, air-cored design rather than variable reluctance. However this would have provided an adequate demonstration of all the theory used at that stage of development.

Alternative Design: Linear-Rotary Generator

Early in the research I explored the possibility of driving a rotary mechanism with a translating screw. This used the theory of a variable reluctance generator

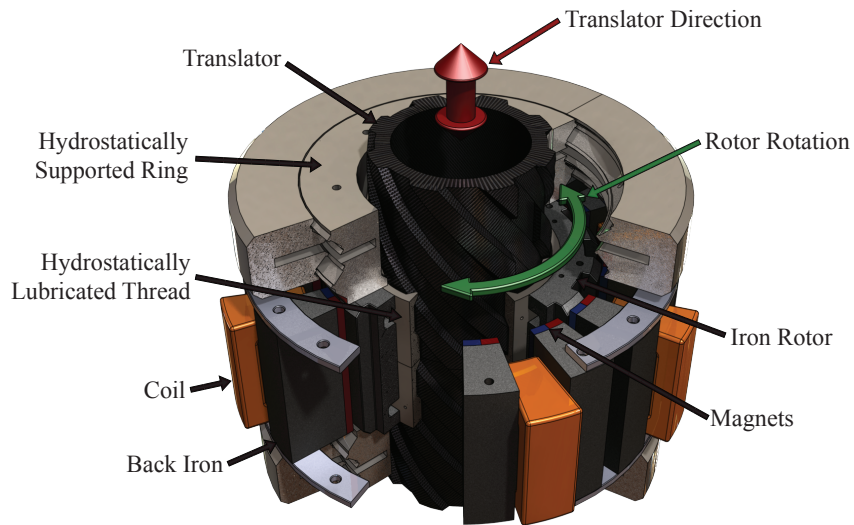


Figure B.10: Linear-Rotary Generator with Sections

adapted to work with a hydrostatically supported rotating core. The intention was to pump fluid into the rotary bearings which would then also feed into the screw bearings, therefore requiring only 1 inlet and pump to support the whole mechanism, however it would require high pressures and throughput.

Appendix C - Laser Position Sensor

The laser position sensor was an attempt to make an inexpensive device capable of tracking sub-millimetre variations in the position of parts within a generator during operation without directly interfering with its operation. The intent was to use it to monitor parts supported by hydrostatic bearings in real-time when the variation in position was likely to be very small. Although its design and testing were successful it was never applied in practice.

Concept

In order to monitor small changes in the position of parts within the hydrostatic support structure it is necessary to have a sensor system that is capable of measure sub-millimetre changes. Existing methods/sensors are either expensive or suffer from repeatability issues. The laser sensor potentially provides a more reliable method of recording surface displacements.

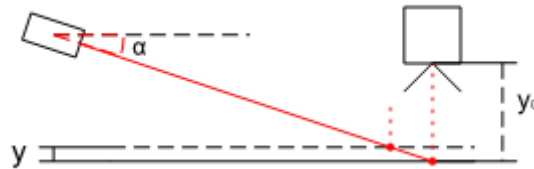


Figure C.11: Schematic Device Arrangement

$$y = x \tan(\alpha) \Rightarrow y \approx x\alpha \because \alpha \rightarrow 0$$

$$\Delta y \approx \alpha \Delta x \tag{C.16}$$

Since the path of a laser, for all intents and purposes, is always a straight line and

does not apply any force or have any moving parts, this device should be limited only by the technology used to register the position of the beam. Since there are no moving parts there will be no inaccuracies caused by slip-stick characteristics of the measuring device. Also there is scope for continuous measurement leading to potential for easy measurement of motions in real time, within the capture rate of the camera used.

Theory

The Laser

The position of the laser dot is easily predictable using the standard formula for a line. As described in the following equations, the resolution improves the smaller the angle becomes.

$$\Delta x = \frac{\Delta y}{\alpha} \therefore \frac{\Delta x}{\Delta y} = \frac{1}{\alpha} \therefore \alpha \rightarrow 0 \Rightarrow \frac{\Delta x}{\Delta y} \rightarrow \infty \quad (\text{C.17})$$

$$x = m_g y + c \Rightarrow m_g = \frac{1}{\alpha} \quad (\text{C.18})$$

If designed correctly changes in vertical displacement (Δy) can be easily derived from the changes in the position of the laser dot, (Δx). However the observed change in position is not the same as the true change because of problems of perspective. As the surface moves towards and away from the camera the observed size of an object varies. A simple approximation for this is as follows;

$$x_s = \frac{fx}{y} \quad y_s = \frac{fz}{y} \tag{C.19}$$

Derived from;

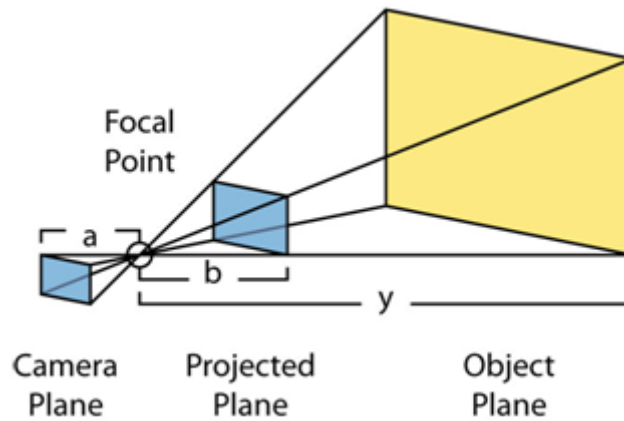


Figure C.12: Perspective Projection

Depending on the application the scale factor f/y used to scale anything intersecting the object plane is either a/y or b/y . However these two are not used concurrently so a and b are replaced by the single value f . Since the camera plane is on the other side of the focal point it could easily be represented on either side with a reversal of signs in both directions.

These equations are used for 3-dimensional projection in computer renderers and computer games. In general the focal point is assumed to be the observers eye and the projected plane is the computer display/TV.

x_s and y_s are screen coordinates derived from the real world coordinates x , y and z . f is a factor that converts the scale of real world coordinates to the scale used on the computer screen or in this case the camera. The value of f is something that for this device at least would need to be found through experimentation.

$$\Delta x_s = \frac{f \Delta x}{\Delta y + y + 0} \quad (\text{C.20})$$

For this purpose the above equation is required. The y_0 value is required in order to set a datum for the camera. Since the real world x is described as $x = m_g y + c$ the Δx can be replaced by $m_g \Delta y$ to give;

$$\Delta x_s = \frac{f m_g \Delta y}{\Delta y + y_0} \Leftrightarrow \Delta y = \frac{\Delta x_s y_0}{f m_g - \Delta x_s} \quad (\text{C.21})$$

a suitable y_0 is chosen, so that $y_0 \gg \Delta y$ then the equation could be simplified to;

$$\Delta x_s = \frac{f m_g \Delta y}{y_0} \Leftrightarrow \Delta y = \frac{\Delta x_s y_0}{f m_g} \quad (\text{C.22})$$

However this does introduce some inaccuracies into the system.

In practice, y_0 would be found experimentally since it would be hard to predict its value. However once the device has been calibrated both y_0 and f are constant.

The Camera

It may seem a simple task to record the location of the bright red dot in an image, however in order to register the position of the laser dot multiple steps are required. These stages will vary depending on the type and capabilities of the camera used in the device.

In the original plan only two steps were required;

1. To screen out all but the brightest pixels in the image since in the majority

of cases these will be the pixels representing the laser dot. In this case the top 25% of pixels are used based on brightness in the Red channel.

2. Determine the centre of the bright section of the image. This is done via interpolation which will be described later.

A later version includes a mechanism for scanning and recording multiple bright areas. This was due to the fact that such a device might be subject to bright surrounding conditions and adequate filtering might not be in place. This method requires an extra step;

1. The first stage is unchanged
2. This stage now scans the image and locations every contiguous bright area within it. The areas are found using a flood routine that expands from the first unrecorded bright pixel until threshold conditions are reached. These areas are stored with an identifying number.
3. For each area the centre is determined via interpolation and stored

Both method recorded and stored the information using a CSV formatted files for later analysis in Microsoft Excel.

The top 25% of pixels are chosen by;

1. Finding the maximum and minimum pixel value in the image.
2. Subtracting the minimum value from all pixel values

3. Multiplying all pixel values by $\frac{255}{max-min}$. This expands the range of the image to the full 0-255 that can be used.
4. A value of 192 is subtracted from all pixel values
5. Any negative values are set to zero
6. Stages 1-3 are repeated to re-expand the range.

This yields the top 25% of pixels from the original image after the first range expansion. These are the values that are then used by the interpolation algorithms.

Interpolation

The interpolation process determines the centre of a bright mass in the image by using a biased summation of vectors.

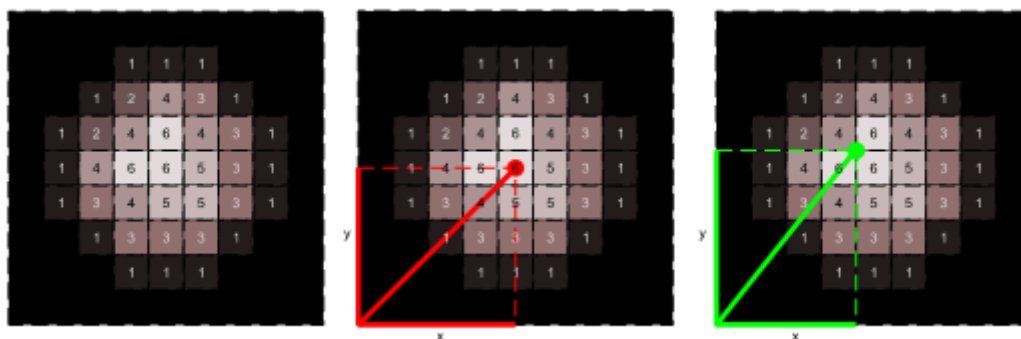


Figure C.13: Interpolation Method

The vector of each pixel, relative to the origin of the image is multiplied by the brightness of the pixel in question.

$$x_w = V_{xy}x \quad y_w = V_{xy}y \quad (\text{C.23})$$

The x_w and y_w are the weighted values. The V_{xy} is a scalar value taken from the pixel brightness. The range of this value is only of interest as far as the greater it is the more accurate the method should be.

$$x_c = \frac{\sum V_{xy}x}{\sum V_{xy}} \quad y_c = \frac{\sum V_{xy}y}{\sum V_{xy}} \quad (\text{C.24})$$

By summing the weighted values and dividing by the sum of the weights the theoretical centre is determined.

Applying this method to the whole image works if there is only a single light source, if this is attempted with an image with multiple bright areas then it will fail unless each of the bright areas is identified and checked separately.

Flood Area Detection

Flood Area Detection works by selecting one pixel and examining the pixels around it. Each pixel is checked to see if it is within certain parameters. If the parameters are met then the algorithm moves to that pixel and continues the expansion.

Single Area Detection

The single area detection algorithm begins by creating a blank buffer with the same dimensions as the image. This buffer is essentially binary and starts off as all zero.

The process of area selection works as follows;

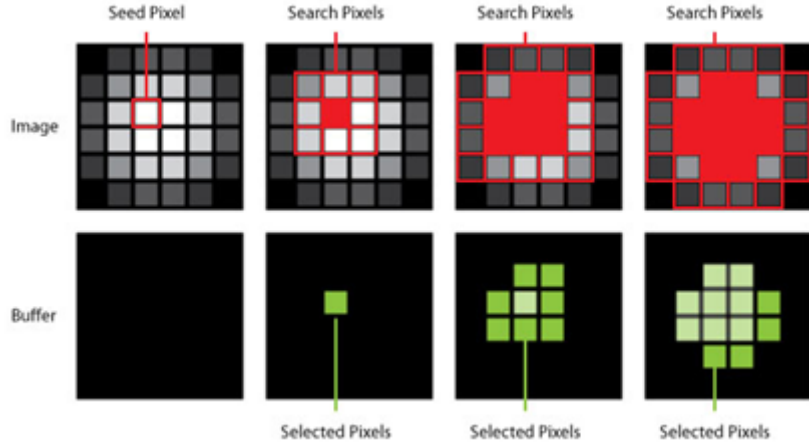


Figure C.14: Flood Selection Method

1. A seed pixel is chosen, normally one of the brightest pixels in the image, value of 255.
2. This pixel is registered by changing the value of the buffer to a 1 for this location.
3. The algorithm then checks the pixels surrounding that location and runs itself on any that are suitable, ie. Meets parameters.
4. Stage 3 repeats until no more suitable pixels are found and then terminates.

The final selection is taken as the non-zero values in the buffer layer. This makes for easy application to the interpolation routine as well;

$$x_w = B_{xy}V_{xy}x \quad y_w = B_{xy}V_{xy}y \quad (\text{C.25})$$

$$x_c = \frac{\sum B_{xy}V_{xy}x}{\sum B_{xy}V_{xy}} \quad y_c = \frac{\sum B_{xy}V_{xy}y}{\sum B_{xy}V_{xy}} \quad (\text{C.26})$$

This will give the centre of the flooded area biased by pixel values. To improve speed the interpolation routine should only be run within the bounds of the selected area, otherwise it would attempt to interpolate the whole image area. Although this would not affect the values produced, it would slow the program down.

The flood algorithm is a recursive algorithm meaning that it calls itself during operation. This makes it very efficient on code however there is a limit to the size of area it can capture thanks to limitations in the number of times it can call itself.

Multiple Area Detection

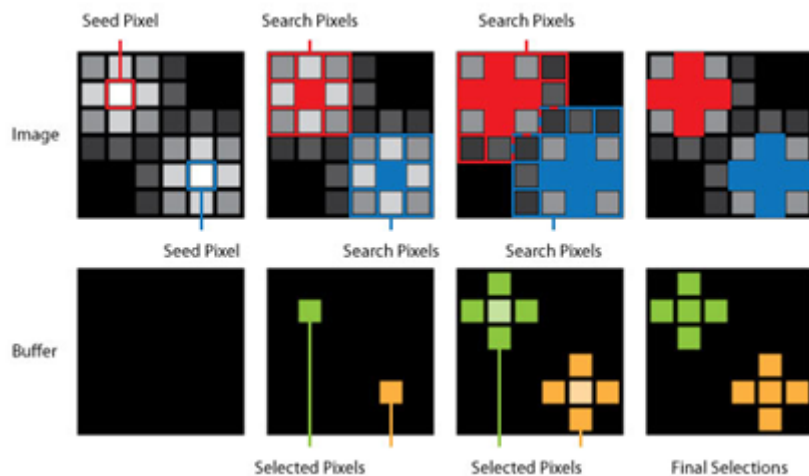


Figure C.15: Multi-Area Flood Selection Method

The multiple area detection uses the same basic routine as the single area, however instead of recording ones and zeros to the buffer, a number related to the order in which they were mapped. Although the above diagram shows the areas being mapped concurrently, they would in fact be mapped sequentially for reliability. Concurrent operation introduces the problems of overlapping areas; by allowing each area detection routine to run its course this is avoided.

The process is now;

1. Find seed pixel
2. Check buffer for zero value, if zero then continue, if not go back to 1
3. Perform area detection algorithm using seed pixel entering sweep number into buffer
4. Repeat until no new seed pixels are found

Once areas have been defined they are selected individually and the location of the centre of each area is determined and exported. Since the buffer values are no longer binary the method reverts to the original formulae with a Boolean condition applied. The Boolean condition checks if the values from the buffer match the selected value.

Additionally each position is tracked so that if an area disappears or becomes untrackable the area numbers are maintained. For example, if 2 areas exist initially and the first area becomes unusable for some reason, then the remaining area is still tracked as number 2.

This is done by maintaining the previous location of each centre from one frame to the next and checking against it on each update. When an area is found its centre is compared to all previous centres and it is given the number of the previous centre it was closest to. As can be seen in Figure C.16, this isnt always enough to ensure success.

The coloured circles represent the distance to the nearest previous point. The blue circle indicates that the previous red point is closer than the previous blue and as

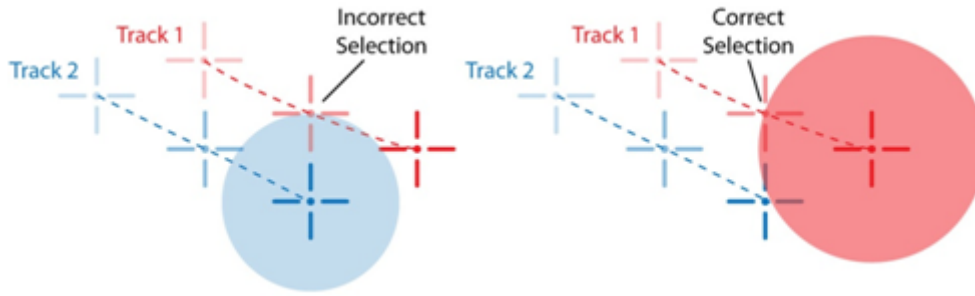


Figure C.16: Range Point Discrimination

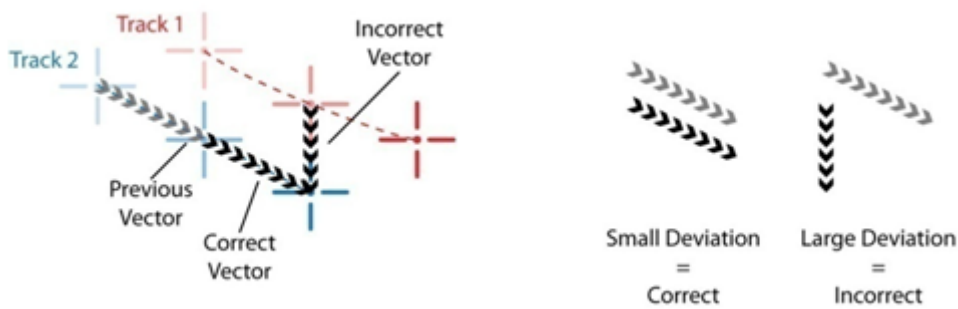


Figure C.17: Motion Vector Point Discrimination

such, based purely on distance, the wrong point would be chosen to continue the blue path. The red circle however shows that the reds closest previous point is the previous red point so both paths could potentially claim that point based on distance.

To solve this, the vector for each position change is stored as well. By comparing the new vector to the previous one it is possible to determine if the closest point is the one that lies on the path. A simplified version is shown in Figure C.17;

If the vectors are plotted between the 2 closest points in the blue path and the previous vector it becomes readily apparent that the red point cannot be part of the blue path. Therefore the next closest is checked instead to see if it is a closer match.

$$D = \left| \overline{V_{old}} - \overline{V_{new}} \right| \quad (\text{C.27})$$

By finding the closest point with the smallest value of D the method should reliably pick the correct points.

This provides a check against 2 points being mixed up when moving past one another, since it is assumed that the velocity change will be smaller than the displacement change.

$$\left| \frac{d^2s}{dt^2} \right| < \left| \frac{ds}{dt} \right| \quad (\text{C.28})$$

Therefore even if the two points could be mixed up based on their position relative to previous positions, the velocity vectors would not match and would tell them apart.

As a result of these two methods, area numbers are maintained unless they coalesce or split. At present if two areas coalesce then they are reduced to a single area number and the second track will be lost. It does form the basis for a future system which is capable of overcoming temporary coalescence.

This makes analysis easier since an individual trace is maintained for each area irrespective of the order in which they are discovered in the sweep.

Hardware

The prototype uses a <1mW, 670nm laser to project a dot towards a flat surface. A webcam, in this case a basic Logitech model, is mounted such that the CCD/FPA

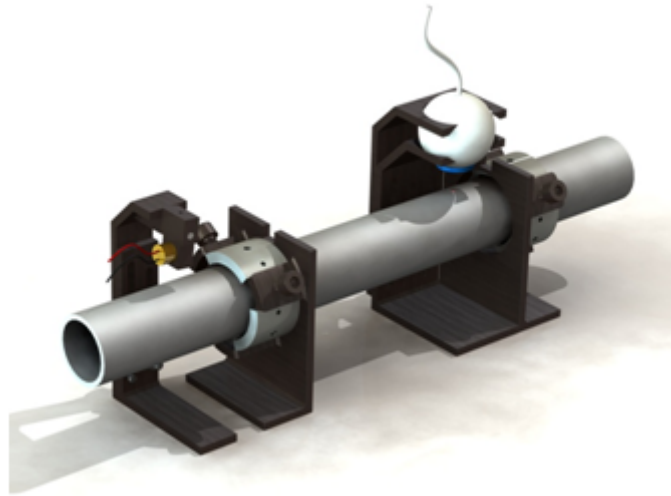


Figure C.18: Original Concept Design of Device

of the webcam is parallel to the surface being tracked. The laser is mounted at a fixed angle relative to the surface (α) and the camera is mounted at a distance y_0 . Note that y_0 is a parameter distance and may not match the physical distance, it is defined as the theoretical separation of the focal plane and the surface at datum.

Practical Tests

Programming Test

The programming tests probably occupied the majority of the testing time to date. In the first instance this was due to the software picking up the first available light source rather than the light source most likely to be the laser. This is a failing in the webcam and drivers used. A lack of manual controls for the gain and exposure meant that light reflected from surrounding sources was bleaching the camera and causing the original software to misinterpret the image. Also the external light

sources were often causing bright areas large enough to exceed the memory limits of the programs flood routine.

As both a solution to the original problems and for future applications, the multi-area algorithm was created. By tracking the centres of multiple areas at the same time it overcame the problems of external light sources and allowed for the near continuous tracking of the laser dot. Unfortunately if the object being observed does not have smooth edges, the scattered laser light can confuse the software and cause the formation of additional bright patches in the image.

Calibration Test

For the first practical tests of this device a stepped bar was used. This bar had 0.05” steps cut into it using a milling machine. This provided an easily repeatable experiment and a very simple and quite accurate set of measurements against which to calibrate.

After the computer had recorded the position data of the laser, it was taken into Microsoft Excel where it was processed and compared to the data from the theoretical model. The results are shown in Figure C.19;

The experimental data and the model data are plotted against one another for the given vertical displacement. The linear trend-line fits to the data with an R^2 value of 0.997 indicating that the model is very close to the experimental data. This shows that the model is a good first approximation.

There is however the issue of the deviation of the blue line from the black. Although the fit is statistically very good, the deviation does not look like it should be the

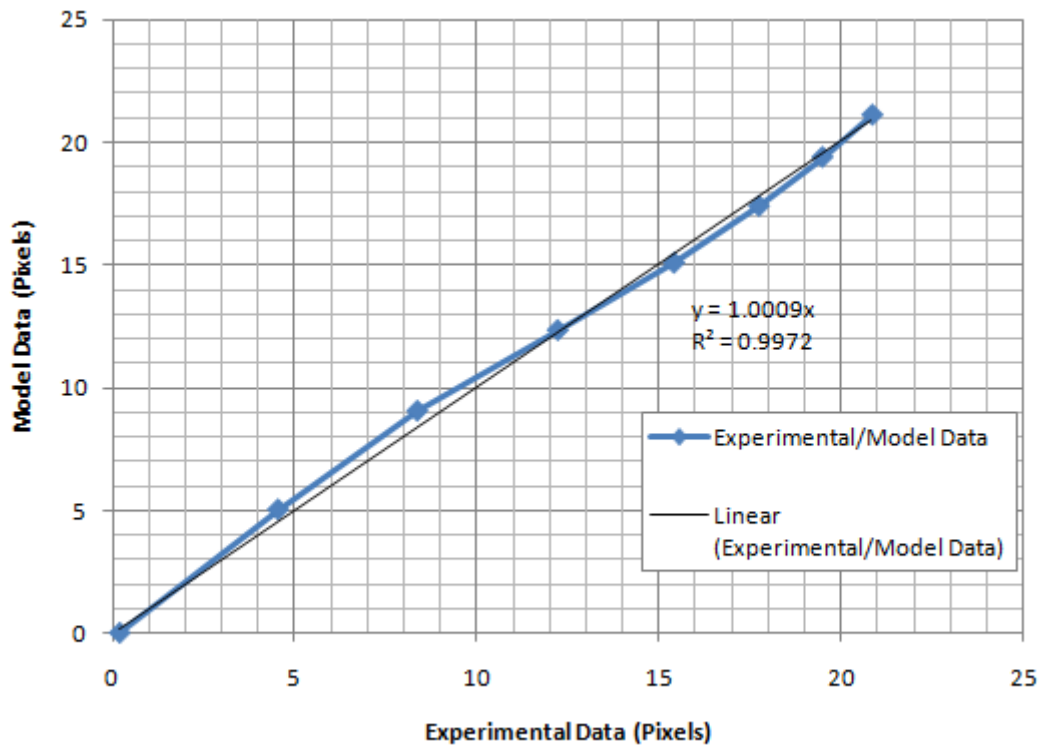


Figure C.19: Comparison of Experimental & Practical Data

result of random errors. In all likelihood the deviation from the model is due to an earlier assumption to do with the 3D projection equations. This is that the lens does not distort the image before it reaches the CCD/FPA of the camera. Since this variation is visible as the values move away from the datum and appears roughly sinusoidal in nature it is logical to assume that it is due to the curvature of the lens in the camera. The webcam in question uses a fairly simple/cheap lenses and it is likely that distortion is not a concern for its given task.

Conclusions

Although not viable as a commercial product in its current form this device was cheap and easy to construct. The software presented some challenges and there is still considerable room for improvement it is behaviour however it has proven that this type of device is technically viable if used correctly. With enough test data it should be possible to accurately predict the distortion caused by the lense of a given camera or it may prove feasible to replace the camera with a CCD/FPA and lense with known characteristics. Even with the distortion the accuracy of the readings is well into the sub-millimetre range and therefore potentially extremely useful.

The addition of filters to account for flare in the lense and to reduce the intensity of all light sources, laser and background should also make it easier to identify the primary laser spot and make the device more accurate. It would prevent bleaching of the camera and reduce the size of the spot observed by the software. It would also reduce the number of individual light sources the software is attempting to track.

References

1. **Bacelli, G.; Gilloteaux, J. C. and Ringwood, J.** State space model of a hydraulic power take off unit for wave energy conversion using bondgraphs. *In Proceedings World Renewable Energy Conference.* Glasgow 2008
2. **Baker, N. J.; Mueller, M. A.; Spooner, E.** Permanent magnet air-cored tubular linear generator for marine energy converters. *Proceedings of the 2nd IEE international conference on power electronics, machines and drives.* 2004, p.862-867
3. **Baker, N.J.; Mueller, M.A.; Ran, L.; Tavner, P.J.; McDonald, S.** Development of a linear test rig for electrical power take off from waves. *Proceedings of IMarEST - Part A - Journal of Marine Engineering and Technology.* 2007, Vol.2007(10), p.3-15
4. **Bhushan, B.** *Introduction to Tribology.* s.l.:John Wiley and Sons, 2002. p.441.
5. **Brooking, P.R.M.; Mueller, M.A.** Power conditioning of the output from a linear vernier hybrid permanent magnet generator for use in direct drive wave energy converters. *Generation, Transmission and Distribution, IEE Proceedings.* 2005, Vol.152(5), p.673-681
6. **Caraher, S.L.; Chick, J.P.; Mueller, M.A.** Investigation of Fluid Film Bearings for use in Direct Drive Linear Generators in Submerged Wave Energy Converters. *Proceedings of the Eighteenth International Offshore and Polar Engineering Conference.* Vancouver 2008
7. **Cengel & Turner.** *Thermal-Fluid Sciences.* s.l.:McGraw-Hill, 2001. p.133.

8. **Clement et al.** Wave energy in Europe: current status and perspectives. *Renewable and Sustainable Energy Reviews*. 2002, Vol.6(5), p.405-431
9. **Cruz J.; Gunnar H.; Barstow S.; Mollinson D.; Joao Cruz. Ed.** Green Energy and Technology. *Ocean Wave Energy*. 2008, p.93
10. **Danielsson, O.** *Master's Degree Project: Design of a linear generator for wave energy plant*. s.l.:Uppsala University, School of Engineering, 2003.
11. **Douglas, J.F.; Gasiorek, J.M. & Swaffield, J.A.** *Fluid Dynamics*. s.l.:Pearson Education, 2005 (5th ed.). p.547-549.
12. **Du Bois, H.** *The Magnetic Circuit in Theory and Practice*. s.l.:Longmans, London, Republished online 2010.
13. **Ernst, S. G.; Brekken, T. K. A.** A novel linear generator for wave energy applications. *MSc Thesis*. 2009
14. **Ferdinand, P.; Beer, J. T. DeWolf.** *Mechanics of Materials*. s.l.:McGraw-Hill, 2004. p.530-661.
15. **Ferraris, S.; Volpone, L.M.** Aluminium Alloys in Third Millenium Shipbuilding: Materials, Technologies, Perspectives. *The Fifth Internation Forum on Aluminium Ships*. Tokyo 2005
16. **Goldman, A.** *Modern Ferrite Technology*. s.l.:Springer Science & Business, 2006. p.2.
17. **Gunn, K.; Taylor, C.J.** Genetic algorithms for the development and optimisation of wave energy converter control systems. *European Institute for*

Applied Research Workshop on Advanced Control and Diagnosis. Coventry
2008

18. **Henderson, R.** Design, simulation and testing of a novel hydraulic power take-off system for the Pelamis wave energy converter. *Renewable Energy*. 2006, Vol.31(2), p.271-283
19. **Jean Frêne; Nicolas, D.; Degueurce, B.** *Hydrodynamic Lubrication: Bearings and Thrust Bearings*. s.l.:Elsevier, 1997. p.21.
20. **Kastinger, G..** Design of a novel transverse flux machine. *Robert Bosch GmbH*. Retrieved 2010
21. **Khonsari, M. M.; Booser, E. R.** *Applied Tribology: bearing design and lubrication*. s.l.:John Wiley and Sons, 2001. p.298-318.
22. **Morris-Thomas et al.; Irving, Rohan J.; Thiagarajan, Krish P.** An Investigation Into the Hydrodynamic Efficiency of an Oscillating Water Column. *Journal of Offshore Mechanics and Arctic Engineering*. 2007, Vol.129(4), p.273-278
23. **Mueller, M. A.; Baker, N. J.** Direct drive electrical power take-off for offshore marine energy converters. *Journal Proceedings of the Institution of Mechanical Engineers, Part A: Journal of Power and Energy*. 2006, Vol.219(3), p.223-234
24. **Mueller, M.A.; Baker, N.J.** Modelling the performance of the vernier hybrid machine. *Electric Power Applications, IEE Proceedings*. 2003, Vol.150(6), p.647-654

25. **Mueller, M.A.; Baker, N.J.; Spooner, E.** Permanent Magnet Air-Cored Tubular Linear Generator for Marine Energy Convertors. *Power Electronics, Machines and Drives, Second International Conference on.* 2004, Vol.2, p.862-867
26. **Pierson, W.J.; Moskowitz, L.A.** Proposed Spectral Form for Fully Developed Wind Seas Based on the Similiarity Theory of S.A Kitaigorodskii. *Journal of Geophysical Research.* 1964, Vol.69, p.5181-5190
27. **Polinder, H.; Damen, M.E.C.; Gardner, F.** Linear PM Generator system for wave energy conversion in the AWS. *Energy Conversion, IEEE Transactions on..* 2004, Vol.19(3), p.583-589
28. **Ralph E. Tarter.** *Solid-state power conversion handbook.* s.l.:John Wiley and Sons, 1993. p.10.
29. **Rhinefrank, K.; Agamloh, E.B.; von Jouanne, A.; Wallace, A. K.** Novel ocean energy permanent magnet linear generator buoy. *Renewable Energy.* 2006, Vol.31(9), p.1279-1298
30. **Rhinefrank, F.; Agamloh, E.B.; von Jouanne, A.; Wallace, A.K.; Prudell, J.; Kimble, K.; Aills, J.; Schmidt, E.; Chan, P.; Sweeny, B.; Schacher, A.** Novel ocean energy permanent magnet linear generator buoy. *Renewable Energy.* 2006, Vol.31, p.1279-1298
31. **Roberge, Pierre R.** *Handbook of Corrosion Engineering.* s.l.:McGraw-Hill, 2000. p.339-344.
32. **Salter, S.H.** Wave Power. *Nature.* 1974, Vol.249, p.720-724

33. **Shabana, A.A.** *Theory of vibration: an introduction*. s.l.:Springer, 1996. p.63.
34. **Taylor, C. J.; Chotai, A.; Young, P. C.** State space control system design based on non-minimal state-variable feedback: Further generalisation and unification results. *International Journal of Control*. 2000, Vol.73, p.1329-1345
35. **Taylor, J.R.** *Classical Mechanics*. s.l.:University Science Books, 2005. p.163-192.
36. **Yavuz, H.; Stallard, T.J.; McCabe, A.P.; Aggidis, G.A.** Time series analysis-based adaptive tuning techniques for a heaving wave energy converter in irregular seas. *IMEchE Proceedings, Journal of Power and Energy*. 2007, Vol.221, p.77-90
37. **Young, P.C.** *Recursive Estimation and Time Series Analysis*. s.l.:Springer, 1984.
38. **Young, P.C.; Behzadi, M.A.; Wang, C.L.; Chotai, A.** Direct digital and adaptive control by input-output, state variable feedback pole assignment. *International Journal of Control*. 1987, Vol.46, p.1867-1881
39. **Zbigniew, O.** *Damping of vibrations*. s.l.:A. A. Balkema, 1998. p.24.
40. **Roadmap 2050.** Roadmap 2050: A Practical Guide to a Prosperous, Low Carbon Europe. *Roadmap 2050 Website*. [Online] April 2010. [Accessed: 9 Nov. 2011.]
<http://www.roadmap2050.eu/>

41. **Roy Beardmore.** Rolling Bearing Friction. *RoyMech Website*. [Online] 23 Jun. 2010. [Accessed: 9 Nov. 2011.]
http://www.roytech.co.uk/Useful_Tables/Tribology/Bearing%20Friction.html
42. **BP.** Statistical Review of World Energy 2009. *BP Corporate Website*. [Online] 6 Jun. 2009. [Accessed: 6 Jun. 2010.]
http://www.bp.com/liveassets/bp_internet/globalbp/globalbp_uk_english/reports_and_publications/statistical_energy_review_2008/STAGING/local_assets/2009_downloads/statistical_review_of_world_energy_full_report_2009.pdf
43. **BP.** Statistical Review of World Energy 2010. *BP Corporate Website*. [Online] 6 Jun. 2010. [Accessed: 6 Jun. 2010.]
http://www.bp.com/liveassets/bp_internet/globalbp/globalbp_uk_english/reports_and_publications/statistical_energy_review_2008/STAGING/local_assets/2010_downloads/statistical_review_of_world_energy_full_report_2010.pdf
44. **WEC.** World Wave Resource. *Wind Waves and Solar Website*. [Online] 2005. [Accessed: 9 Nov. 2011.]
<http://www.windwavesandsun.com/WaveResource.html>
45. **Pelamis Wave Power.** The Pelamis. *Pelamis Wave Power*. [Accessed: 9 Nov. 2011.]
<http://www.pelamiswave.com/our-technology/the-pelamis>
46. **The American Society of Mechanical Engineers.** The Kingsbury

Thrust Bearing. *Holtwood Hydroelectric Station*. [Online] 5 Apr. 2001.

[Accessed: 9 Nov. 2011.]

<http://files.asme.org/ASMEORG/Communities/History/Landmarks/5583.pdf>